

39500202 —

# **Groundwater Flow and Transport Subregional Model: Giroux Wash Tailings Impoundment**



**Prepared for:**

**Nevada Division of  
Environmental Protection**

**October 15, 1997**

  
**Geomega**



39000202

Geomega

2995 Baseline Road  
Suite 202  
Boulder, CO 80303

Tel: 303-938-8115  
Fax: 303-938-8123

October 14, 1997

Mr. Leo Drozdoff, P.E.  
Chief, Bureau of Mining Regulation and Reclamation  
Nevada Division of Environmental Protection  
Capitol Complex  
333 W. Nye Lane  
Carson City, Nevada 89710

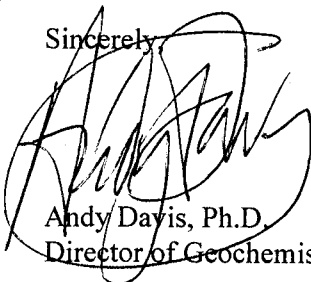
RE: Groundwater Flow and Transport Subregional Model: Giroux Wash Tailings  
Impoundment, for BHP Copper-Robinson Operations.

Dear Mr. Drozdoff:

Please find attached the final version of the modeling report *Groundwater Flow and Transport Subregional Model: Giroux Wash Tailings Impoundment*. The text incorporates your comments and suggestions as per your letter transmittal dated September 11, 1997. A written response to these comments were previously forwarded to you in a letter dated September 16, 1997.

A minor revision to this final report is that the tables and figures for each Section are included at the end of each individual Section. Please note that the numerical modeling which was completed to evaluate the Giroux Wash impoundment incorporates geologic heterogeneities by specifying unique hydraulic properties for each individual rock type described in the subsurface. This report was prepared for BHP pursuant to Section 2.9 of the February 27, 1997 *Work Plan—Robinson Operations* that was prepared in accordance with the Consent Agreement between BHP Copper-Robinson Operations and the Nevada Division of Environmental Protection (NDEP). Please contact me or George Fennemore directly with any comments or questions concerning this document at 303/938-8115.

Sincerely,



Andy Davis, Ph.D.  
Director of Geochemistry

cc: Ms. Cindi Byrns, CEM, Environmental Manager, BHP Copper-Robinson Operations  
Ms. Lisa Shevenell, Nevada Bureau of Mines and Geology





**Groundwater Flow and Transport  
Subregional Model:  
Giroux Wash Tailings Impoundment**

**Prepared for  
Nevada Division of Environmental Protection**

**Prepared by  
Geomega, Inc.  
2005 Baseline Road  
Boulder, Colorado 80303**

**for  
BHP Copper–Robinson Operations**

**October 15, 1997**



# Giroux Wash Groundwater Modeling Report

## CONTENTS

<b>Executive Summary</b>	<b>ES-1</b>
<b>1. Introduction</b>	<b>1</b>
1.1 Objectives of the Investigation	2
1.2 Scope of Work	2
1.3 Previous Data Acquisition and Analyses	3
1.3.1 The Model for the 1994 EIS	4
1.3.2 Field TDS Mobility Study	4
1.3.3 Water Chemistry of Tailings Solution and Background Groundwater	5
<b>2. Geologic Description</b>	<b>7</b>
2.1 Summary	7
2.2 Detailed Description of the Site Geology (after Welsh 1991)	7
2.2.1 Stratigraphy	8
2.2.2 Tectonism, Volcanism, and Structure	11
<b>3. Hydrogeologic Description</b>	<b>12</b>
3.1 Regional Hydrogeology	12
3.2 Local Hydrogeology	13
3.2.1 Paleozoic Rocks	13
3.2.2 Alluvial Aquifers	13
3.2.3 Fault Disruption of Aquifers	14
3.3 Summary Description of Groundwater Occurrence and Movement	14
<b>4. Vadose Zone Flow and Solute Transport</b>	<b>15</b>
4.1 Vadose Zone Description	15
4.1.1 Tailings Material	15
4.1.2 Paleozoic Limestone	15
4.1.3 Tertiary Sandstone	16
4.1.4 Quaternary Alluvium	16
4.2 Infiltration Modeling	16
4.3 Conditions Assumed in the Infiltration Model	18



4.4 Model Parameters	19
4.4.1 Recharge Rate	20
4.4.2 Hydraulic Properties of the Wash Materials	20
4.4.3 Solute Transport Properties	21
4.4.4 Depth to Groundwater	22
4.5 Model Discretization	22
4.6 Initial Conditions	22
4.7 Boundary Conditions	23
4.8 Model Results: Rates of Infiltration and Solute Transport	23
4.9 Sensitivity Analysis	24
<b>5. Groundwater Flow Modeling</b>	<b>27</b>
5.1 Conceptual Flow Model	27
5.1.1 Inflow of Groundwater into the Model Domain	27
5.1.2 Groundwater Flow Beneath the Impoundment Site	28
5.2 Mathematical Model	30
5.3 Model Design	31
5.3.1 Model Domain	32
5.3.2 Model Boundary Conditions	32
5.3.3 Hydraulic Properties	33
5.3.4 Aquifer Stresses	34
5.4 Calibration	35
5.4.1 Observation Points	35
5.4.2 Results of Steady-State Calibration	36
5.5 Verification and Sensitivity Analysis	37
5.6 Predictive Simulations	38
5.7 Interpretation of Modeling Results	38
5.8 Model Limitations and Assumptions	38
<b>6. Transport Modeling</b>	<b>40</b>
6.1 Conceptual Transport Model	40
6.2 Mathematical Model	40
6.3 Model Design Parameters	42
6.3.1 Solute Fluxes	42



6.3.2 Dispersivity	42
6.3.3 Molecular Diffusion	42
6.3.4 Chemical Reactions	43
6.4 Predictive Transient Simulations	43
6.5 Interpretation of Modeling Results	43
6.5.1 Case 1—3,000 mg/L TDS and 2,100 mg/L Sulfate Source	43
6.5.2 Case 2—4,000 mg/L TDS and 2,400 mg/L Sulfate Source	44
6.5.3 Case 3—5,000 mg/L TDS and 3,000 mg/L Sulfate Source	45
6.5.4 Simulations of the Barge-Operating Channel	45
6.5.5 Maximum Solute Concentrations at the Vadose Zone/Water Table Interface	47
6.6 Model Limitations and Assumptions	47
<b>7. Conclusions</b>	49
7.1 Tailings Solution Percolation Through the Unsaturated Zone	50
7.2 Potential for Groundwater Degradation	50
7.3 Barge-Operating Channel	51
7.4 Summary	51
<b>8. Recommendations</b>	52
<b>9. References</b>	53

## TABLES

1-1	Comparison of Modeling Efforts
1-2	Summary of Tailings Data for Robinson District
2-1	Stratigraphy, Lithology, and Average Thickness of Geologic Units
4-1	Hydraulic Parameters for the Unsaturated-Zone Model
4-2	Solute Transport Parameters
5-1	Transmissivities and Hydraulic Conductivities of Rock Types in Model
5-2	Storage Properties Used in Model
5-3	Groundwater Flow Model Calibration Statistics
5-4	Sensitivity Analysis
6-1	Solute Transport Parameters Used in Model



## **FIGURES**

### **Section 1—Introduction**

- 1-1 Giroux Wash Area
- 1-2 Giroux Wash Modeling Approach
- 1-3 Process Flow Diagram of Numerical Modeling

### **Section 2—Geology**

- 2-1 Geologic Map of Giroux Wash Area
- 2-2 Geologic Cross-Section (East-West) Beneath Impoundment
- 2-3 Geologic Cross-Section (South-North) Beneath Impoundment

### **Section 3—Hydrogeology**

- 3-1 Approximate Water Table Map with Monitoring Well and Boring Locations

### **Section 4—Vadose Zone Flow and Solute Transport**

- 4-1 Cross-Section of the Giroux Wash Vadose Zone
- 4-2 Plan View of Unsaturated Zone Model Domain
- 4-3 Conceptual Vadose Zone Model
- 4-4 Model Domain Cross-Section
- 4-5 Solute Concentration at  $t = 0$
- 4-6 Solute Concentration at  $t = 16$  Years
- 4-7 Solute Concentrations at  $t = 100$  Years
- 4-8 Solute Discharge to Groundwater
- 4-9 Predicted Flow Field
- 4-10 Sensitivity Analysis to Increased (2×) Recharge

### **Section 5—Groundwater Flow Modeling**

- 5-1 Regional Water Table and FDM Model Domain
- 5-2 East-West Conceptual Flow Schematic
- 5-3 North-South Conceptual Flow Schematic
- 5-4 Giroux Wash Impoundment Finite Difference Model Grid
- 5-5 Finite Difference Model Discretization, Section View
- 5-6 Boundary Conditions Assigned, Layer 6
- 5-7 Hydraulic Conductivity Distribution, Layer 6
- 5-8 Hydraulic Conductivity Distribution, Layer 7
- 5-9 Recharge Rates Applied to Top Active Model Layer
- 5-10 Calibrated Summary of Steady-State Flow Model
- 5-11 Observed vs. Predicted Water Table Map, Layer 6
- 5-12 Giroux Wash Area Hydrographs
- 5-13 Comparison of Transient vs. Steady-State Heads
- 5-14 Predicted Water Table Map, Layer 6, at 100 Years

## Section 6—Transport Modeling

- 6-1 Modeled Sulfate Concentrations vs. Time at WCC-G1, Assuming 3,000 mg/L TDS Source
- 6-2 Modeled TDS Concentrations vs. Time at WCC-G1, Assuming 3,000 mg/L TDS Source
- 6-3 Predicted Sulfate Isoconcentrations in Layer 5 at 96 Years
- 6-4 Predicted Sulfate Isoconcentrations in Layer 6 at 96 Years
- 6-5 Predicted Sulfate Isoconcentrations in Layer 7 at 96 Years
- 6-6 Predicted Sulfate Isoconcentrations in Layer 6 at 548 Years
- 6-7 Predicted Sulfate Isoconcentrations in Layer 7 at 548 Years
- 6-8 Predicted Sulfate Isoconcentrations in Layer 6 at 1,644 Years
- 6-9 Predicted Sulfate Isoconcentrations in Layer 7 at 1,644 Years
- 6-10 Modeled Sulfate and TDS Concentrations vs. Time at WCC-G1, Assuming 4,000 mg/L TDS Source
- 6-11 Modeled Sulfate and TDS Concentrations vs. Time at WCC-G1, Assuming 5,000 mg/L TDS Source
- 6-12 Predicted Solute Concentrations in the Vadose Zone for the Barge-Operating Channel and 5-Foot Head Simulations (West Part of Giroux Wash Impoundment)
- 6-13 Predicted Solute Concentrations in the Vadose Zone not covered by the Barge-Operating Channel and 5-Foot Head Simulations (West Part of Giroux Wash Impoundment)
- 6-14 Predicted Solute Concentrations in the Vadose Zone for the Barge-Operating Channel and 5-Foot Head Simulations (East Part of Giroux Wash Impoundment)
- 6-15 Predicted Vadose Zone and Groundwater Sulfate Concentrations
- 6-16 Predicted Vadose Zone and Groundwater TDS Concentrations

## APPENDIX

### Appendix on CD-ROM:

Unsaturated Flow Model Data (HYDRUS\_2D)

Groundwater Flow Model Data (MODFLOW)

Transport Model Data (MT3D96)



## Executive Summary

In accordance with the Consent Agreement between BHP Copper–Robinson Operations and the Nevada Division of Environmental Protection (NDEP), groundwater flow and solute transport modeling was completed for the Giroux Wash Tailings Impoundment. The purpose of conducting this modeling effort was threefold:

- to evaluate tailings water percolation through the unsaturated zone below the impoundment and
- to assess the potential for solute transport and degradation of state waters.

A detailed, subregional flow and transport model for the Giroux Wash Tailings Impoundment was constructed by refining the regional model developed for the Environmental Impact Statement (EIS) (PTI 1994). The Giroux Wash Tailings Impoundment model incorporated three well-benchmarked codes:

- HYDRUS\_2D for unsaturated zone flow and transport,
- MODFLOW for saturated zone flow,
- MT3D96 for saturated zone transport, and

These three numerical codes were coupled to predict flow and transport through the unsaturated and saturated zones. The subregional impoundment model quantified water flow and solute transport through the vadose zone to groundwater, followed by saturated zone solute transport to the downgradient groundwater compliance point (well WCC-G1). A process flow diagram of how these numerical models were inter-related is shown in Figure 1-3. The model implemented the following conservative flow and solute transport assumptions:

- Seepage will occur over the entire footprint of the impoundment for the operational life of the facility.
- The supernatant pond was assumed to provide an equivalent head across the lateral extent of the impoundment.
- No sorption or retarded transport of solutes will occur.
- The solutes will not be subjected to any chemical reactions.
- Worst-case scenarios for source concentrations were modeled.
- Low permeability soils (i.e., "B" horizon) were not incorporated in the vadose zone model.

← uniform ponding depth of 5 ft

The model also accounted for future impoundment development through sequentially increased impoundment surface area and volume.

On the basis of the permitted TDS and solute discharge levels into the impoundment, three tailings disposal cases were evaluated via fate and transport modeling. These cases

simulated varying source concentrations to establish a range of outcomes from the currently observed highest concentrations to progressively worse scenarios:

- Case 1. The highest levels actually observed to date in the solution samples—i.e., TDS = 3,000 mg/L and sulfate = 2,100 mg/L.
- Case 2. A case simulated with higher levels—i.e., TDS = 4,000 mg/L and sulfate = 2,400 mg/L.
- Case 3. A worst-case simulation—i.e., TDS = 5,000 mg/L and sulfate = 3,600 mg/L.

The unsaturated zone beneath Giroux Wash extends from the surface of the impoundment to a depth of 750 feet in the western part of the impoundment and to a depth of 250 feet in the eastern part of the impoundment. The variation in water levels is due to a hydraulically sealing fault that trends north-south which acts as an east-west flow barrier. The geologic material beneath the impoundment consists of four main components (Figure 4-1):

- tailings,
- Paleozoic limestone,
- Tertiary sandstone, and
- Quaternary alluvium.

Within the area of investigation groundwater originating in the mountain ranges is encountered at or near the surface and flows south towards the central portion of the White River Valley. Groundwater is first encountered at approximately 250 feet below ground surface (bgs) in the Tertiary Volcanic rocks on the east side of the Giroux Wash Impoundment, whereas groundwater in the Quaternary alluvium on the west side of the impoundment is first encountered at approximately 750 feet bgs. A combination of normal faulting and variation in stratigraphy account for this hydraulic separation across the impoundment.

A series of 40 stress periods (5,000 days each) was run using MT3D96 to simulate sulfate transport from the tailings impoundment area during disposal and post-disposal when the vadose zone was subjected to infiltration of impoundment water. The transport model was then run for an additional 1,096 years at pre-disposal conditions to estimate maximum sulfate concentrations at the point of compliance (POC) well, WCC-G1. Modeling was incorporated to predict flow and transport for more than 1,644 years in the future.

Three scenarios for source solute concentration were simulated. The interpreted results from the solute transport modeling are discussed below.

*Case 1—3,000 mg/L TDS and 2,100 mg/L Sulfate Source*

A graph of predicted concentration vs. time for the entire 1,644 year simulation show sulfate concentrations reaching a maximum of 44 mg/L 750 years in the future at the POC well, WCC-G1 (Figure 6-1). Sulfate concentrations are predicted to decrease at the POC well after 1,200 years of transport from the surface source, at which time they begin a return to pre-disposal background concentrations. The estimated TDS concentrations at the POC well reach a maximum of 395 mg/L 750 years from now. A concentration vs. time curve for TDS at the POC well, assuming a 3,000 mg/L source, is shown in Figure 6-2. On the basis of these concentration vs. time curves, it is apparent that sulfate and TDS will not exceed the State of Nevada Drinking Water Standards.

*Case 2—4,000 mg/L TDS and 2,400 mg/L Sulfate Source*

By adjusting these predicted values for a 4,000 mg/L TDS source in the impoundment, the resulting TDS at the POC well will reach maximum concentration of 400 mg/L approximately 750 in the future. Maximum sulfate concentration will occur at the same time as in case one, but is estimated at 44 mg/L. On the basis of these analyses, it is apparent that sulfate and TDS will not exceed the State of Nevada Drinking Water Standards.

*Case 3—5,000 mg/L TDS and 3,000 mg/L Sulfate Source*

The same relationship as described above was incorporated to predict TDS concentrations for a 5,000 mg/L source. By adjusting these predicted values for a 5,000 mg/L TDS source in the impoundment, the resulting TDS at the POC well will reach maximum concentration of 405 mg/L approximately 750 in the future. Maximum sulfate concentration will occur at the same time as TDS, but is estimated at 48 mg/L. On the basis of these modeling results, it is apparent that sulfate and TDS once again will not exceed the State of Nevada Drinking Water Standards.

Potential impacts to groundwater quality from these disposal operations are predicted to be minimal. Model results predict no substantial increase in solute concentrations in groundwater at the compliance monitoring point (WCC-G1). Conservative solute transport was assumed in the model input parameters. It will take over 100 years for the infiltration front from the disposed tailings solution to reach the water table on the west side of the facility. On the basis of this unsaturated and saturated zone flow and transport modeling, there will be no impact, above the State of Nevada Drinking Water Standards, to groundwater subjacent to the Giroux Wash Tailings Impoundment at the POC well, WCC-G1. The modeling results support continued operation of the tailings impoundment throughout the remaining mine life of approximately 16 years.

## 1. Introduction

Pursuant to Section 2.9 of the February 27, 1997, *Work Plan—Robinson Operations*, prepared in accordance with the Consent Agreement between BHP Copper—Robinson Operations and the Nevada Division of Environmental Protection (NDEP), groundwater flow and solute transport modeling has been completed for the Giroux Wash Tailings Impoundment. The purpose of conducting this modeling effort is threefold:

- to evaluate tailings solution percolation through the unsaturated zone below the impoundment and
- to assess the potential for solute transport and degradation of state waters.

This report describes the modeling effort and presents results of flow and solute transport simulations from the tailings impoundment, in accordance with Section 2.9.2 of the February 27, 1997, *Work Plan—Robinson Operations*.

The study area is located in the Robinson District south of Ruth, in White Pine County, east-central Nevada (Figure 1-1). This impoundment will ultimately cover an approximate lateral extent of 1,800 acres at the head of the White River Valley, which represents the confluence of White River Wash and Giroux Wash. BHP is disposing of flotation tailings from its mill process into the impoundment at Giroux Wash. At maturity this facility will hold over 200 million tons of tailings. A complete description of the disposal process at Giroux Wash is provided in the *Robinson Project Draft Environmental Impact Statement* (BLM 1994). Previous investigations performed by Welsh Engineering, Inc. (1991), and WESTEC (1994) described the impoundment facility area and provided the initial engineering design for implementation.

Groundwater flow and solute transport modeling for the impoundment was performed in two stages. First, the existing regional groundwater flow model (PTI 1994), developed to support the Environmental Impact Statement (EIS), was updated to incorporate new geologic and hydrogeologic data obtained since BHP began mining in the Robinson District. Next, a more detailed subregional model consistent with the existing regional model was constructed for the Giroux Wash Tailings Impoundment. The EIS regional groundwater flow model (PTI 1994) was originally developed to evaluate

- the potential influence of pumping in the mine area on the regional water table,
- the effects of tailings disposal in Liberty pit on the groundwater system, and

- the flux of water into the open pits after cessation of mining, for the purpose of predicting the water quality in the pit lakes.

Although the regional model was ideal to achieve its objectives, the Giroux Wash Tailings Impoundment model required finer resolution than the regional model could provide. Thus, in the current modeling effort, the regional model provided the basis for development of a more detailed subregional tailings impoundment model. The Giroux Wash Tailings Impoundment model incorporated the results of three well-benchmarked codes:

- HYDRUS\_2D for unsaturated zone flow and transport,
- MODFLOW for saturated zone flow, and
- MT3D for saturated zone solute transport.

The subregional impoundment model quantified water flow and solute transport through the vadose zone to groundwater, followed by saturated zone solute transport to the downgradient groundwater compliance point (well WCC-G1, a monitoring well installed in 1991 south of the impoundment and near the center of the structure [Woodward Clyde 1992]). The model source area for seepage flow included the permitted and operational tailings impoundment and barge-operating channel. The impoundment model implemented a range of tailings solution TDS concentrations (from 3,000 to 5,000 mg/L). Finally, the model accounted for future development and enlargement of the impoundment as tailings deposition continues throughout the remaining mine life of approximately 16 years.

### **1.1 Objectives of the Investigation**

The objective of this investigation was to predict the impact, if any, that mill tailings disposal at the Giroux Wash impoundment may have on water quality of the aquifers potentially affected by the facility. To fulfill this objective, three major tasks were completed:

- the vadose zone infiltration rate and solute flux to the water table was estimated,
- the groundwater flow regimes in the areas adjacent to the impoundment were resolved, and
- the migration of sulfate ions and total dissolved solids (TDS) downgradient of the impoundment were predicted.

### **1.2 Scope of Work**

Groundwater flow models for both the unsaturated and saturated zones were developed to solve the problems posed in Section 1.1. Figure 1-2 is a conceptual flow model of how the several numerical models were incorporated to address both flow and transport problems at the site.



An accurate unsaturated flow and transport model was developed to estimate infiltration and solute flux to the water table through the base of the Giroux Wash impoundment. The finite-element method (FEM) numerical code HYDRUS\_2D was used as the approach of choice for solving the unsaturated flow and transport equations because of its proven applicability to a wide variety of field problems (Simunek et al. 1996).

A detailed subregional groundwater model was constructed to evaluate groundwater flow and transport of solutes from the Giroux Wash Tailings Impoundment. A conceptual hydrogeologic model was developed for the site as a basis for construction of the saturated-zone groundwater flow and contaminant transport models. This model included review of all available relevant site data—including boring logs, aquifer test data, climatic data, groundwater elevations, and distribution of contaminants of concern (COCs) in soil and groundwater.

From the conceptual hydrogeologic model, a steady-state, numerical, groundwater flow model was constructed by using the U.S. Geological Survey (USGS) Modular Three-Dimensional Finite-Difference Ground-Water Flow Model (MODFLOW) (McDonald and Harbaugh 1988). Construction of the model was facilitated by the use of Groundwater Vistas, version 1.88, a graphical pre- and post-processor for use with MODFLOW and MT3D (Rumbaugh 1997).

Transport modeling to determine concentrations of COCs at the point of compliance (POC) was performed with MT3D96 (Zheng 1996). Inputs to the contaminant transport model included

- groundwater flow and heads, obtained from the MODFLOW groundwater flow model, and
- concentrations of COCs that may infiltrate to the water table, as predicted by the HYDRUS\_2D unsaturated flow and solute transport model.

Construction of the MT3D input files was also facilitated by the use of Groundwater Vistas.

A process flow diagram of how these numerical models were inter-related is shown in Figure 1-3. Inputs to and outputs from the different models are documented in this diagram.

### **1.3 Previous Data Acquisition and Analyses**

Mobility of solutes in the subsurface underlying the Giroux Wash Tailings Impoundment was examined initially in the site EIS (PTI 1994) and more recently by

Geomega (1997a). In addition, the chemical composition of the tailings solution in the impoundment has been monitored monthly since disposal commenced in January 1996. The databases developed during these studies were used in the current evaluation and are summarized below.

### *1.3.1 The Model for the 1994 EIS*

The simulation of flow and transport presented in support of the 1994 EIS incorporated a one-dimensional unsaturated zone model and groundwater flow results taken from the regional flow model. The main assumptions influencing the solute transport predicted by the 1994 model were

- the average infiltration rate was of 0.004 feet/day,
- the solute transport in the subsurface was conservative (i.e., no chemical reactions or retardation was assumed), and
- sulfate is the analyte of concern for transport modeling.

These assumptions were reexamined during the total dissolved solids (TDS) mobility study and during the current modeling effort. A comparison of central features of the various modeling efforts is included to show their similarities and differences (Table 1-1).

The model used in the 1994 EIS predicted that sulfate concentrations at a downgradient monitoring point (well WCC-G1) will be <250 mg/L and the maximum concentration will reach this location after approximately 900 years (PTI 1994).

### *1.3.2 Field TDS Mobility Study*

Angle bores from the impoundment embankment collected soil samples from beneath the impoundment in December 1996 (Geomega 1997a). Chemical analyses of these soil samples were used to determine the extent to which the tailings solution had transported solutes into the subsurface material. The fastest-moving solute front measured in these samples had traveled approximately 18 inches during the year between deposition of tailings and soil sampling (0.004 feet/day). The advective flow velocity should decrease following closure of the impoundment because ponded water will no longer be present to drive the infiltration.

In addition, bore holes approximately 100 feet south of the impoundment embankment drilled in 1997 did not identify horizontal flow downgradient of the impoundment area (Geomega 1997a). These data indicate that potential infiltration from the tailings impoundment, if any, is moving vertically downward and is not flowing laterally.

Another aspect of the 1996 field studies conducted in Giroux Wash was the examination of the hydraulic properties of the upper strata of the regional soil. The B-

horizon consists of very fine, clay-sized particles that are present in layers as much as 20 feet thick below the surface of the impoundment area. Column tests demonstrate that this material has a low hydraulic conductivity and acts as a barrier to water infiltration and solute transport (Geomega 1997b).

### *1.3.3 Water Chemistry of Tailings Solution and Background Groundwater*

The water chemistry of the tailings solution and the background solute concentrations have been measured since tailings disposal commenced. The solute concentrations in the tailings solution were determined from analyses of tailings material recovered from the Repulp House, Pump House, Reclaim Barge, Mill Slurry, entrained impoundment water, and the tailings thickeners (Table 1-2). These analyses identify TDS and sulfate as the constituents of concern for the modeling effort because concentrations of other chemicals generally meet drinking water standards. Averages of analytical results of groundwater obtained from unaffected wells in Giroux Wash (WCC-G1, WCC-G2, WCC-G3, MW-4G, and MW-5G) were used to represent the background solute concentrations. These data were used to determine the solute concentrations that were modeled in this study.

Investigation of the tailings impoundment and the February 1996 excursion have demonstrated that the tailings are not generating acid. Further, the composition of the tailings solution is such that it has a buffering capacity; therefore, any acid generated will be neutralized by the tailings solution. This finding is supported by the results of the TDS mobility study in which an alkaline pH was observed in the impoundment and in the subjacent alluvium. In addition, on a quarterly basis, in compliance with Water Pollution Control Permit NEV92013, BHP will analyze a solid tailings sample for acid-generating potential.

The average TDS concentration in the 90 samples of the tailings solution was 1,912 mg/L; the maximum TDS concentration was 3,000 mg/L. The time-weighted TDS average is 1,928 mg/L. Sulfate accounted for approximately 60% of the TDS in the tailings solution. Sulfate concentrations in these samples averaged 1,308 mg/L; the maximum sulfate concentration was 2,100 mg/L. The other major TDS component was calcium, which accounted for approximately 27% of the TDS. The average calcium concentration was 604 mg/L; the maximum calcium concentration was 1,400 mg/L.

The average concentrations of the 90 samples do not violate the permitted standards for tailings impoundment operations. However, 41 individual samples exceeded the permitted TDS limit (which is  $\leq 2000$  mg/L in tailings discharge into the impoundment), and 19 individual samples exceeded the permitted sulfate level (1500 mg/L). The average of 34 background groundwater samples indicated that background TDS in Giroux Wash was 378 mg/L, background sulfate was 30 mg/L, and background calcium was 61 mg/L.

On the basis of the permitted TDS and solute discharge levels into the impoundment, three cases were evaluated via fate and transport modeling. These cases simulated varying source concentrations to establish a range of outcomes from the currently observed highest concentrations to progressively worse scenarios:

- Case 1. The highest levels observed to date in the solution samples—i.e., TDS = 3,000 mg/L and sulfate = 2,100 mg/L.
- Case 2. A case simulated with higher levels—i.e., TDS = 4,000 mg/L and sulfate = 2,400 mg/L.
- Case 3. A worst-case simulation—i.e., TDS = 5,000 mg/L and sulfate = 3,000 mg/L.

The worst-case TDS concentration was predicted from an assumed net evaporation rate of 48 inches/year and an average 3-day residence time of recirculated tailings solution in the impoundment. In this calculation, the increase in TDS was a result of linear evapoconcentration (i.e., no mitigating reactions were considered).

**Table 1-1. Comparison of Modeling Efforts**

Model feature	Geomega (1997)	PTI (1994)
Grid node spacing	200 feet, uniform	Telescoping from 8,000 feet to 400 feet in the Giroux Wash area
Geologic description	Included current BHP characterization of the Giroux Wash area	Included data that were available in 1994
Hydraulic conductivity and lithologies	39 different rock types were assigned over the model domain Five different conductivities were assigned to the alluvial strata	23 different rock types were assigned Only one conductivity was assigned for alluvial strata
Unsaturated-zone modeling	2-D slices over the lateral footprint of the impoundment were incorporated to address surface disposal variations	1-D vertical column was used for the entire impoundment area
Groundwater modeling of Giroux Wash area	3-D FDM numerical model that addressed subsurface heterogeneities 3-D groundwater flow and solute transport were simulated	2-D analytical solution that could not address subsurface heterogeneities 2-D groundwater flow and solute transport equations were solved

*Note:* 1-D = one-dimensional, 2-D = two-dimensional, 3-D = three-dimensional, FDM = finite-difference method.



**Table 1-2. Summary of Tailings Data for Robinson District**

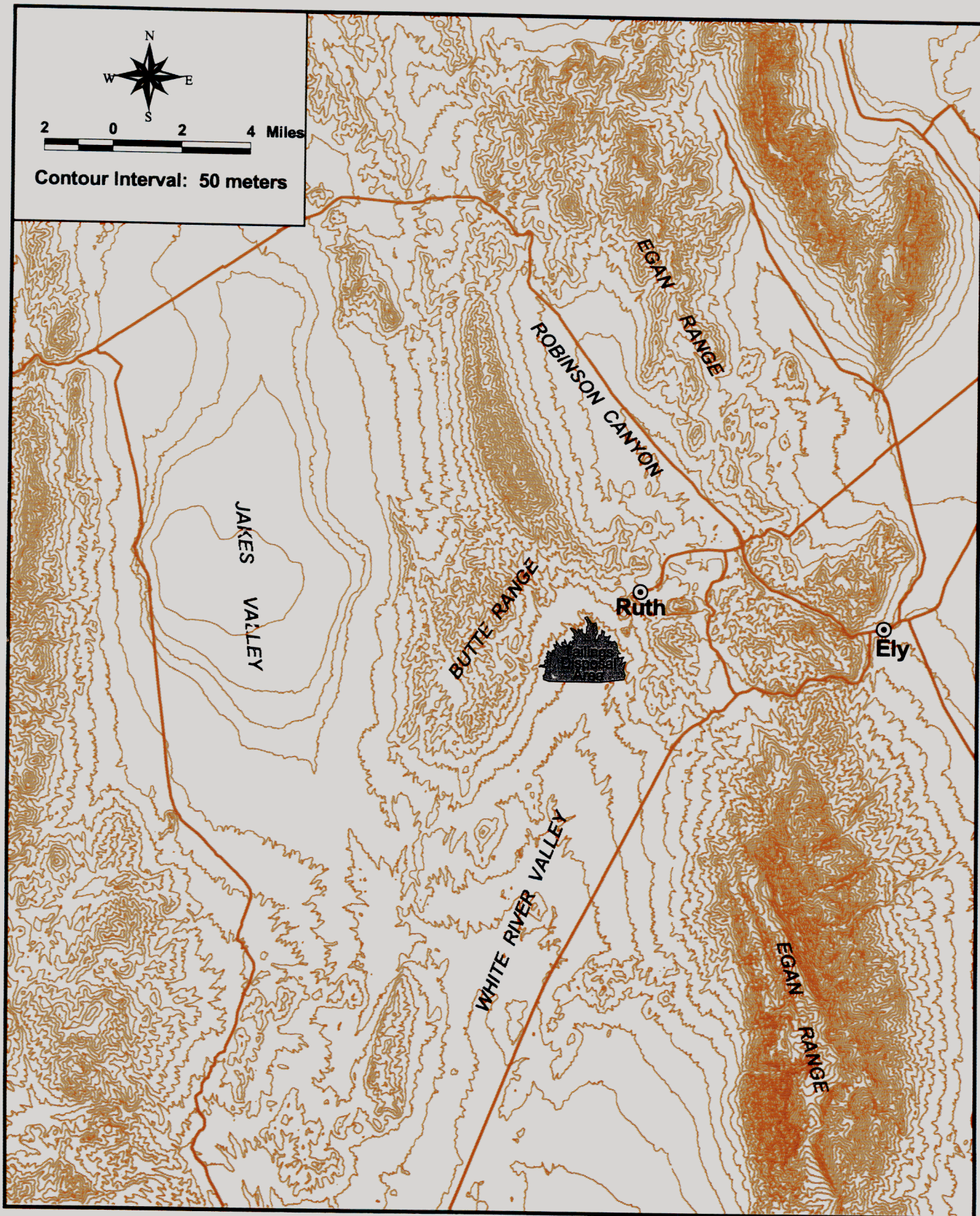
Sample identification	Parameters				
	Date	pH	TDS	Calcium	Sulfate
Repulp House	1/31/96		1790	520	1030
	2/28/96	10.7	2530	731	1450
	3/26/96	10.1	2470	689	1520
	7/11/96	10.38	2590	668	1600
	4/15/96	9.22	2150	573	1330
	5/14/96	9.49	2360	398	1370
	1/31/96	10.4	1790	520	1030
	2/28/96	10.7	2530	731	1450
	3/26/96	10.1	2470	689	1520
	4/15/96	9.22	2150	573	1330
	5/14/96	9.49	2360	598	1370
	6/12/96	9.84	1610	924	1610
	6/20/96	9.29	2620	761	1640
	6/27/96	10.48	2580	676	1430
	7/3/96	9.88	2710	723	1640
	7/25/96	5.33	2510	787	1650
	8/2/96	9.63	2500	699	1480
	8/16/96	8.79	2010	557	1160
	8/23/96	6.47	1640	407	904
	9/20/96	6.95	2680	653	1810
	10/31/96	6.9	1290	348	699
	11/15/96	8.62	1540	387	896
	12/2/96	9.28	1390	384	842
	12/19/96	8.65	1410	304	766
	12/31/96	9.8	1450	389	842
10:00	3/16/97		1310		
3:00	3/16/97		1880		
10:00	3/17/97		1732		
3:00	3/17/97		2152		
5:30	3/18/97		1540		
9:00	3/18/97		2280		
10:00	3/19/97		1500		
3:00	3/19/97		1364		
10:00	3/20/97		1370		
3:00	3/20/97		1464		
10:00	3/21/97		1512		
3:00	3/21/97		1444		
10:00	3/22/97		496		
3:00	3/22/97		1444		
10:00	3/23/97		1732		
3:00	3/23/97		1608		
10:00	3/24/97		1576		
3:00	3/24/97		1176		
10:00	3/25/97		660		
3:00	3/25/97		688		
10:00	3/26/97		1180		
3:00	3/26/97		1140		

**Table 1-2. Summary of Tailings Data for Robinson District, *continued***

Sample identification	Parameters				
	Date	pH	TDS	Calcium	Sulfate
Repulp House, <i>cont.</i>	10:00	3/27/97	1420		
	15:00	3/27/97	1288		
	10:00	3/28/97	1256		
	15:00	3/28/97	1368		
		5/28/97	2256		
		5/28/97	1956		
Pump House		1/5/96	1260	283	782
		2/27/96	2070	599	1390
		3/26/96	2170	479	1240
		4/15/96	2110	564	1330
		5/14/96	1300	312	730
		6/12/96	2380	862	1500
		6/20/96	2590	605	1670
		6/27/96	2800	813	1520
		6/27/96	2580	817	1480
		7/3/96	2680	693	1620
		7/11/96	2540	677	1560
		7/25/96	2470	647	1560
		8/2/96	2600	566	1470
		8/2/96	2540	679	1480
		8/9/96	2550	807	1470
		8/16/96	1990	550	1130
		8/23/96	1650	405	840
Reclaim		1/3/96	1720	382	1100
		1/8/96	1570	412	954
		2/27/96	2460	634	1400
Mill Slurry		12/16/95	2310	1400	641
		12/18/95	1480	332	946
		12/30/95	1450	328	916
Impoundment		3/28/96	2490	589	1520
		4/15/96	2150	573	1330
		7/11/96	2660	824	1510
		7/25/96	2490	804	1520
		1/13/97	3040	674	2100
Thickener		6/20/96	9.1		
		7/3/96	10.5	2660	683
		7/11/96	10.94	2390	661
<b>Average</b>		<b>9.31</b>	<b>1912.93</b>	<b>603.87</b>	<b>1308.30</b>
<b>Standard Deviation</b>		<b>1.29</b>	<b>565.86</b>	<b>195.85</b>	<b>325.28</b>
<b>Average TDS for Samples with Ca and SO<sub>4</sub> data</b>			<b>2192.68</b>		

**Table 1-2. Summary of Tailings Data for Robinson District, *continued***

Sample identification	Parameters				
	Date	pH	TDS	Calcium	Sulfate
MW-4G	8/10/95	7.87	325	59.8	35.9
MW-4G	11/7/95	7.77	281	38.5	35.6
MW-4G	3/11/96	7.82	260	26.6	19
MW-4G	4/23/96	7.94	252	33.1	16
MW-5G	8/9/95	7.69	338	36.1	30.8
MW-5G	11/9/95	7.99	287	38.2	26.3
MW-5G	3/25/96	7.86	282	47.3	23
MW-5G	4/28/96	7.94	284	46.2	22
WCC-G1	5/17/93	7.89	634	107	34.5
WCC-G1	10/8/93	7.7	542	101	32.5
WCC-G1	3/29/94	7.63	606	103	33.9
WCC-G1	9/23/94	7.86	580	91	28.7
WCC-G1	4/5/95	8.11	552	92.5	26.3
WCC-G1	8/2/95	7.87	572	93.7	30.3
WCC-G1	9/22/95	7.94	551	92.4	28
WCC-G1	3/20/96	8.12	578	93	27
WCC-G1	4/23/96	8.05	528	77.9	25
WCC-G2	5/14/93	8.44	580	44.4	40
WCC-G2	10/7/93	8.1	239	46.4	28.9
WCC-G2	3/28/94	8.26	246	43.2	28.8
WCC-G2	9/7/94	8.24	271	44.5	28.1
WCC-G2	4/5/95	8.22	260	44.9	27.5
WCC-G2	8/1/95	8.04	255	45.1	29
WCC-G2	9/22/95	8.07	250	45.5	27.8
WCC-G2	11/20/95	8.12	265	42.4	28.7
WCC-G2	3/22/96	8.29	266	43.1	30
WCC-G2	4/28/96	8.22	264	45.8	28
WCC-G3	3/28/94	8.25	269	41.8	32.7
WCC-G3	9/23/94	8.28	272	44.1	33.2
WCC-G3	4/5/95	8.98	395	75.5	41.7
WCC-G3	8/2/95	8.15	260	44	32.1
WCC-G3	9/22/95	7.67	489	85	30.5
WCC-G3	11/20/95	7.74	601	127	25.6
WCC-G3	4/23/96	7.73	224	30.8	36
<b>Average</b>		<b>8.03</b>	<b>378.18</b>	<b>60.91</b>	<b>29.51</b>
<b>Standard Deviation</b>		<b>0.27</b>	<b>144.64</b>	<b>26.83</b>	<b>5.25</b>

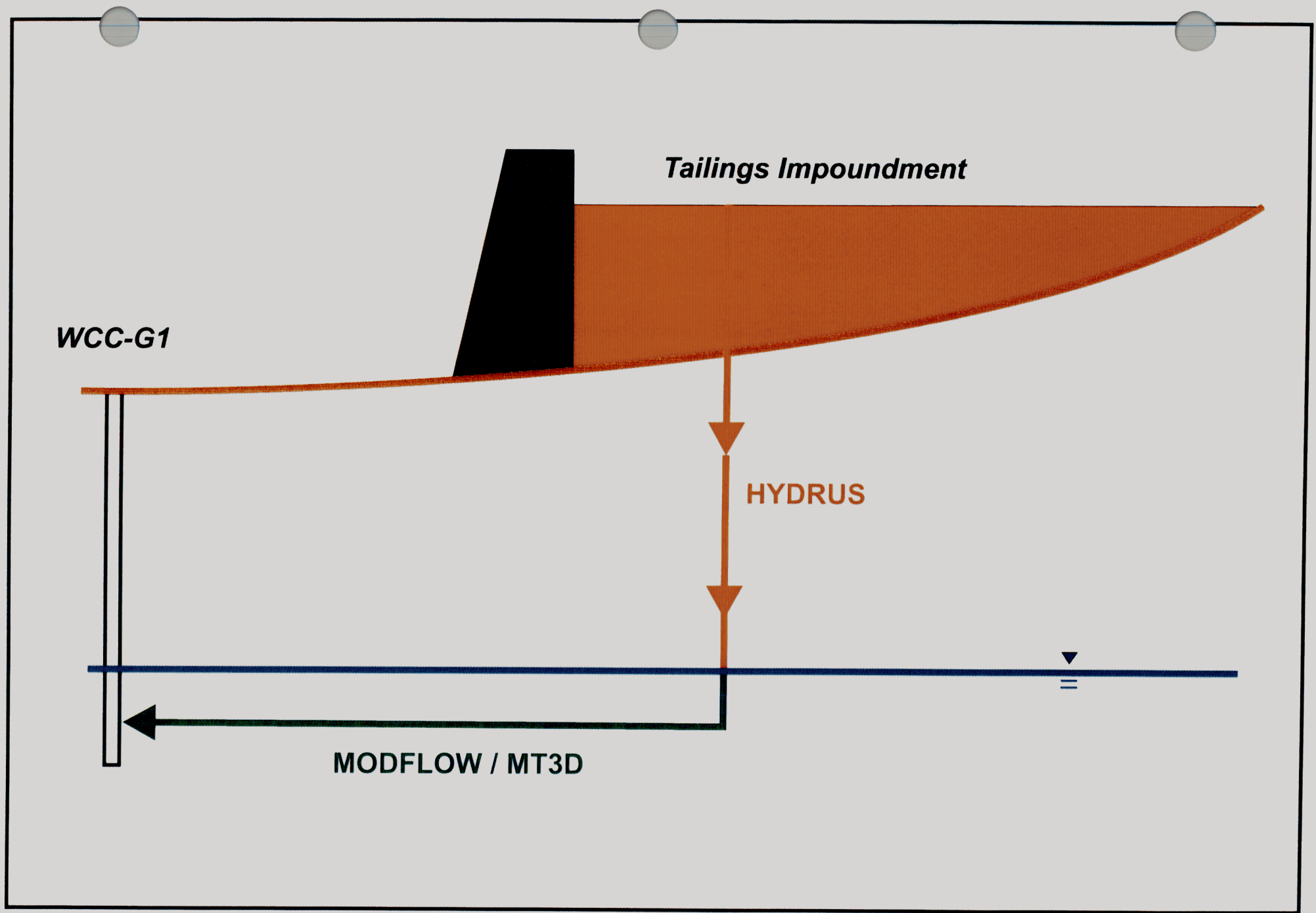


Generation  
Date:  
8/7/97

Figure 1-1. Giroux Wash Area.



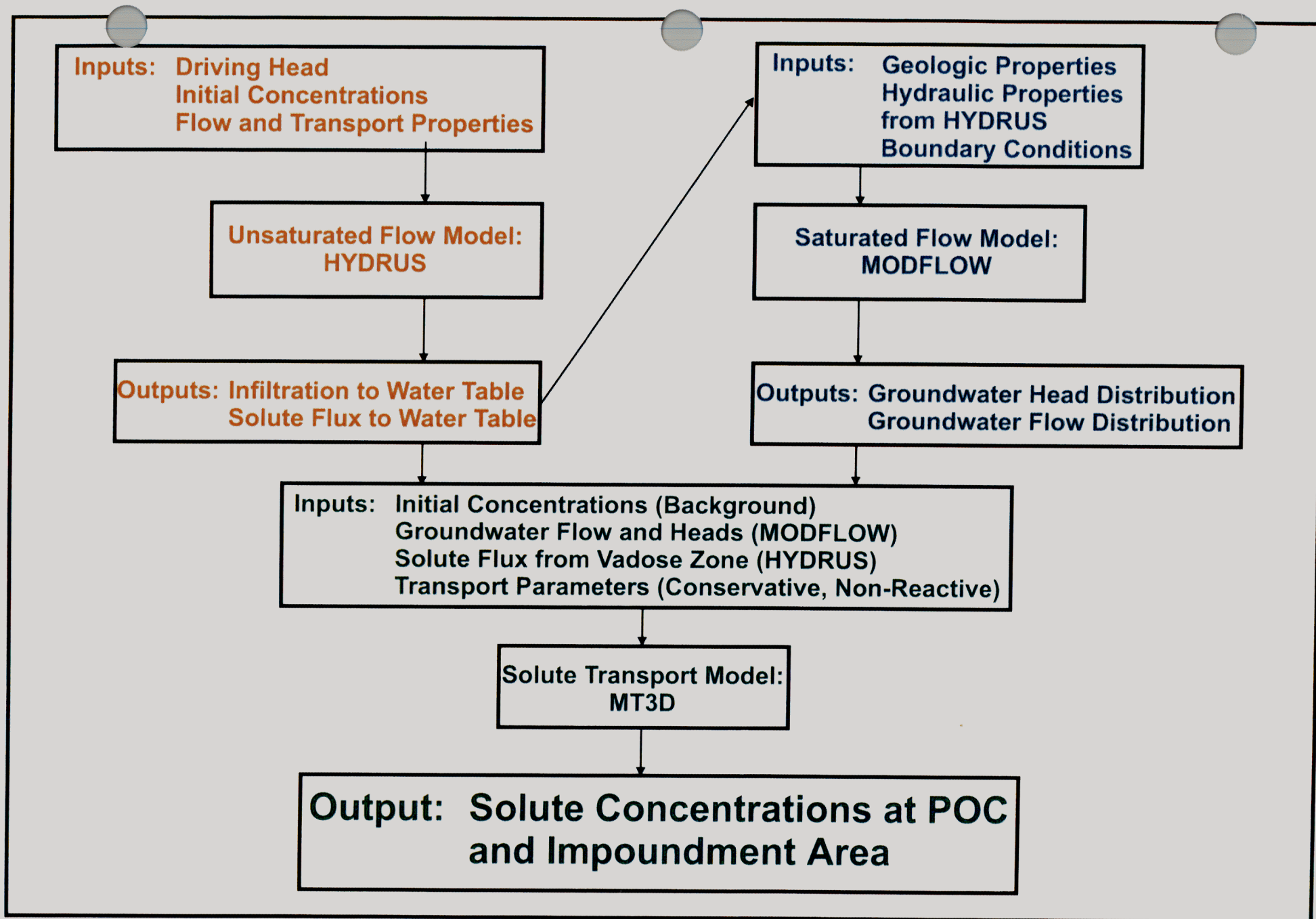




Generation  
Date:  
8/7/97

Figure 1-2. Giroux Wash Modeling Approach.





Generation  
Date:  
8/4/97

Figure 1-3. Process Flow Diagram of Numerical Modeling.

## **2. Geologic Description**

### **2.1 Summary**

Previous work by a variety of authors described the geology of Robinson Mining District and the Giroux Wash impoundment area. References include Brokaw and Barosh (1968), Einaudi (1982), Fournier (1967), James (1976), Gans and Miller (1983), Hose and Blake (1976), Seedorf (1993), Smith (1976), and Westra (1982). Past consulting investigations that described the geology of the area include Dames & Moore (1982), PTI (1994), Welsh Engineering (1991), WESTEC (1991), and Woodward Clyde (1991, 1992).

As shown in a geologic map of the Giroux Wash area (Figure 2-1) and an east-west hydrogeologic cross section located just south of the dam that forms the basin for the impoundment (Figure 2-2), the stratigraphic section directly underlying the western two thirds of the impoundment consists of a thick deposit of Quaternary alluvium. This alluvial deposit comprises unconsolidated, interbedded gravels, sands, and clays to a depth of more than 1,000 feet, on the basis of boring logs taken just south of the Giroux Wash dam. The Quaternary alluvium is truncated to the east by the first of a series of normal faults.

The eastern third of the impoundment is characterized by a series of normal faults cutting Tertiary volcanic rocks. A north-south cross section through the eastern part of the impoundment area displays geologic strata encountered (Figure 2-3). Within the vadose zone, relatively impermeable Tertiary volcanic rocks, varying from ash flows to rhyolitic lava flows, crop out at the surface outside of the tailings impoundment footprint and dip between 9° and 30° to the west. Near the surface, parts of these formations have been eroded and filled with Tertiary and Quaternary alluvial deposits.

### **2.2 Detailed Description of the Site Geology (after Welsh 1991)**

At the tailings impoundment site, the Paleozoic sedimentary rocks are more than 11,000 feet thick. In stratigraphic order from oldest to youngest, they include the limestones of the Devonian Guilmette Formation, the limestone of the Permian Kaibab Formation, and the siltstone, sandstone, and limestone of the Permian Arcturus Formation. The Kaibab and Arcturus Formations are well exposed in the Egan and Butte Ranges above the valley floor on which the tailings dam is located. In the easternmost part of the site, the Paleozoic rocks are capped by a sequence of Tertiary volcanic rocks that dip 9° to 30° to the west.

The westernmost two thirds of the site is composed of a fault block or "half-graben" structure tilted steeply to the west and filled with Tertiary to Quaternary alluvium; the half-graben is bounded on the west by the Radar Range fault. The easternmost third

of the site is composed of small, west-dipping structural blocks separated by steep normal faults. These blocks are composed of Tertiary volcanic rocks overlying Paleozoic strata.

Although the topographically high areas (<8,000 feet) to the east and west of Giroux Wash (about 6,700 feet) represent source areas for the thick alluvium filling the graben, the dominant source area appears to be the mountains (about 8,500 feet) to the west of the site. This interpretation is supported by the fact that to the west of Giroux Wash, the landscape is dominated by a series of coalescing alluvial fans. These fans have pushed the main channels of White River Wash and Giroux Wash (which drain southward and join to form the White River Valley) eastward against fault scarps formed of the west-dipping Tertiary volcanic rocks.

Subsequent to the alluvial filling of the graben was a relatively recent period of stream rejuvenation. The main channel of the White River Wash–Giroux Wash and its major tributaries were incised into the surface of the Tertiary–Quaternary alluvium. The incised channels were then filled with younger silt-sized and fine-sand-sized alluvium.

### 2.2.1 Stratigraphy

Ten geologic units have been identified at the Giroux Wash site (see Figure 2-1). They are described below from oldest to youngest. Table 2-1 summarizes the stratigraphy, lithology, and average thickness, based on USGS geology maps (Langenheim and Larson 1973).

#### *Pennsylvanian–Permian Sedimentary Rocks, Undivided (Pz)*

This unit consists of the Kaibab Limestone, the Arcturus Formation, the Rib Hill Sandstone, the Reipe Spring Limestone, and the Ely Limestone.

- The Kaibab Limestone is a light to medium gray, fine to moderately crystalline massive limestone with indistinct bedding. It contains abundant light brown to gray modular chert.
- The Arcturus Formation is a predominantly yellow to reddish-gray siltstone and fine-grained sandstone interbedded with thin, platy, tan limestone. At the base of the upper unit is a thin evaporite sequence of calcareous siltstone, gypsum, and impure gray limestone. The lower part of the Arcturus Formation consists of a massive, ledge-forming gray limestone, interbedded with sandstone and siltstone.
- The Rib Hill Sandstone is a medium- to fine-grained sandstone and siltstone.
- The Reipe Spring Limestone consists of a medium to gray, finely to moderately crystalline, thin-bedded to massive, bioclastic limestone.
- The Ely Limestone consists of a light olive gray to brownish gray, thin- to thick-bedded cherty limestone.

### *Tertiary Sheep Pass Formation (Tsp)*

This unit consists of a light tan to brown, silty to sandy limestone with sparse gastropod fossils and root casts.

### *Tertiary Smoky Quartz Rhyolite (Tvf and Tvt)*

These are the oldest volcanic rocks in the area. They are typified by phenocrysts of light gray to black smoky quartz. The smoky quartz rhyolite includes both lava flows (Tvf) and unwelded ash-flow tuffs (Tvtu and Tvtl). The rhyolitic lavas range from flow-banded, devitrified, vapor-phase-altered rocks to fresh, vitrophyric, vesiculated, and autobrecciated rocks. The rock contains 30% to 35% phenocrysts of alkali feldspar, clear to smoky quartz, biotite, and rare hornblende in a devitrified glass groundmass. In some areas the formation appears as steep-sided rubbly outcrops of glassy, massive rhyolite.

The ash-flow tuffs range from pink to white and are expressed as rounded or bouldery outcrops mainly in the southern part of the area. The tuffs consist of about 20% crystals, 5% to 30% rock fragments, 5% white pumice, and 45% to 70% devitrified glass groundmass. Lithic fragments consist mainly of devitrified or glassy volcanic rocks with minor sedimentary rocks and rare plutonic lithic fragments. These lithic fragments range from sand-size particles to 5-foot-diameter boulders.

### *Tertiary Volcaniclastic Sedimentary Rocks (Tvs)*

This unit consists of a sequence of tuffaceous sandstone and conglomerate with intercalated ash-flow and ash-fall deposits. The sediments that formed this unit were derived directly from erosion of the underlying ash-flow tuffs. The unit consists of angular to subrounded quartz, feldspar, sparse biotite, and volcanic lithic fragments with variable amounts of devitrified glass groundmass. In places, the sedimentary rocks are hard to distinguish from ash-flow or ash-fall tuffs and may include slightly reworked or even primary tuffs. Most of these rocks, however, display well-developed sedimentary structures—such as bedding, cross-bedding, and conglomerate channels—that indicate deposition in an alluvial-fan or braided-stream environment.

### *Tertiary Biotite Rhyolite Tuff (Tvb)*

This unit consists of platy, locally columnar-jointed, biotite-rich tuff. The rocks range from moderately welded and pumiceous tuff with up to 40% phenocrysts of alkali feldspar, biotite, quartz, and magnetite to unwelded, pumice-rich tuff with 25% to 30% phenocrysts.

### *Tertiary Crystal-Poor Ash-Flow Tuff (Tva)*

Crystal-poor tuff is predominantly tan to brown, with 5% to 20% pumice, 5% to 10% lithic fragments, and 1% to 5% crystals in a fine ash matrix. The pumice is tan to

white, unwelded, and silky in appearance. Phenocrysts include sparse quartz, feldspar, and biotite, and lithic fragments are mostly sedimentary or plutonic. Portions are oxidized to a brick red color, perhaps indicating extended subaerial exposure.

#### *Tertiary Alluvium (Ta)*

This unit—consisting of poorly cemented calcareous conglomerate and sandstone with minor lacustrine limestone—overlies most of the Tertiary units in the White River Wash–Giroux Wash area. It commonly caps low ridges. Clasts in the conglomerate range up to 15 centimeters across and are subrounded to subangular. The clasts consist of Paleozoic limestone, silicified limestone, hornfels, porphyritic intrusive igneous rocks, and rarer Tertiary volcanic rocks in a calcareous sandy matrix.

#### *Quaternary Alluvial Terraces (Qat)*

These materials also consist of poorly sorted sands and gravels similar to the above-described older alluvial materials. However, they were laid down on relatively flat terraces associated with stream deposition during the middle to late Quaternary at a higher base level of erosion.

#### *Older (Tertiary–Quaternary) Alluvium (Qoal<sub>1</sub>, Qoal<sub>2</sub>, Qoal<sub>3</sub>, and Qoal<sub>4</sub>)*

These materials consist primarily of poorly sorted sands and gravels with a high percentage of cobble-sized clasts. The larger gravel- and cobble-sized clasts vary from rounded to subangular but are predominantly subrounded to subangular, indicating a source for the sediments that was relatively close. The older alluvium unit fills the deep “half-graben” structure located directly east of the Radar Range fault. Active deposition in this west-tilted basin has continued from late Tertiary through late Quaternary time.

The numerical sequencing assigned to the older alluvium subunits is less a function of relative age and more a function of geomorphic characteristics. The alluvial deposits designated as Qoal<sub>1</sub> represent the alluvial-fan deposits that form an apron along the mountain front to the west of the site. These deposits are found primarily in the wedge located between the two largest alluvial fans (designated Qoal<sub>2</sub> and Qoal<sub>3</sub>) that appear to have been responsible for most of the basin in-filling during the late Quaternary. The Qoal<sub>4</sub> alluvial materials form a relatively thin veneer of pediment gravels and colluvial soils.

#### *Quaternary (Recent) Alluvium (Qal)*

These are recent soil materials associated with stream deposition in the entrenched segments of the valley floor. They consist primarily of well-sorted, fine-grained sands and silts.

### 2.2.2 *Tectonism, Volcanism, and Structure*

During Tertiary time, there were two major periods of tectonic activity in the study area, which had previously been tectonically quiet. The first, during the late Mesozoic to early Tertiary, resulted in the development of both low- and high-angle thrust faults. However, the most significant activity was the development of a large low-angle thrust fault (or fault complex) over much of eastern Nevada, structurally known as a decollement. Remnants of a low-angle thrust that may have been associated with this deformation have been mapped across the northernmost and easternmost parts of the tailing dam site. As the trace of this feature is followed southward, it appears to terminate in younger high-angle normal faults with the downthrown side to the east.

Following this Late Cretaceous–early Tertiary crustal shortening, Eocene to Oligocene lacustrine limestones and conglomerates were deposited in shallow depositional basins. Early Oligocene andesitic and rhyolitic lavas and tuffs erupted from isolated vent areas, followed by the eruption of intermediate volcanic rocks coinciding with the onset of the large-scale extension and crustal thinning that formed the Basin and Range structural province.

As much as 250% extensional deformation from middle to late Tertiary time has produced the Basin and Range horst-and-graben structure that dominates the landscape today. The horsts are represented by the north-trending, elongate mountain ranges, and the grabens form the intervening, wide, flat-bottomed valleys filled with deep alluvium deposits.

The early crustal thinning was accompanied by extensive volcanic activity. Although most volcanism in east-central Nevada had reached quiescence by early to middle Miocene time, extension continues to the present, as evidenced by multiple generations of imbricate normal faults, the youngest of which cut late Tertiary and Quaternary conglomerate and lacustrine valley-fill deposits.

On this site, tilting of the Paleozoic to lower Tertiary section ranges from 9° to 30° to the west. Dips in the youngest Tertiary sedimentary rocks are shallower, consistent with syndepositional growth faulting along the Radar Ridge fault to the west. To the east, several north-trending, downthrown blocks, which possibly represent two generations of normal faulting, are inferred to cut the Tertiary sequence but do not appear to disturb Quaternary alluvium or older (Tertiary–Quaternary) alluvium and, hence, do not affect the foundation of the impoundment.



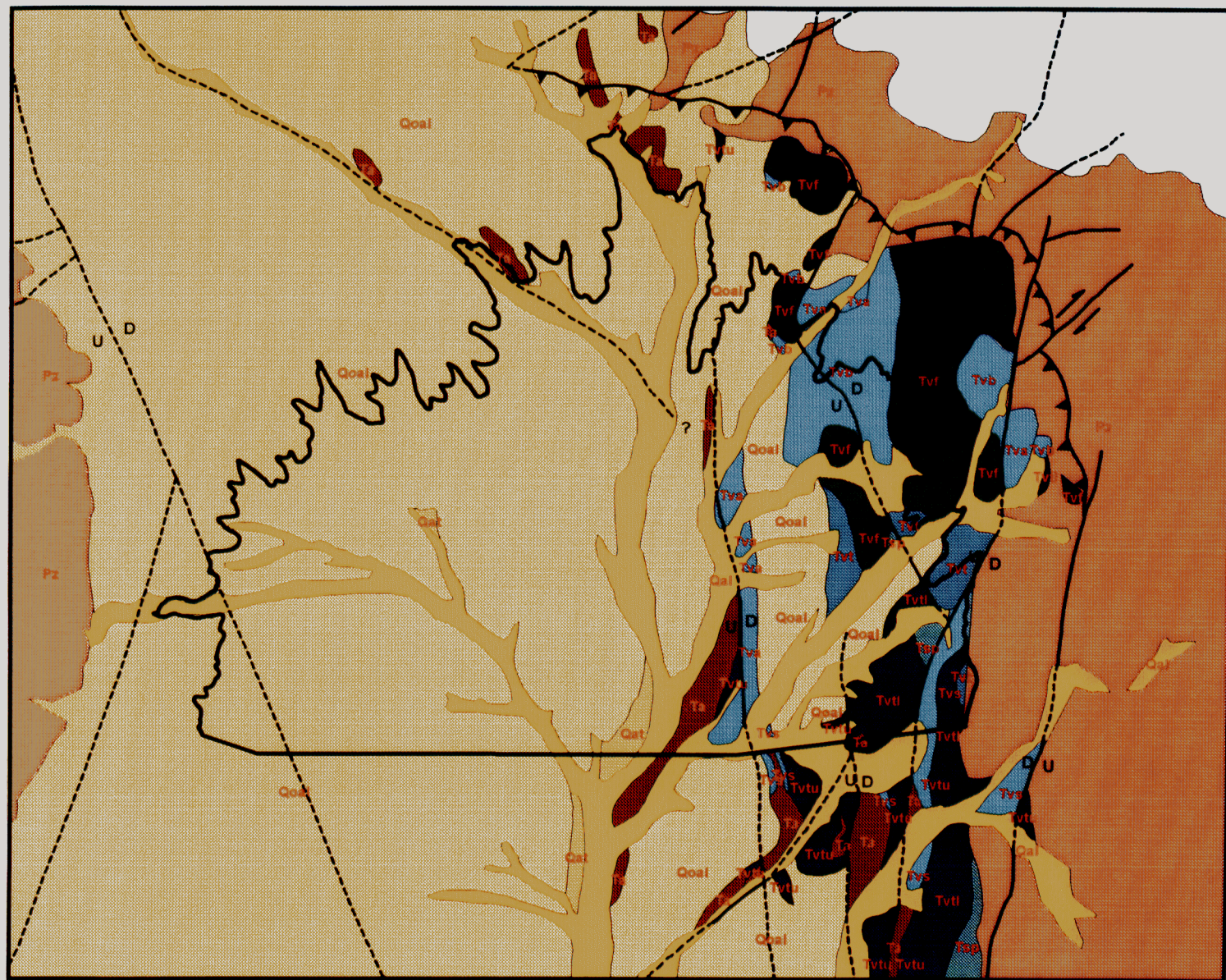
**Table 2-1. Stratigraphy, Lithology, and Average Thickness of Geologic Units**

Symbol	Lithologic Code	Thickness* (ft)	Age	Formation and Lithologic Description
Qal and Qoal	1	0-2,000+	Quaternary	Alluvium and older alluvium
Tvb	2	1,000+	Tertiary	Welded tuff (porphyritic rhyolite)
Tsp	3	1,000+	Tertiary	Sheep Pass Formation (conglomerate and limestone)
Tvf	2	na	Tertiary	Quartz rhyolite lava flows
Tvt	2	na	Tertiary	Unwelded tuff (rhyolite)
Tva	2	na	Tertiary	Ash and agglomerate
Pk	4	150-400	Permian	Kaibab Limestone
Pau Pal	5	1,500-1,600 (Pau) 1,200-1,500 (Pal)	Permian	Upper and lower members of Arcturus Formation (siltstone interbedded with limestone)
Prh	3	1,100-1,200	Permian	Rib Hill Sandstone (with interbedded limestone)
Prs	4	275-350	Permian	Riepe Spring Limestone of Steele
Pe	4	2,450-2,600	Permian	Ely Limestone (with interbedded sandstone)

*Note:* Information based on USGS geologic quadrangle maps for Ely area and on Welsh Engineering Inc. (1991); na = not available.

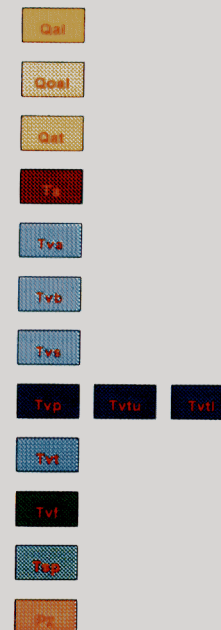
\* Thickness of Steptoe valley alluvium up to 11,000 ft near McGill (Frick 1985).





# LEGEND

- Inferred Normal Fault
- - - Concealed Normal Fault
- ▲ Thrust Fault (saw teeth on upper plate)



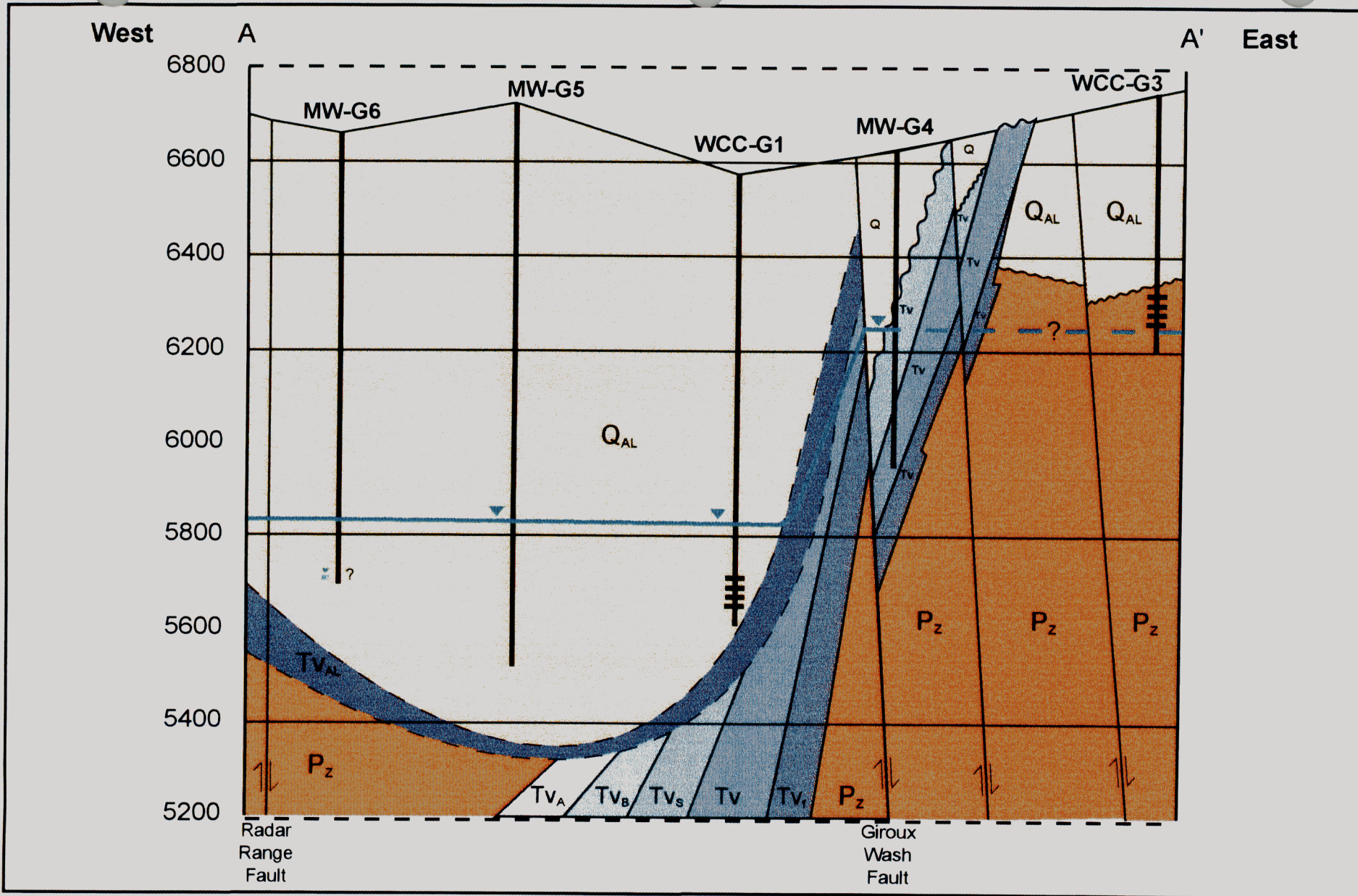
2000 0 2000 4000 Feet

Generation  
Date:  
8/4/97

Figure 2-1. Geologic Map of Giroux Wash Area.







Generation

Date:  
8/4/97

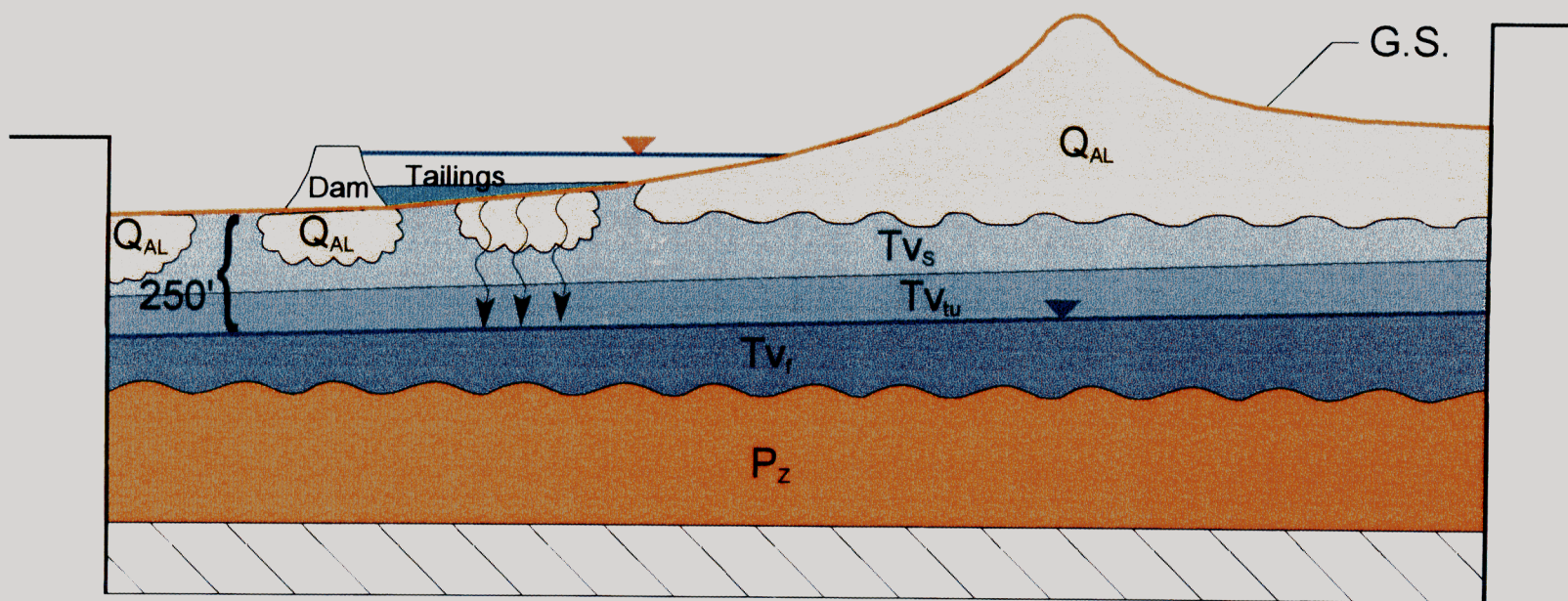
Figure 2-2. Geologic Cross-Section (East-West) Beneath Impoundment.



# Eastern Portion

South

North



Generation

Date:

8/4/97

Figure 2-3. Geologic Cross-Section (South-North) Beneath Impoundment.



Geomega

### **3. Hydrogeologic Description**

The hydrogeology of the Giroux Wash area has been included as part of various regional and local hydrogeologic investigations.

#### **3.1 Regional Hydrogeology**

A description of the regional hydrogeology documented in previous investigations (eg. PTI 1994) performed for the Robinson District is included in this section of the report.

The Giroux Wash area is located in the Carbonate-Rock hydrologic province of the Great Basin, as defined by Burbey and Prudic (1991), which covers approximately the eastern half of Nevada. Groundwater in this region occurs in two hydrologic regimes: alluvial sediments filling the basins or valleys between the high ranges, and Paleozoic rocks that are exposed within the mountain ranges and dip beneath the alluvial sediments of the basins.

Water moves from the mountain ranges by surface flow in streams, evaporation, plant transpiration and by subsurface flow through the aquifers. Groundwater through-put within the regional aquifers is controlled by localized hydraulic features that result from primary (rock matrix) and secondary diagenetic processes.

Water is lost from the basins by evaporation, plant transpiration, and by surface water flow via streams out of the basins. Water is also lost from the shallower alluvial aquifers to the deeper Paleozoic rock system by flow out of one region and into another. There is variable inter-basin hydrogeologic communication throughout the regional groundwater system.

In the study area, the main ridge of the Egan Range is believed to be a major divide, not only for surface water but also for the groundwater systems (Figure 1-1). On the west side of this divide (e.g., Jakes Valley, White River Valley), the regional flow is south toward the Colorado River Basin, whereas on the east side of the divide, the regional system flows northeast toward the Great Salt Desert.

Hydraulic heads are generally lower in the deeper Paleozoic rocks than in the overlying alluvial aquifers, indicating that the Robinson District is an area of groundwater recharge, which comes principally from precipitation in the mountain ranges (Thomas et al. 1986). Precipitation is strongly correlated to elevation, ranging from 6 inches/year in the valleys to more than 20 inches/year in the surrounding mountains. Snowmelt recharges the Paleozoic rocks directly, and surface flow down mountain streams reaches the alluvial valleys and descends into the coarse alluvium along the mountain fronts to recharge the alluvial aquifers. Direct rainfall also contributes to recharge in both aquifer systems.



The percentage of precipitation and runoff that reaches groundwater varies, from a regional average of 5% for the Paleozoic rocks (Burbey and Prudic 1991) to local values as high as 25% (5 inches/year) for the mountainous areas of White Pine County (Maxey and Eakin 1949). There is a net groundwater discharge in some valley-bottoms areas (e.g., Steptoe Valley near McGill) where evaporation and transpiration losses from shallow groundwater exceed annual precipitation rates (Bedinger et al. 1984).

### **3.2 Local Hydrogeology**

Primary aquifers in the Giroux Wash consist of the Paleozoic rocks and the Quaternary alluvial basin-fill deposits. These strata range widely across a broad spectrum of gross thickness, lithology, and hydraulic properties.

#### **3.2.1 Paleozoic Rocks**

Paleozoic bedrock aquifers can vary locally from unconfined or confined, depending on topography and degree of burial. At higher elevations where meteoric water recharges the systems, these aquifers are unconfined. In the basins (valleys) where the Paleozoic rocks dip below other strata, they act as confined aquifers.

Groundwater flux through the Paleozoic rock sequences is determined by localized hydraulic features within their gross thickness. Formation of conductive flow units is controlled by both primary and secondary hydraulic features including; fracture development, original matrix porosity, and secondary diagenetic features (both dissolution and mineralization). These primary and secondary geohydraulic features contribute to the average hydraulic conductivity of individual flow units within these rocks. Thickness of the preferential flow units determines their ability to transmit groundwater flow to adjacent hydrostratigraphic units. Hydraulic conductivity within these rock types varies over several orders of magnitude, depending on the formation of secondary features.

#### **3.2.2 Alluvial Aquifers**

Alluvial aquifers in the area are typically unconfined. Thickness of these strata varies depending on spatial positioning within the basin proper. At the edge of the valleys, the alluvial deposits are thinner than in the center of the basin; more than 1,000 feet of alluvial material was encountered in monitoring well WCC-G1, just south of the Giroux Wash Tailings Impoundment.

Hydraulic conductivity of these alluvial deposits varies several orders of magnitude. Higher conductivity is encountered near the center of the basins, as corroborated by aquifer testing in Steptoe Valley (PTI 1994). Besides location, particle size

distribution, degree of sorting, and amount of secondary alteration also determine the hydraulic conductivity of this hydrostratigraphic unit.

### **3.2.3 Fault Disruption of Aquifers**

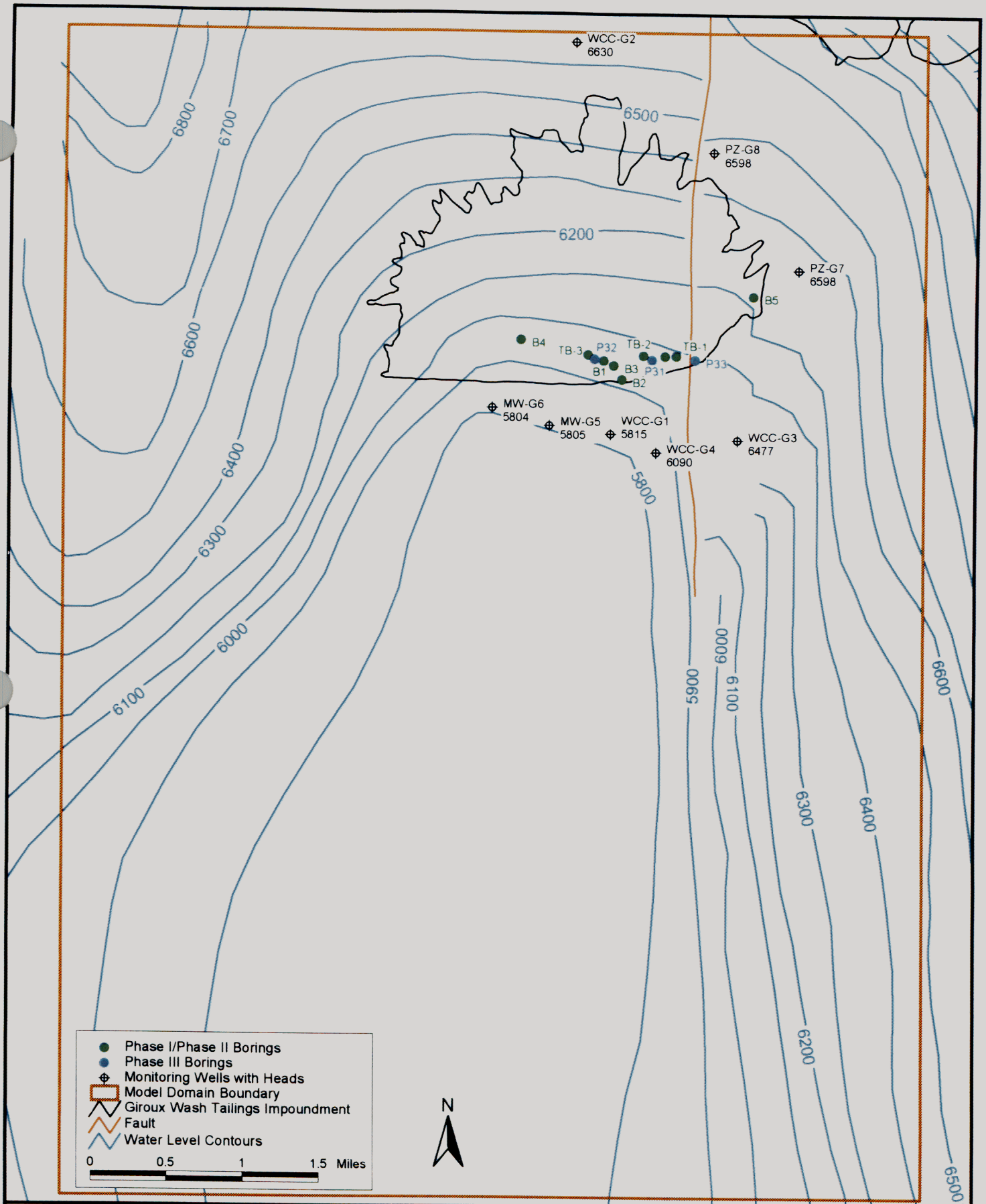
The north-trending faults that cross the tailings impoundment area and bound bedrock blocks form hydraulically significant barriers to groundwater flow. Either these faults act as flow barriers themselves, or movement along them has juxtaposed lower-conductivity volcanic rocks against higher-conductivity alluvial strata. There is more than 500 feet of head difference between monitoring wells WCC-G1 and WCC-G3. The latter is approximately 4,500 feet to the east of WCC-G1.

This faulting separates the groundwater system on the western part of the Giroux Wash impoundment from that of the eastern part. Outcropping strata in the western part are unconsolidated Quaternary alluvium, whereas those on the eastern part are Tertiary volcanic rocks and unconsolidated alluvial sediments.

### **3.3 Summary Description of Groundwater Occurrence and Movement**

On the west side of the Egan Range, groundwater and surface water generally flow south, toward the Colorado River Basin. Groundwater originating in the mountain ranges is encountered at or near the surface, and it flows toward the axis of the White River Valley as it makes its way south. Groundwater is encountered at greater depths in the basins. Figure 3-1 is a water table map for the study area; the map is based on the monitoring wells rimming the impoundment as well as USGS maps (Thomas et al. 1986). Heads are higher to the north, east, and west than in the White River Valley. Hydraulic gradients are typically steeper in the area surrounding the valley because of greater recharge and generally lower hydraulic conductivity. Gradients become flatter farther south and in the center of the valley. Hydraulic heads are usually lower in the deeper Paleozoic rocks; therefore, the shallower alluvial aquifers function as a source of groundwater recharge for the regional aquifers.

Groundwater in the Tertiary volcanic rocks on the east side of the Giroux Wash impoundment is first encountered at approximately 250 feet below ground surface (bgs), whereas groundwater in the Quaternary alluvium on the west side of the impoundment is encountered at approximately 750 feet bgs. A combination of normal faulting and variation in stratigraphy account for this hydraulic separation across the impoundment. Groundwater flow is southward from the tailings impoundment toward the axis of the White River Valley.



Generation  
Date:  
10/9/97

Figure 3-1. Approximate Water Table Map  
with Monitoring Well and Boring Locations.





## 4. Vadose Zone Flow and Solute Transport

The focus of this part of the study is to determine the analyte concentrations in water infiltrating from the tailings impoundment in Giroux Wash to the water table. The depth to groundwater varies between 250 feet on the eastern side to approximately 750 feet on the western side of the impoundment. Because of these distances and the concomitant long period of time needed for water to move from the impoundment to the water table, practical assessment of the infiltrating water requires that the infiltration be modeled.

### 4.1 Vadose Zone Description

In the western part of Giroux Wash, the unsaturated zone extends from the surface to a depth of approximately 750 feet bgs. In the eastern part of the wash, it extends to approximately 250 feet bgs. This variation in water levels is due to a fault running parallel to the axis of the wash, which acts as an east-west flow barrier. The material in the wash consists of tailings, Paleozoic limestone, Tertiary sandstone, and Quaternary alluvium (Figure 4-1).

#### 4.1.1 Tailings Material

The tailings material consists of fine-grained particles that currently cover the existing impoundment footprint to depths of  $\leq 50$  feet. The extent of the impoundment coverage changes during its life. Initially, the tailings were deposited along the impoundment embankment; additional areas north of the embankment will be covered during filling. The elevation to which the impoundment will fill can be expressed as a temporal empirical function (SRK 1997), i.e.,

$$E = 0.0259t + 6,695, \quad (4-1)$$

where

$E$  is the contour elevation and

$t$  is the time in days since January 1, 1996.

Hydraulically, the fine tailings have a relatively low saturated conductivity ( $1 \times 10^{-6}$  cm/s) and a saturated water content equivalent to the porosity (0.30; PTI 1994). These parameters were used to determine the infiltration rate from the saturated tailings (Section 4.4.1).

#### 4.1.2 Paleozoic Limestone

The Paleozoic limestone (part of map unit Pz; Figure 2-1) crops out along the extreme east and west edges of the wash. The limestone dips from both sides toward the center

of the wash, forming the "trough" below the other materials. Because of uplift of blocks along the series of north-trending faults (see Figure 2-2), the limestone is only 100 feet below the tailings impoundment at its eastern edge but is more than 1,000 feet below the impoundment in the middle and western parts of the wash.

Unsaturated flow through the limestone is limited by the relatively low saturated conductivity of the material ( $10^{-5}$  cm/s) and the low porosity (0.08) and residual water content (0.04) (WESTEC 1991, PTI 1994). The conductivity value reported here is probably representative of the effective porosity of the material where water flow is occurring primarily in fractures.

#### **4.1.3 Tertiary Sandstone**

The Tertiary sandstone (part of map unit Tvs; Figure 2-1) overlies the limestone across the breadth of the wash. Because of block faulting, the sandstone is as shallow as 10 feet beneath the ground surface on the east side of the wash, reaches a depth of >1,000 feet in the middle of the wash, and occurs at a depth of 200 feet on the western edge. The tailings impoundment does not cover the sandstone surface exposure, which occurs adjacent to the limestone exposure on the eastern edge of the wash.

Unsaturated flow through the sandstone is limited by the relatively low saturated conductivity ( $5 \times 10^{-5}$  cm/s), porosity (0.08), and residual water content (0.04) of the material (WESTEC 1991, PTI 1994). The conductivity value is probably representative of the effective porosity of the material, through which water flows primarily in fractures.

#### **4.1.4 Quaternary Alluvium**

The alluvium fill, the source of which is the adjacent ranges, is approximately 1,000 feet thick at its deepest point in the middle of the wash. All parts of the tailings impoundment are underlain by at least 10 feet of alluvium, and the alluvium reaches from the ground surface to the water table across most of the wash.

Most of the unsaturated flow in the wash occurs in the alluvium, which is more conductive (up to  $10^{-2}$  cm/s) and has greater porosity (0.25) and residual water content (0.07) compared to the bedrock (WESTEC 1991, PTI 1994). Assuming a saturated conductivity value of  $10^{-2}$  cm/s (28.5 feet/day) for the alluvium is a conservative estimate of the true conductivity, given the impermeable nature of the contained B-horizon layers (Geomega 1997b).

### **4.2 Infiltration Modeling**

Infiltration was modeled by using the numerical code HYDRUS\_2D (Simunek et al. 1996). HYDRUS\_2D is an updated version of SWMS\_2D, a well-documented and well-benchmarked U.S. Department of Agriculture computer code that uses a finite-

element approach to simulate groundwater flow and solute transport in the unsaturated zone. HYDRUS\_2D solves a finite-element analogue of well-established, governing flow and transport equations in two dimensions. HYDRUS\_2D outputs moisture profiles in the soil at time intervals designated by the user.

The partial differential equation for groundwater flow is Richards equation, a nonlinear partial differential equation based on mass conservation that models water flow in the unsaturated zone of the subsurface:

$$\frac{\partial}{\partial x} \left( K_{xx} \frac{\partial h}{\partial x} \right) + \frac{\partial}{\partial z} \left[ K_{zz} \left( \frac{\partial h}{\partial z} - 1 \right) \right] = S \frac{\partial h}{\partial t}, \quad (4-2)$$

where

$K_{xx}$  and  $K_{zz}$  are hydraulic conductivity values along the lateral ( $x$ ) and vertical ( $z$ ) axes [ $L/T$ ],

$h$  is the potentiometric head [ $L$ ],

$S$  is the specific storage of the porous material [ $L^{-1}$ ],

$t$  is time [ $T$ ].

The complexity of physical unsaturated zone flow systems makes modeling them with a tractable set of equations difficult. The computer-based, numerical approaches required to solve these equations add another level of complexity and often entail prohibitive run times. Therefore, to formulate a manageable model, assumptions and approximations that simplify the physical system were required. These assumptions include

- groundwater flow is laminar;
- groundwater is homogeneous, isothermal, and incompressible; and
- the physical parameters do not change with the system's state (e.g., porosity of the vadose zone will not vary with variation in unrelated parameters such as TDS).

These assumptions are reasonable for application to the unsaturated zone in Giroux Wash, as the flow rate is slow enough that turbulence is unlikely to occur and ambient climatic conditions do not alter the state of water in the subsurface (e.g., groundwater will not freeze and thaw at depth).

The partial differential equation for contaminant fate and transport modeling is the advective dispersion equation:

$$\frac{\partial}{\partial x} \left( D_{xx} \frac{\partial c}{\partial x} \right) + \frac{\partial}{\partial z} \left( D_{zz} \frac{\partial c}{\partial z} \right) - q_x \frac{\partial c}{\partial x} - q_z \frac{\partial c}{\partial z} - \lambda_w c - \frac{\lambda_s \rho_b K_d}{\theta} s = \frac{\partial c}{\partial t} + \frac{\rho_b K_d}{\theta} \frac{\partial s}{\partial t}, \quad (4-3)$$

where

$D_{xx}$  and  $D_{zz}$  are dispersion coefficients along the lateral ( $x$ ) and vertical ( $z$ ) axes,  
 $q_x$  and  $q_z$  are advective velocities of the groundwater along the lateral and vertical axes,  
 $\lambda_s$  and  $\lambda_w$  are the soil and groundwater decay rates of contaminants,  
 $\rho_b$  is the bulk density of the soil,  
 $K_d$  is the adsorption partitioning coefficient,  
 $\theta$  is the water content,  
 $c$  is the contaminant concentration in groundwater, and  
 $s$  is the contaminant concentration sorbed to the soil.

#### **4.3 Conditions Assumed in the Infiltration Model**

The Giroux Wash Tailings Impoundment model separates the wash into two zones: the region covered by the final tailings impoundment footprint and the region where no tailings will be deposited (Figure 4-2). The covered and uncovered regions allow very different volumes of water to infiltrate through their surfaces.

Infiltration in the uncovered region is dominated by the negative water balance at the site, which experiences a net evaporation of 48 inches/year. Thus, the limited precipitation (about 10 in/year) on the uncovered region is insufficient to wet the Giroux Wash subsurface and result in significant percolation downward several hundred feet to recharge the water table. For this reason the model assumes that there is no percolation through the uncovered region. This assumption is conservative because any percolation through this region would serve to dilute solute concentrations percolating through the region covered by the impoundment.

The region covered by tailings experiences the same evaporative effects; however, the tailings deposition in the form of a slurry provides adequate water to keep the water content of the tailings relatively high. In addition, the ponded water in the impoundment provides a driving force for percolation into the local subsurface that exceeds the evaporative force.

Given these facts, infiltration beyond the ambient recharge (if any) is assumed to occur only in the part of the wash covered by tailings. The percolation through the impoundment area takes place at differing rates depending on the conditions in the impoundment. As the impoundment began to fill, saturated tailings were disposed of immediately behind the impoundment dam while the northern area of the wash remained uncovered. As the area behind the dam filled with tailings, the extent of the saturated zone expanded northward. The tailings will eventually reach the maximum

elevation described by equation 4-1, which expresses the elevation of the tailings in the impoundment as a function of time in order to calculate the period that subsurface soils are in contact with saturated tailings. This model conservatively assumes that the entirety of the impoundment is covered for the operating lifetime of the impoundment.

Saturated tailings are assumed to transmit both moisture and solutes to the subsurface soils from the time the tailings cover the soil until they reach the water table. During this time, the tailings are assumed to remain saturated by tailings solution with constant solute concentrations. Following closure, the water source for the tailings is removed, and the water in the tailings drains down into the subsurface or evaporates because of the ambient precipitation and evaporation conditions. The solute concentrations in the drain-down water are assumed to equal those of the tailings solution. Recharging precipitation entering the top surface of the impoundment is assumed to have solute concentrations equivalent to background groundwater.

Mathematically, the relationship between the concentration of solutes and their advection and dispersion is termed "linear" (equation 4-3). This relationship means that an increase in the initial concentration of a given solute will result in a proportional increase in the predicted concentration of that solute when the infiltrating water reaches the water table. For example, if equation 4-3 predicts that an initial tailings solution concentration of 100 mg/L will be reduced during infiltration to 25 mg/L at the level of the water table, then an initial concentration of 1,000 mg/L would result in a predicted concentration of 250 mg/L (i.e., both the input and predicted result are scaled by the same factor of 10). Therefore, model predictions for the investigated range of initial solute concentrations can be determined from the results presented here (Appendix B) by proportionally rescaling the input and predicted concentrations.

On the basis of data from bore holes, water flow in the Giroux Wash unsaturated zone is assumed to be primarily vertical for the purpose of modeling. In the infiltration model, the water flow occurs in two-dimensional, east-west cross sections of the valley. In actuality, the trough-shaped body of alluvium filling the valley probably contains lateral unsaturated groundwater flow moving toward the center of the trough because of the contact between the permeable alluvium and the less permeable bedrock. In the north-south direction, the contact slopes comparatively slightly (<2%; WESTEC 1991).

#### **4.4 Model Parameters**

The parameters to be assigned to conduct the vadose zone model are recharge rate, hydraulic properties, solute transport properties, and depth to groundwater. (see Table 4-1). Conservative estimates of parameter values were employed when direct measurements were unavailable, and a sensitivity analysis was conducted on the model (Section 4.5)

#### 4.4.1 Recharge Rate

Recharge to groundwater from the impoundment area is due to infiltration of tailings solution and precipitation, tempered by evaporation. A conservative estimate of net recharge (0.008 feet/day) was based on a value double the maximum observed rate (0.004 feet/day). This assumed infiltration rate is in good agreement with the rate conservatively estimated from the hydraulic conductivity of the tailings ( $10^{-6}$  cm/s) (PTI 1994), the hydraulic head (5 feet) expected in the tailings pond (SRK 1997), and the annual precipitation and evaporation expected in the impoundment (SRK 1997). The 5 feet corresponds to the average head occurring when the supernatant pond is lying directly over a segment of the impoundment. This hydraulic head is applied across the entire impoundment area resulting in an overestimate of seepage from the areas not beneath the supernatant pond where a hydraulic head of 1 foot was estimated (SRK 1997). The rate of advance of the seepage front,  $q$ , from tailings solution infiltration is calculated by

$$q = K_{\text{sat}} H = 2.76 \times 10^{-3} \text{ feet / day} \times 5 = 1.38 \times 10^{-2} \text{ feet / day}, \quad (4-4)$$

where

$K_{\text{sat}}$  is saturated permeability and

$H$  is average head.

The net evaporation rate,  $E_n$ , is  $1.1 \times 10^{-2}$  feet/day at the surface of the impoundment. However, using the evaporation rate defined at the surface of the tailings overestimates the rate of evaporation at depth within the tailings. Assuming that evaporation rate linearly decreases from a maximum at the surface of the tailings to zero at a depth of 10 feet (Maurer 1996), the average evaporation rate in the tailings is approximately  $6 \times 10^{-3}$  feet/day. Hence, the infiltration rate,  $I$ , will be approximately 0.0078 feet/day. This infiltration rate is approximately double the rate used in the previous modeling effort (PTI 1994) and agrees well with the rate assumed for this investigation.

Following the closure of the impoundment, the model assumes a recharge rate of  $6.6 \times 10^{-4}$  feet/day, which is consistent with the assumed recharge of the saturated zone model (see Section 5). This assumption is conservative given the negative water balance of the area and the relatively low permeability of the tailings and B-horizon soils that limit infiltration. Hydrogeologic evaluations of the possibility of recharge to deep aquifers in other areas of Nevada have concluded that there is actually extremely limited recharge to deep groundwater through valley-floor alluvium (Zones 1961).

#### 4.4.2 Hydraulic Properties of the Wash Materials

Hydraulic properties (e.g., saturated conductivity, porosity, and residual water content) of the alluvium, sandstone, and limestone were determined from the

geotechnical study performed for construction of the impoundment (WESTEC 1991, PTI 1994) (Table 4-1). The unsaturated model requires selection of van Genuchten curve-fitting parameters to define the conductivity of the materials as a function their water content (Table 4-1). The curve-fitting parameters were inferred from the saturated conductivity values by using parameter values reported in the literature for materials with similar conductivities.

For the modeling purposes, flow in the sandstone and limestone bedrock units was treated as flow in porous media rather than fracture-controlled flow. The hydraulic parameter values used for these units represent the effective properties of the media.

#### *4.4.3 Solute Transport Properties*

Solute transport parameters used in the model were obtained from site-specific field observations and conservative estimates of the unsaturated zone properties (Table 4-2).

Solute adsorption and precipitation were observed during the field TDS mobility study (Geomega 1997a). During the study, the solute front in the bore hole samples taken from the impoundment embankment infiltrated approximately half the distance of the wetting front. This result corresponds to a retardation factor of  $R = 2$  and a sorption partitioning coefficient of  $K_d = 0.16$ . In addition, material recovered from the subsurface showed evidence of calcite precipitation on soil grains. Calcium accounts for approximately 27% of the TDS present in the tailings solution, which is supersaturated with respect to calcite. Therefore, TDS concentrations will probably be reduced in the subsurface owing to precipitation of calcite and other minerals from solution.

Despite the above results, the modeled transport of solutes in the Giroux Wash unsaturated zone assumed that the solutes do not participate in any chemical reactions. This solute transport assumption represents a conservative evaluation of the transport mechanisms in the subsurface (e.g., transport without solute retardation or reaction).

The rate of diffusion and dispersion of solutes through the Giroux Wash subsurface was taken to be 20 cm<sup>2</sup>/day in the alluvium and 10 cm<sup>2</sup>/day in the bedrock. These values were based on the upper bound of typical dispersion rates in permeable and impermeable soil materials (Jury et al. 1991). The dispersion values used were reported literature values (Jury et al. 1991) and were realistic for application to the Giroux Wash subsurface according to the geotechnical properties of the subsurface material. Jury et al. reported the range of dispersion values to be between 5 and 20 cm<sup>2</sup>/day for various soil types.

#### **4.4.4 Depth to Groundwater**

The depth to groundwater was determined from the steady-state conditions in the wash prior to infiltration through the impoundment (Figure 4-1). The depth to groundwater beneath the impoundment varies: the maximum depth of 750 feet occurs under the west side of the impoundment, and the minimum depth of 250 feet occurs under the east side. The water table is simulated in the model by fixing the head in the finite elements located at that depth to zero.

#### **4.5 Model Discretization**

Numerical discretization divided the Giroux Wash impoundment into 50,694 finite elements.

- Each of 14 horizontal layers (rows) was divided into 51 slices (along the east-west direction) and 71 columns (along the north-south direction).
- Each slice and each column were 200 feet wide. They formed a grid of 200 foot  $\times$  200 foot squares that was coincident with the impoundment area (Figure 4-2).
- In the vertical dimension (Figure 4-3), a slice through the subsurface was discretized into 14 rows of unequal thickness as well as the 71 uniform-width columns. The rows near the top of the model domain are thinner than those at depth. The spacing of the rows increases with depth to a maximum of 75 feet at the water table.

The top of the model domain represents the surface of the tailings impoundment. In map view, each of the 200 foot  $\times$  200 foot two-dimensional squares in each row correlates with a corresponding three-dimensional cell in the groundwater flow model. Thus it is possible to accurately predict the wetting and solute fronts as they move downward from element to element, i.e., from the vadose zone into the water table.

Each model element is assigned hydraulic and transport properties based on the subsurface material found at that element's location. The discretized subsurface geology of Giroux Wash (Figure 4-4) features alluvium throughout most of the model domain on the west side and volcanic rocks on the east side with Paleozoic sedimentary rock on the edges.

#### **4.6 Initial Conditions**

The initial conditions for the unsaturated zone model were designed to approximate the conditions in Giroux Wash prior to the disposal of tailings (i.e., the pre-1996



conditions). The modeled subsurface material has a residual moisture content consistent with a chemical composition identical to background groundwater.

#### **4.7 Boundary Conditions**

The bottom boundary condition of the unsaturated zone model fixes the hydraulic head of those elements to zero to represent the saturated condition at the water table.

The surface boundary condition is a variable flux condition that accounts for seepage from the impoundment during its operation, followed by a period of drain down and drying after closure during which the infiltration rate decreases.

The side boundaries of the model domain are free drainage boundaries that would allow water and solutes to move through the sides of the model domain if flow were to extend laterally to that distance. However, the side boundaries were taken sufficiently far from the flow areas that flow and solute transport do not reach the boundaries, and so the choice of boundary conditions for the lateral boundaries was inconsequential.

#### **4.8 Model Results: Rates of Infiltration and Solute Transport**

The model predictions conserved mass for both the water and the solutes in the Giroux Wash unsaturated zones. Both the water mass balance and the solute mass balance had errors of less than 1%.

Initially, solutes are transported downward from the surface at a relatively rapid rate under the driving force of the ponded tailings solution. Under these conditions, the solute front propagates approximately 231 feet during the 16 years of impoundment operation (Figures 4-5 through 4-7). The movement rate of the solute front decreases gradually over the next 20 years after closure of the impoundment while the tailings drain under the influence of gravity and ambient precipitation and evaporation without constant recharge by additional tailings solution. After the impoundment drains, the solute front propagates relatively slowly, as the sole remaining driving forces are

- the limited infiltration of precipitation under ambient conditions and
- dispersion, which has a significant impact on solute mobility at this low advective velocity.

The solute concentrations reaching the water table range up to 33% of the original concentration in the tailings solution. This maximum concentration is predicted in the shallower water table on the eastern part of the impoundment. The solutes are completely flushed from the subsurface by precipitation recharge and dispersion after approximately 550 years (Figure 4-8). Infiltration is fastest in the alluvium-filled part

of the wash, especially near the contact between alluvium and bedrock where water preferentially flows in the more permeable alluvium (Figure 4-9). However, the predicted infiltration reaches groundwater in the bedrock on the east side of the impoundment sooner because the groundwater in that area more than 500 feet closer to the surface.

Solute transport takes place at comparable speeds in the bedrock (e.g., the volcanic rock in the eastern part of the area) and alluvium. The lower porosity of the bedrock units allows solute transport at a rate comparable to that in the alluvium, as advective velocity is inversely proportional to porosity, i.e.,

$$q_a = \frac{i}{\phi}, \quad (4-5)$$

where

$q_a$  is the advective velocity,

$i$  is the flow velocity, and

$\phi$  is the porosity.

The maximum solute concentration reaches the water table in the bedrock on the east side of the impoundment because of the shallower depth to groundwater in that area.

#### **4.9 Sensitivity Analysis**

Conservative parameter values were assumed when site-specific data were not available for the entirety of the model domain. Many of these assumptions (alluvial saturated conductivity, chemical adsorption, chemical reactivity, etc.) represent the conservative bound of appropriate parameter choices, indicating that any sensitivity evaluation of these parameters would result in a prediction of less solute transport to the water table.

The conservative chemical transport assumptions made in the model (e.g., no reaction, no solute retardation) cause the predicted solute concentrations in the vadose zone to be relatively insensitive to changes in the model because in each simulation, the entire mass of the solute is transported from the impoundment to the water table. Hence, resulting solute concentrations in the groundwater are more dependent on the rate of flow through the vadose zone (i.e., a greater volume of solute is added to the groundwater by virtue of a faster flow rate rather than higher solute concentrations). Sensitivity analysis was performed by using the low-end (5 cm<sup>2</sup>/day) dispersion value. Model results were insensitive to variation in dispersion compared to variation in recharge rate and retardation.

For the western part of the impoundment, solute breakthrough took approximately 25 years longer with the lower dispersion value, and transport of solutes from the subsurface (total flushing) was completed approximately 50 years sooner than with the initially modeled dispersion rate (Section 4.4.3). The maximum solute concentrations reaching the groundwater were equivalent for both dispersion values; the peak concentration (8% of the initial concentration) persisted approximately 25 years longer for the lower dispersion value (137 years as opposed to 112 years).

For the eastern part of the impoundment, solute breakthrough and flushing occurred at the same time for both dispersion cases. The maximum solute concentration reaching the water table increases in the prediction using the lower dispersion, from 33% of the initial concentration to 34%. In the eastern part of the impoundment, dispersion is a less important transport mechanism because solute transport to the shallower groundwater is driven by advective flow during the operating life of the tailings impoundment. The advective flow caused by the operating impoundment is not rapid enough to cause percolation to the deeper groundwater under the western part of the impoundment during the same time span. Dispersion becomes a more important mechanism when advective flow is slower (e.g., for the deeper groundwater in the western part of the impoundment) and is therefore relatively unimportant as a result of the low concentrations being predicted in the western part of the study area.

Overall, the most important parameter in predicting transport is the recharge rate (Section 4.4.1). The recharge rates (both during operation and after closure) were doubled to determine model sensitivity to this parameter. Transport from doubling the recharge rate resulted in an approximately twofold increase in predicted transport speed but only a slight increase in predicted solute concentrations (Figure 4-10). Conversely, when the modeled operating recharge rate was retained and the postclosure recharge rate was reduced to zero, as suggested by Zones (1961), predicted infiltration in the impoundment area was insufficient to transport solutes to the water table.

To quantify the variability in predicted solute concentration due to variation in recharge rate, modeled recharge to groundwater was increased by 50%. This increased rate was the maximum recharge that would allow model convergence when the calibrated saturated hydraulic conductivity values were used. Predicted solute concentrations in the vadose zone did not vary significantly; however, the rate at which these concentrations mixed with background groundwater increased 50% because the hydraulic conductivity of the vadose zone was sufficiently high to transmit the increased recharge. In the saturated zone, this increase in recharge resulted primarily in a rise in the level of the water table (approximately 11 feet on average), whereas the flow rates increased only slightly owing to the low conductivity of the bedrock underlying the eastern part of the wash. Groundwater flow rates in the impoundment area increased by an average of 7%, and there was an average 49% increase in the volume of water in the model cells located at the water table. Hence, the mass of solute entering the water table from the vadose zone was increased by

50% for the sensitivity analysis, while the volume of background groundwater that mass mixes with was increased by only 49%. In addition, the rate at which additional background groundwater entered the mixing zone was increased by 7%, resulting in a minor (0.7%) increase in the predicted solute concentrations.

Wetter climates during operation would have minimal effect because the water retained in the impoundment is controlled by operations. Following closure, wetter climates in the Giroux Wash area would possibly increase the flushing of solutes through the vadose zone via increased recharge, but increased recharge will also contribute additional native recharge, resulting in further hydrodynamic mixing of solute with background groundwater. The net effect on solute concentrations in the subsurface is predicted to be minimal. Drier climates would result in decreased recharge and possibly lower solute concentrations than were predicted by the model.

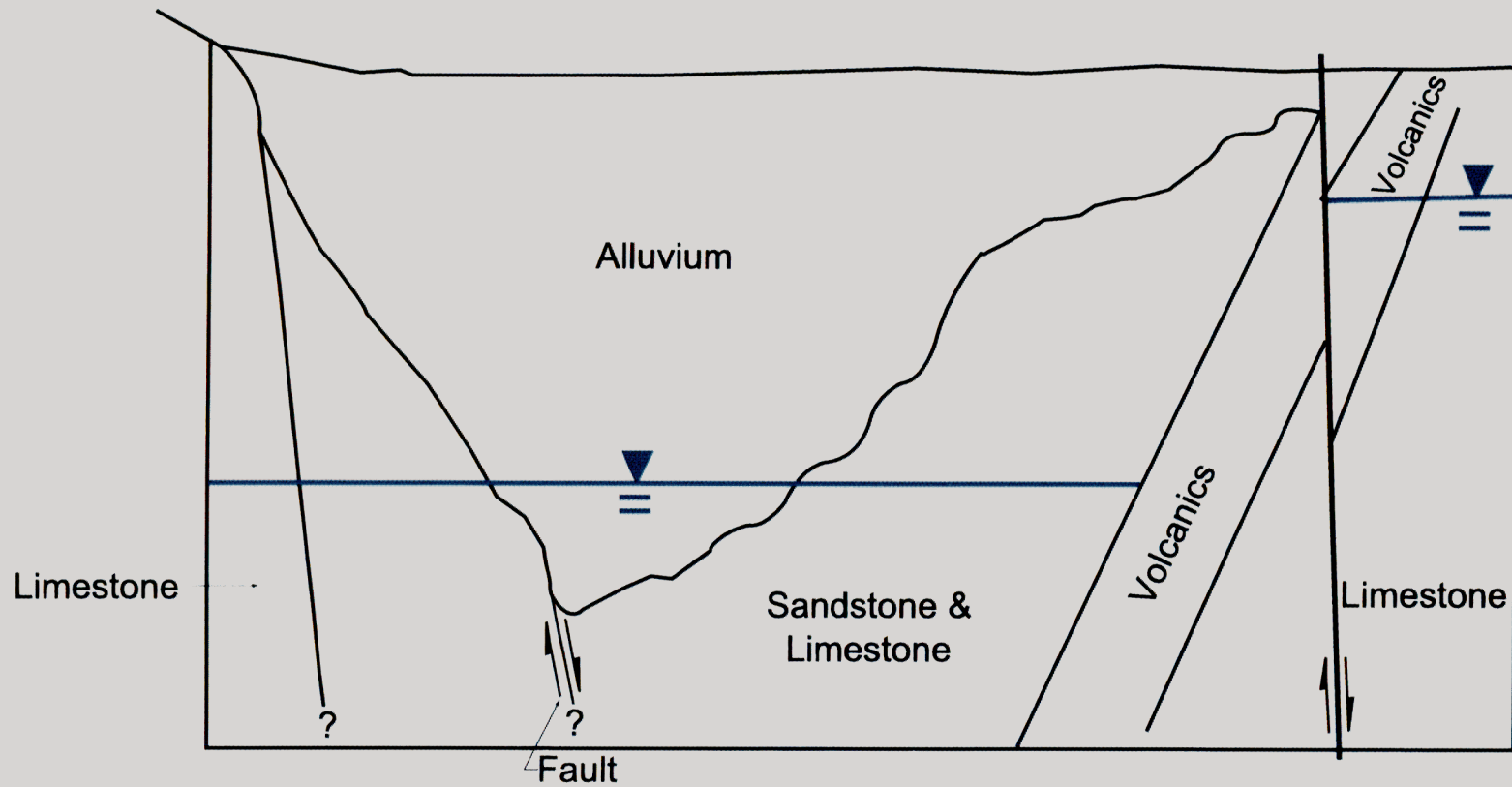
**Table 4-1. Hydraulic Parameters for the Unsaturated-Zone Model**

Parameter	Value	Reference
RECHARGE THROUGH SURFACE OF NATIVE SOILS		
Operating Rate	$7.6 \times 10^{-3}$ ft/day	see Section 2.4.1
Postclosure Rate	$6.6 \times 10^{-4}$ ft/day	saturated-zone model (Section 5)
ALLUVIAL HYDRAULIC PARAMETERS		
Saturated Hydraulic	28.5 ft/day	WESTEC (1991)
Porosity	0.25 $\text{cm}^3/\text{cm}^3$	PTI (1994)
Residual Water Content	0.07 $\text{cm}^3/\text{cm}^3$	PTI (1994)
van Genuchten $\alpha$	0.02 $\text{cm}^{-1}$	Simunek (1996)
van Genuchten $n$	1.41	Simunek (1996)
SANDSTONE HYDRAULIC PARAMETERS		
Saturated Hydraulic	0.014 ft/day	PTI (1994)
Porosity	0.08 $\text{cm}^3/\text{cm}^3$	PTI (1994)
Residual Water Content	0.04 $\text{cm}^3/\text{cm}^3$	PTI (1994)
van Genuchten $\alpha$	0.005 $\text{cm}^{-1}$	Simunek (1996)
van Genuchten $n$	1.09	Simunek (1996)
LIMESTONE HYDRAULIC PARAMETERS		
Saturated Hydraulic	0.014 ft/day	PTI (1994)
Porosity	0.08 $\text{cm}^3/\text{cm}^3$	PTI (1994)
Residual Water Content	0.04 $\text{cm}^3/\text{cm}^3$	PTI (1994)
van Genuchten $\alpha$	0.005 $\text{cm}^{-1}$	Simunek (1996)
van Genuchten $n$	1.09	Simunek (1996)

**Table 4-2. Solute Transport Parameters**

Parameter	Value	Reference
<b>ALLUVIUM</b>		
Bulk Density	1.6 g/cm <sup>3</sup>	WESTEC (1991)
Diffusion Coefficient	20 cm <sup>2</sup> /day	Jury et al. (1991)
Dispersion	20 cm <sup>2</sup> /day	Jury et al. (1991)
Partition Coefficient ( $K_d$ value)	0 L/kg	conservative assumption*
Reactivity	none	conservative assumption*
<b>SANDSTONE</b>		
Bulk Density	2.2 g/cm <sup>3</sup>	WESTEC (1991)
Diffusion Coefficient	10 cm <sup>2</sup> /day	Jury et al. (1991)
Dispersion	10 cm <sup>2</sup> /day	Jury et al. (1991)
Partition Coefficient ( $K_d$ value)	0 L/kg	conservative assumption*
Reactivity	none	conservative assumption*
<b>LIMESTONE</b>		
Bulk Density	2.3 g/cm <sup>3</sup>	WESTEC (1991)
Diffusion Coefficient	10 cm <sup>2</sup> /day	Jury et al. (1991)
Dispersion	10 cm <sup>2</sup> /day	Jury et al. (1991)
Partition Coefficient ( $K_d$ value)	0 L/kg	conservative assumption*
Reactivity	none	conservative assumption*

\* See Section 2.4.3.

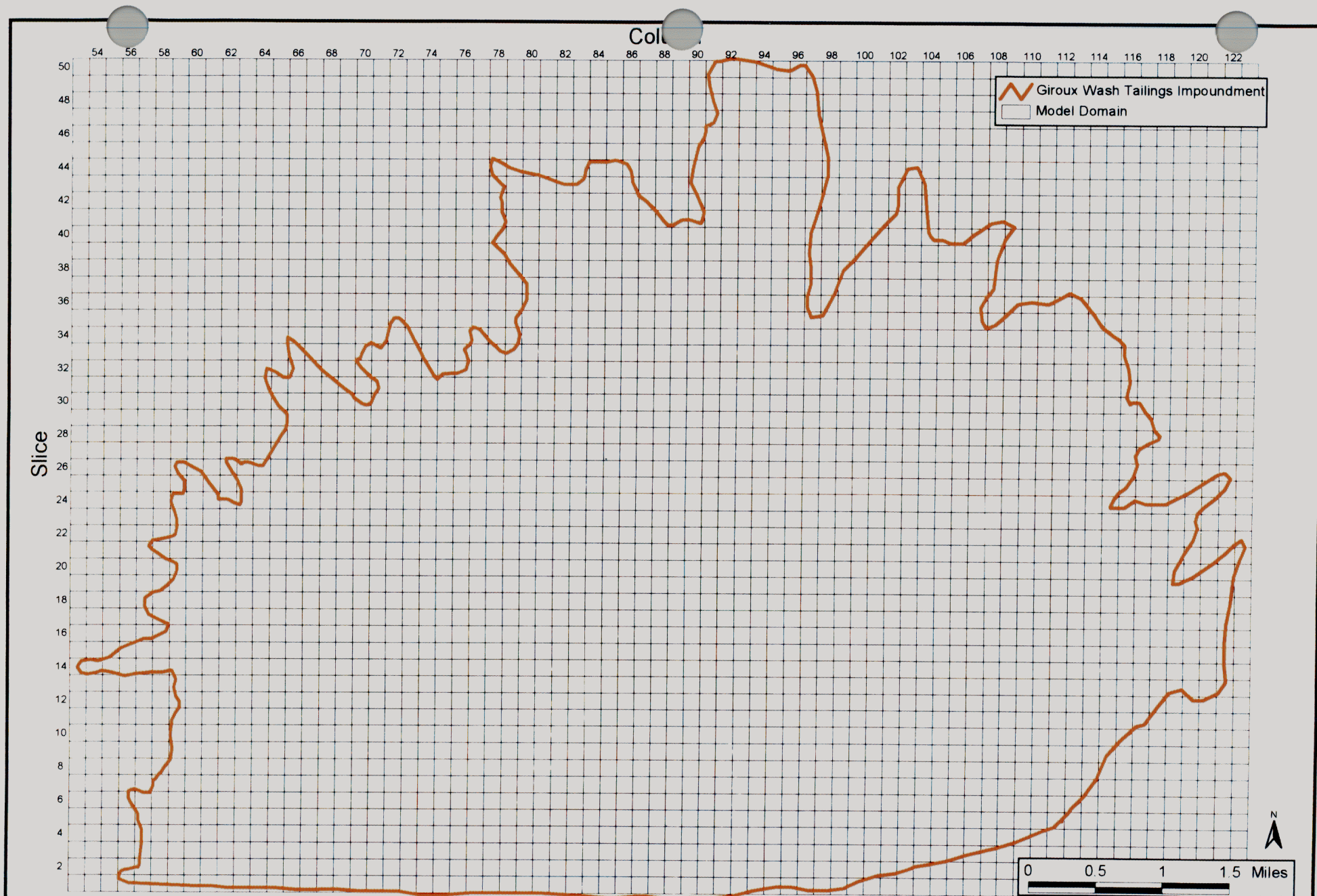


Generation  
Date:  
7/31/97

Figure 4-1. Cross-Section of the Giroux Wash Vadose Zone.



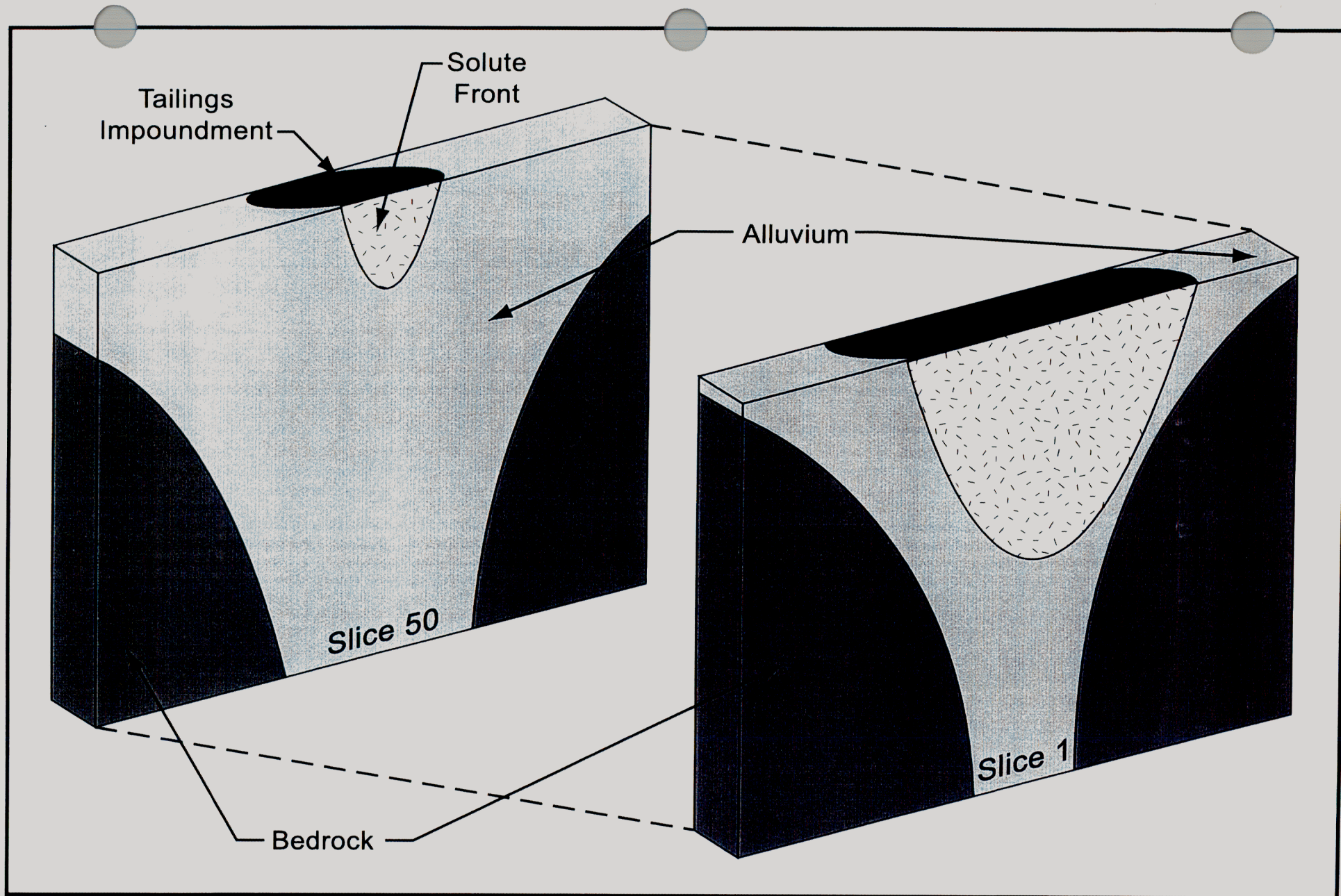




Generation  
Date:  
8/4/97

Figure 4-2. Plan View of Unsaturated Zone Model Domain  
(200' x 200' Squares).



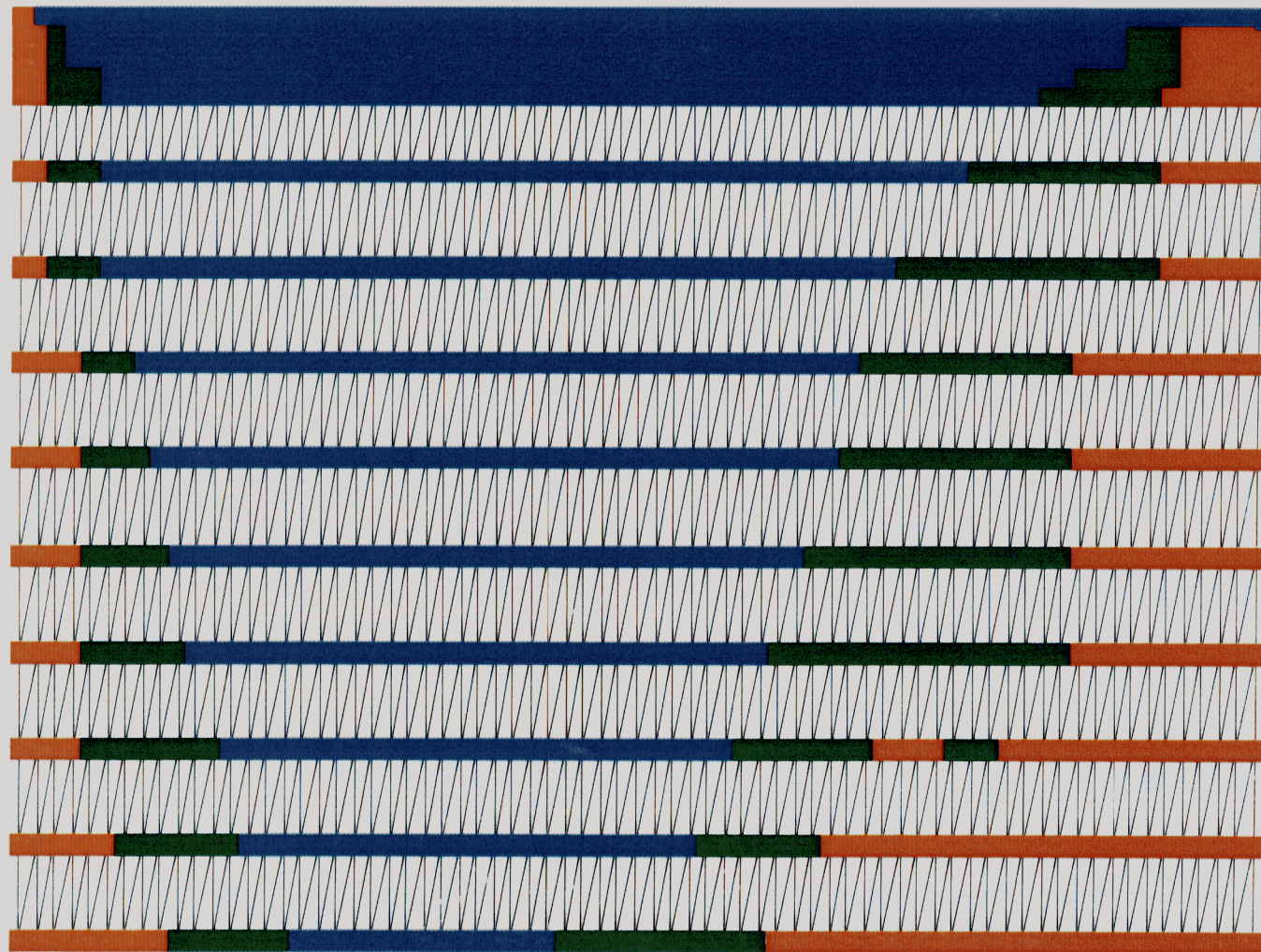


Generation  
Date:  
7/31/97

Figure 4-3. Conceptual Vadose Zone Model.

  
**Geomega**



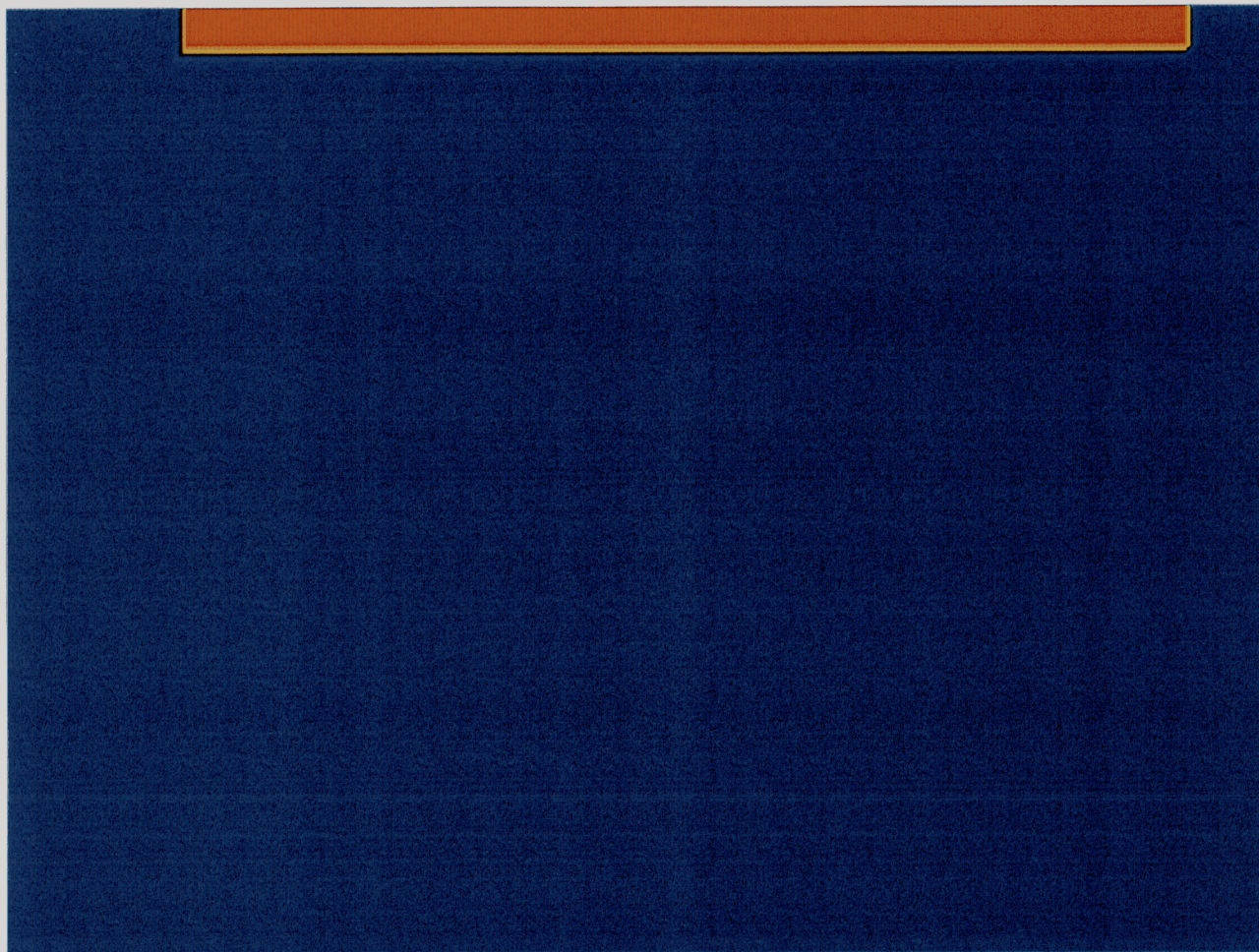


Generation  
Date:  
7/31/97

Figure 4-4. Model Domain Cross-Section  
(Vertical Exaggeration 1:0.075).

  
Geomega



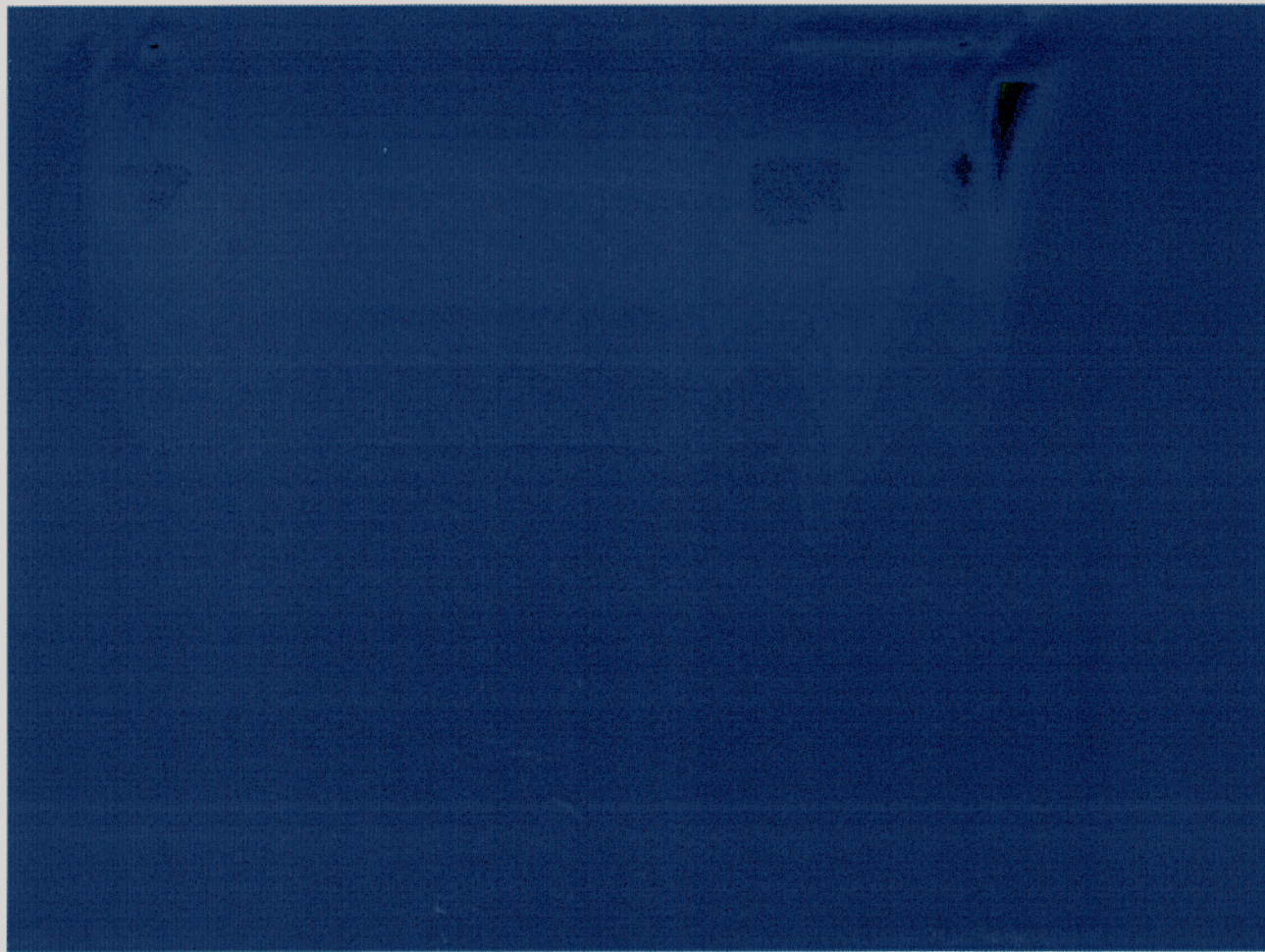


Generation  
Date:  
7/31/97

Figure 4-5. Solute Concentration at  $t = 0$   
(Vertical Exaggeration 1:0.075).

  
**Geomega**



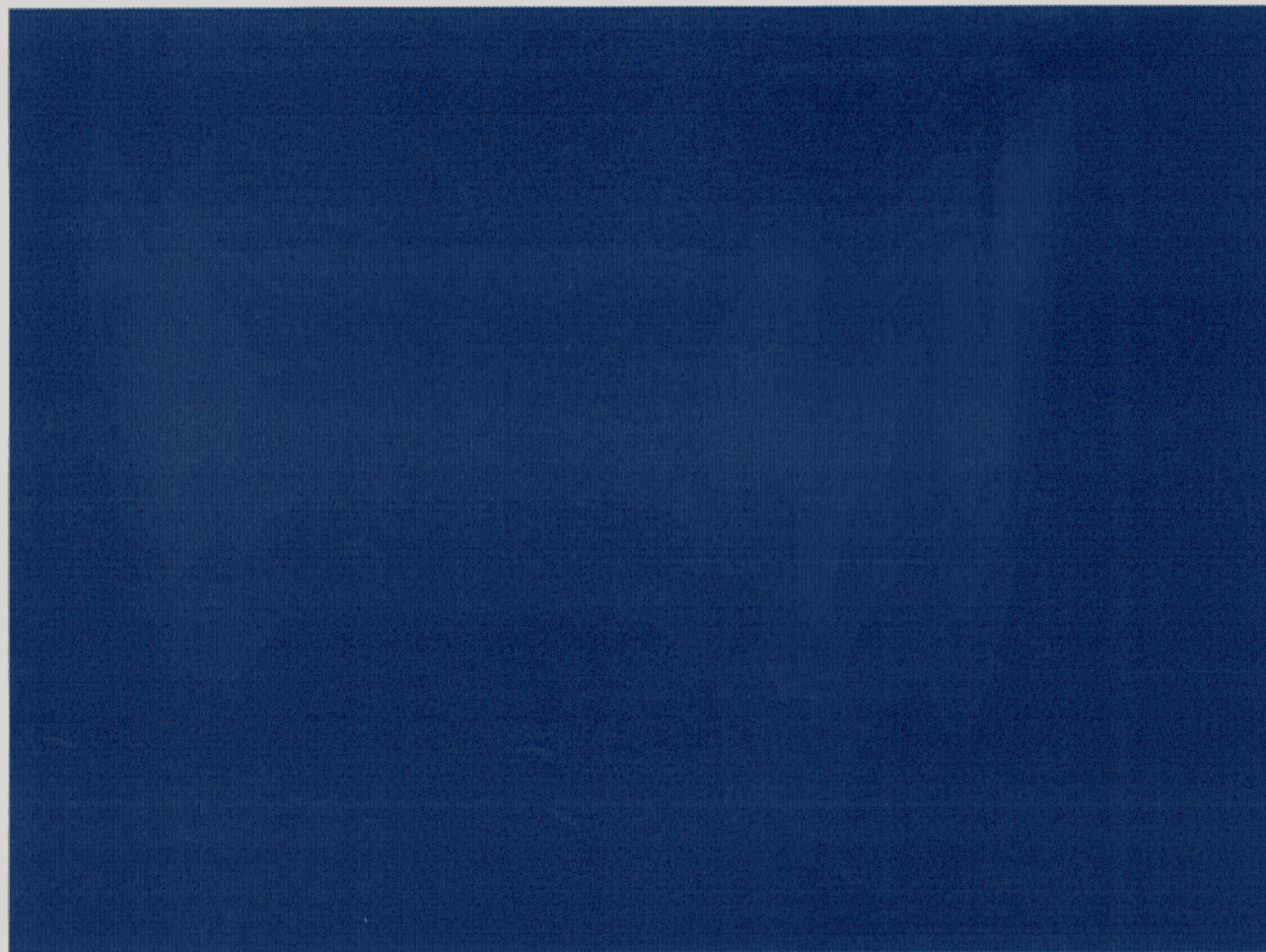


Generation  
Date:  
7/31/97

Figure 4-6. Solute Concentration at  $t = 16$  Years  
(Vertical Exaggeration 1:0.075).

  
**Geomega**

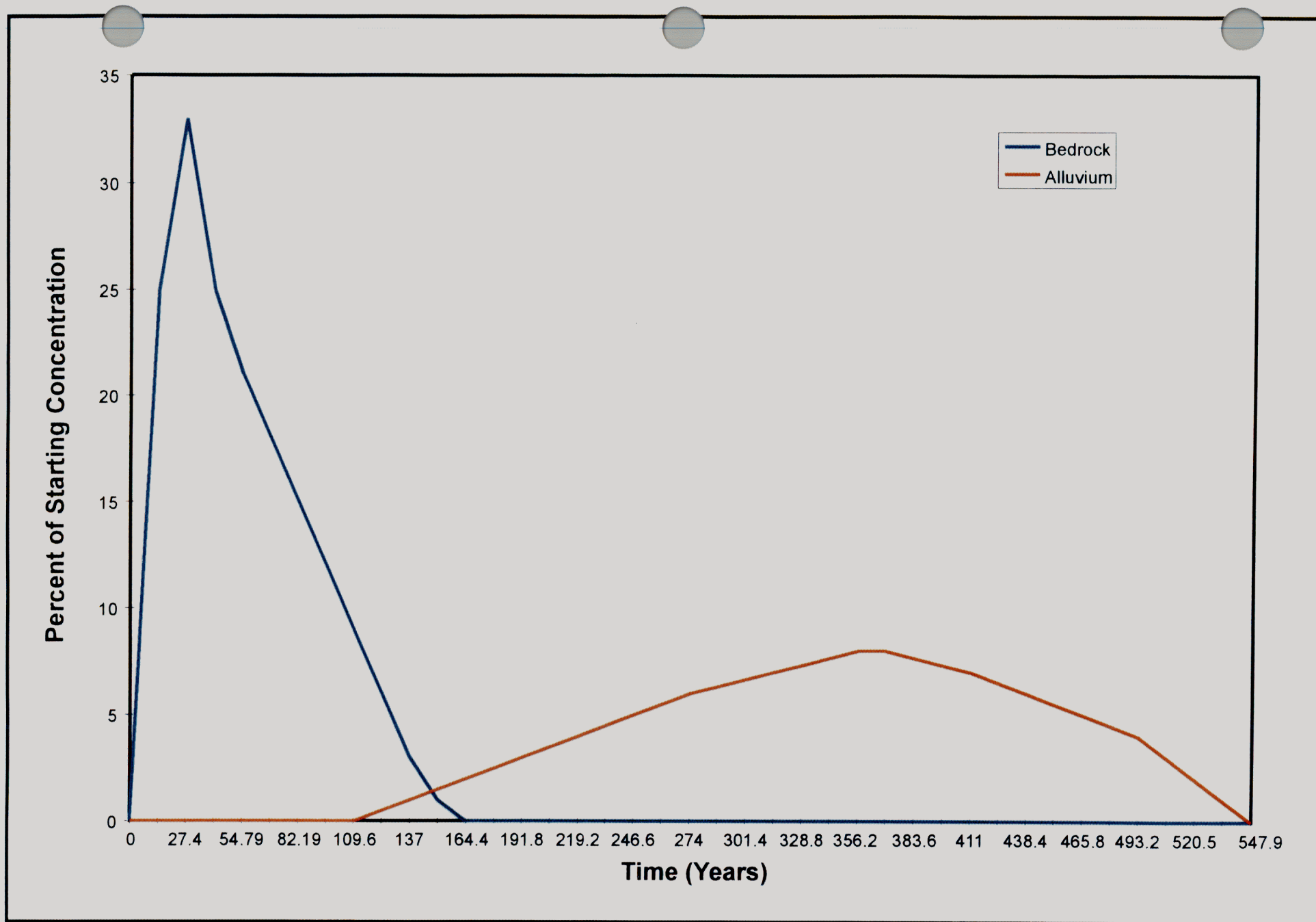




Generation  
Date:  
7/31/97

Figure 4-7. Solute Concentration at  $t = 100$  Years  
(Vertical Exaggeration 1:0.075).

  
**Geomega**

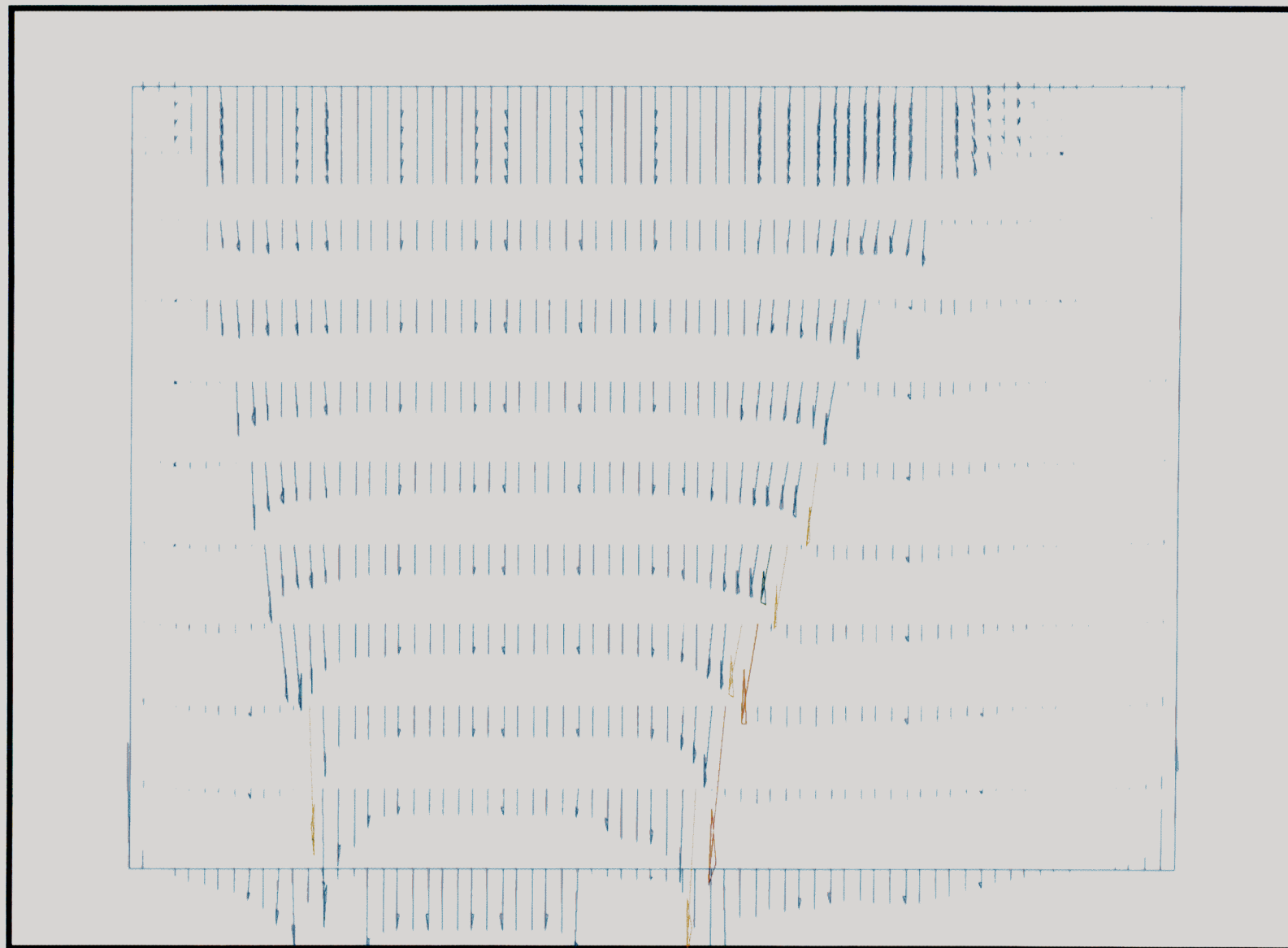


Generation  
Date:  
7/31/97

Figure 4-8. Solute Discharge to Groundwater.



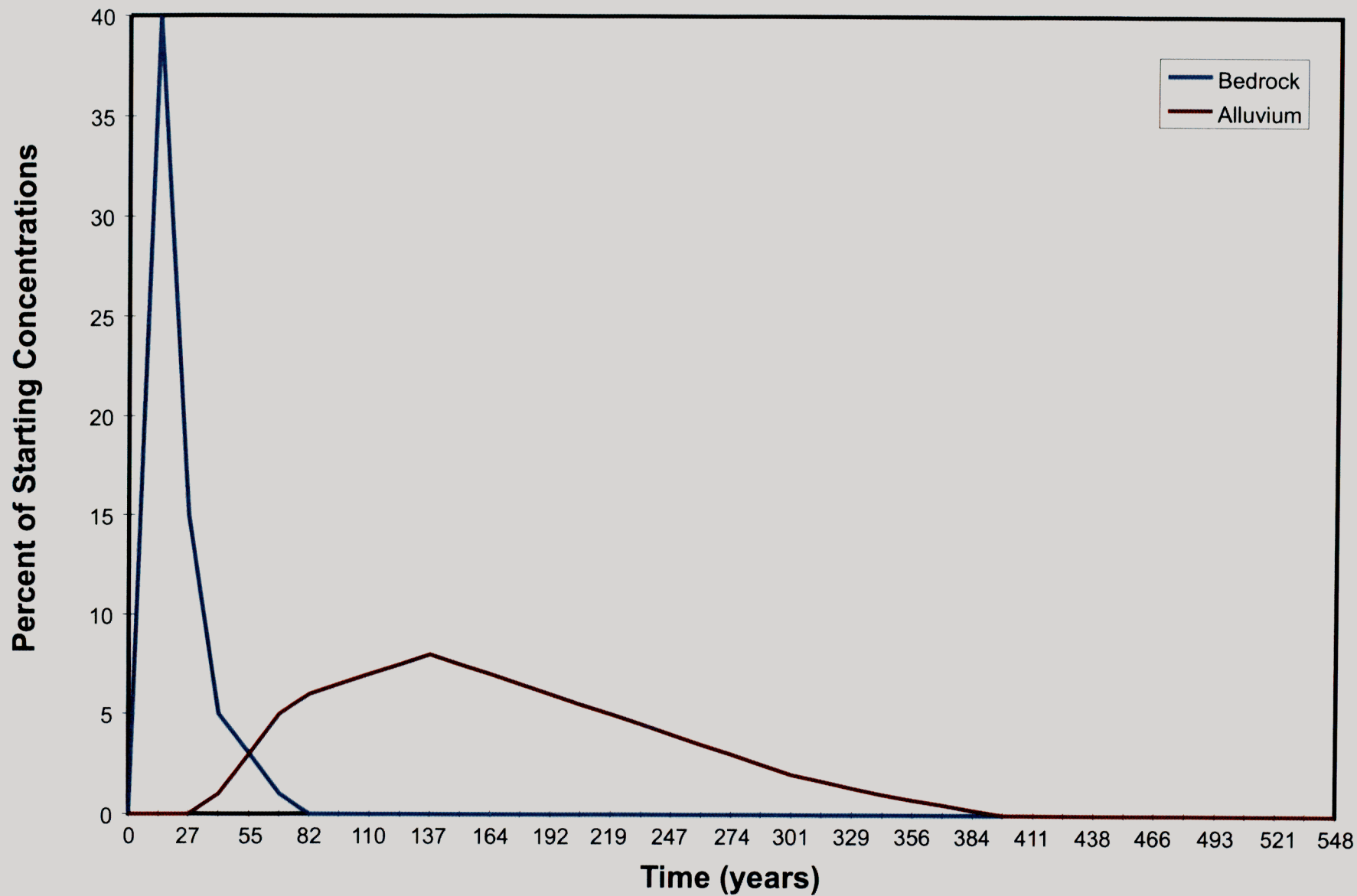




Generation  
Date:  
7/31/97

Figure 4-9. Predicted Flow Field  
(Vertical Exaggeration 1:0.075).

  
**Geomega**



Generation  
Date:  
7/31/97

Figure 4-10. Sensitivity Analysis to Increased (2x) Recharge.

## 5. Groundwater Flow Modeling

Groundwater flow modeling of the saturated zone was completed to continue the unsaturated zone modeling to complete flow through the aquifers beneath Giroux Wash. A numerical model was constructed to quantify the groundwater flow down from the mountain ranges that border the impoundment on three sides and out toward the center of White River Valley. Vertical flow from the shallower basin-fill aquifers into the deeper aquifers was also resolved by modeling. The following sections describe this model development from conceptualization to simulated predictions.

### 5.1 Conceptual Flow Model

Regional groundwater flow is generally toward the south, away from the impoundment area, and it is controlled by several factors. The Giroux Wash model domain is shown on the USGS regional water table map (Figure 5-1; Thomas et al. 1986).

#### 5.1.1 Inflow of Groundwater into the Model Domain

Groundwater flows from the mountains, through the alluvial fans along the sides of the valleys, and into the alluvial aquifers of the valleys. There is groundwater flux into the White River Valley from the Jakes Valley, located just to the northwest. General groundwater flow in the valleys tends to parallel the strike of the valley, flowing to the south in White River Valley.

The mountain ranges adjacent to the Giroux Wash function as regional hydrologic divides for surface and groundwater.

- The Egan Range appears to be a major regional groundwater divide for both the shallow and deeper systems on the east side of the White River Valley. These mountains are interpreted to act as a major water divide separating groundwater on the east, flowing northeast toward the Great Salt Lake, from water on the west side, which flows south toward the Colorado River.
- The White Pine and Grant Ranges form the western boundary of the White River Valley. It is interpreted that these mountain ranges function as water divides on the west side of the White River Valley.
- The Jakes Valley, just northwest of the White River Valley, is separated from the White River Valley by a northeast-trending ridge that is part of the Horse Range. It is interpreted that this ridge acts as a semiconductive hydraulic barrier, allowing flow into the White River Valley (Thomas et al. 1986).

Rainfall originating at higher elevations in the ranges surrounding the tailings impoundment is the source for groundwater in the alluvial basin (valley) south of the facility. This meteoric water infiltrates through the vadose zone and recharges the groundwater aquifers in the area. Evapotranspiration is higher in the valleys than in the mountains and has a major impact on groundwater recharge.

### *5.1.2 Groundwater Flow Beneath the Impoundment Site*

Faulting and relatively impermeable volcanic rocks—expressed at the surface on the east side of the White River Valley and the Giroux Wash impoundment area—create hydraulic barriers that complicate the pattern of groundwater flow. These barriers cause groundwater to be encountered at 250 feet bgs in the alluvium and volcanic rocks on the east side of the valley, whereas it occurs at approximately 750 feet bgs on the west side in alluvial sediments.

A pair of schematic cross sections displays groundwater flow, occurrence of groundwater, and geology across the Giroux Wash area (Figures 5-2 and 5-3). Figure 3-1, a water table map constructed from water-level measurements taken during the first quarter of 1997 and regional data, shows flow generally southward from the impoundment. There is also a large discontinuity in heads across the Giroux Wash fault, with water on the east (downthrown) side being about 500 feet higher than on the west side.

#### *5.1.2.1 Effect of Normal Faulting*

A fault may act as a hydrologic barrier or as a hydrologic conduit or may have no influence on groundwater flow. Hydrologic data from which fault behavior can be inferred are limited in the Giroux Wash area. On the basis of available data, major faults within the model domain were identified and were included in the groundwater model if they appeared to influence groundwater flow. Normal faults in the area form hydraulic barriers to flow, as determined by water-level data.

- Groundwater was encountered at 750 feet bgs in monitoring well WCC-1.
- The water table is interpreted to occur 250 to 300 feet bgs on the east side of the valley where the volcanic rocks are nearer to the surface.
- Monitoring well WCC-3, located 4,500 feet east of WCC-G1, encountered water at 510 feet bgs, and it reached an equilibrium water depth of 250 feet bgs after one month.

#### 5.1.2.2 *Effect of Volcanic Rocks vs. Alluvium*

The preponderance of volcanic rocks on the east side of the valley may also influence the depth to groundwater in the area. These lower-conductivity rocks impede flow laterally and vertically, resulting in higher water table elevations.

Volcanic rocks crop out in a band several thousand feet wide along the western edge of White River Valley, and they are interpreted to terminate about 1 mile south of the Giroux Wash embankment. These Tertiary volcanic flows dip about 9° to 30° to the southwest. It appears that igneous intrusions are related to the extensional forces that created the north-trending normal-faulting regime on the eastern side of the White River Valley.

The Tertiary volcanic rocks tend to have substantially lower hydraulic conductivities than their Tertiary sedimentary counterparts. For example, the hydraulic conductivity of rhyolitic lava flows on the east side of the impoundment area was estimated at 0.0001 feet/day, whereas interpretation of pumping tests of the unconsolidated alluvium near the center of Steptoe Valley estimated hydraulic conductivity of 400 feet/day (PTI 1994).

#### 5.1.2.3 *Description of Aquifers*

The Paleozoic rocks and the alluvial fill in the valleys form the primary aquifers in the region; their hydraulic conductivities range from 0.1 to 400 feet/day. Groundwater in the Paleozoic aquifer can be confined or unconfined, and flow is controlled primarily by the occurrence of faults and fractures, secondary mineralization and alteration, and Tertiary intrusions. Groundwater in the alluvial aquifer is unconfined or, less commonly, semiconfined. Flow is controlled by elevation of the water table above mean sea level (MSL) and hydraulic conductivity contrasts within the alluvial sediments. The thickness of alluvium in White River Valley is greater than 1,050 feet near the impoundment. Monitoring well WCC-G1 was drilled to 1,050 feet near the center of the valley drainage, 1,500 feet south of the impoundment embankment, and the well encountered unconsolidated alluvial material to total depth.

#### 5.1.2.4 *Interaction Between Surface Water and Groundwater*

There are no recognized perennial streams within the model domain. There are ephemeral streams that carry water from the mountain ranges forming the boundary of the valley floor. Giroux Wash, Jakes Wash, and several unnamed drainages at the head of White River Valley are ephemeral, containing surface water during the spring runoff and during storm events.

No naturally occurring surface-water bodies—including lakes, ponds, or springs—occur within the study area.

#### 5.1.2.5 Aquifer Stresses

Precipitation in White Pine County is dependent on elevation; it ranges from approximately 6 inches/year in the valleys to >20 inches/year on the high peaks (Eakin et al. 1967). Recharge to groundwater (precipitation minus losses to evapotranspiration, runoff, and storage) is also dependent on elevation; the overall percentage of precipitation that reaches groundwater can vary from almost zero along the valley floors to as high as 25% in the mountainous areas (Maxey and Eakin 1949).

Snowmelt recharges the Paleozoic aquifers directly, and surface flow down mountain streams reaches the alluvial valleys and descends into the coarse alluvium along the mountain fronts to recharge the alluvial aquifers. Paleozoic aquifers may directly recharge alluvial basin-fill aquifers at depth. Rainfall also contributes to recharge in both aquifer systems.

Evapotranspiration from the groundwater table is most important in the valley floors where the water table is close to the surface. The depth at which evapotranspiration ceases is approximately 20 feet (Frick 1985; LeedsHill 1981a). Evaporative losses are substantial from the pit lakes in the Robinson District; the pan evaporation rate is 48 inches/year (Houghton et al. 1975).

#### 5.1.2.6 Boundary Conditions

No-flow boundaries were proposed for the east and west sides of the study area where the Egan, Butte, and White Pine Ranges form groundwater divides around the White River Valley. However, the eastern boundary of the model domain was not positioned at the Egan Range groundwater divide, and thus there was flow entering the system along this boundary. A constant head was assumed for the northern and parts of the southern boundaries to influence flow toward the south. These boundary conditions were appropriate for the area and were required to solve this mathematical problem using a numerical finite-difference method.

### 5.2 Mathematical Model

The groundwater flow model was implemented for the Giroux Wash site by using the numerical, three-dimensional code MODFLOW. The code uses a block-centered finite-difference model approach to solve the governing groundwater flow equation, which can be expressed as follows (McDonald and Harbaugh 1988):

$$\frac{\partial}{\partial x} \left( K_{xx} \frac{\partial h}{\partial x} \right) + \frac{\partial}{\partial y} \left( K_{yy} \frac{\partial h}{\partial y} \right) + \frac{\partial}{\partial z} \left( K_{zz} \frac{\partial h}{\partial z} \right) - W = S_s \frac{\partial h}{\partial t}, \quad (5-1)$$

where

$K_{xx}$ ,  $K_{yy}$ , and  $K_{zz}$  are the values of hydraulic conductivity along the  $x$ ,  $y$ , and  $z$  coordinate axes ( $LT^{-1}$ ),

$h$  is the hydraulic head ( $L$ ),

$W$  is volumetric flux per unit volume and represents sources and/or sinks of groundwater ( $T^{-1}$ ),

$S_s$  is the specific storage ( $L^{-1}$ ), and

$t$  is time ( $T$ ).

To obtain a solution, the model domain was discretized into a finite-difference grid (see Section 4.5), and appropriate boundary conditions and representative hydrogeologic parameters were assigned to each grid node. MODFLOW then solved equation 5-1 for hydraulic heads and volumetric fluxes.

Development of a numerical groundwater flow model required the use of assumptions and approximations that simplify the physical system. Principal simplifying assumptions implicit in the implementation of MODFLOW include the following:

- groundwater flow is laminar;
- groundwater is isothermal, slightly compressible, and has uniform density;
- hydraulic conductivity is isotropic in the horizontal direction;
- the subsurface can be represented by a grid of cells and hydrogeologic parameters are constant within each cell;
- the physical parameters of the system do not change with the state of the system; and
- groundwater flow between model layers is vertical.

Review of site-specific data and consideration of model objectives indicated that these assumptions are acceptable and do not limit the applicability of the model for Giroux Wash.

A link was made between MODFLOW and HYDRUS\_2D for inputting groundwater flux through the vadose zone to the water table. This structure provided a relatively seamless transition between the unsaturated and saturated flow models. Infiltrated water velocities predicted by HYDRUS\_2D were incorporated into MODFLOW as recharge to the model layer at the water table.

### **5.3 Model Design**

A regional groundwater flow model developed by PTI, Inc., in support of the Environmental Impact Statement of the Robinson Project was used as the basis for the

modeling investigation. The PTI model was refined and modified by incorporating more detailed hydrogeologic data to obtain finer hydraulic detail and resolution of flow vectors in the area of the tailings impoundment. A three-dimensional finite-difference numerical model was employed on a uniform, fine-grid mesh to solve the groundwater flow equation as applied to this study.

### *5.3.1 Model Domain*

A finite-difference model grid mesh oriented north-south and aligned in the principal direction of groundwater flow and contaminant transport was developed (Figure 5-4). The rectangular model domain is 40,600 feet along the north-south dimension by 30,000 feet in the east-west dimension. It covered an area of about 44 square miles ( $1.218 \times 10^9$  square feet). There were nine layers within the model domain that ranged in thickness from 200 to 750 feet.

Model layers were assigned independently of geologic bedding and structure. Figure 5-5 shows the vertical discretization and how the bottom elevations of the nine model layers were held constant. The top elevation for the model, assigned on the basis of a digital topographic map, crossed model layers. Layers 5, 6, and 7 were the most important for resolving the groundwater flow and contaminant transport at the Giroux Wash impoundment. First groundwater is encountered within these layers in the area of interest where contaminant transport to the south may occur.

### *5.3.2 Model Boundary Conditions*

Figure 5-6 displays the boundary conditions set in model layer 6. A no-flow boundary was assigned to the western boundary of the model domain, where the White Pine and Butte Ranges form a surface and groundwater divide. Constant heads were set on the northern and eastern boundaries where groundwater flow enters the model domain. A combination of constant head and no-flow boundaries was assigned to the southern boundary where groundwater exits the modeled system. Constant head values were estimated from water-level measurements of monitoring wells in the Giroux Wash area taken during the first quarter of 1997 and from regional head maps prepared by the USGS.

The normal fault separating rocks on the west side of the facility from those on the east side was incorporated into the model as a steeply east-dipping, linear feature. It was assumed that the fault cut across all of the stratigraphic layers included in the model. Owing to the difference in head of approximately 500 feet across the southern part of the impoundment, the fault was interpreted to act as a hydraulic barrier to groundwater flow. During development of the original EIS, the Giroux Wash fault zone was assigned conductance (conductivity  $\times$  thickness) attributes; these were the basis for modeling the fault as having a thickness of 1 foot and a hydraulic conductivity of  $1.0 \times 10^{-4}$  foot/day. The hydraulic attributes of the fault caused it to form an impediment to horizontal flow across the site. The vertical component of



groundwater flow across the fault zone was somewhat enhanced because of the steep gradient formed at this low-conductance barrier to lateral flow.

The MODFLOW code has a horizontal-flow barrier (HFB) package that allows for modeling of faults, sheet pilings, or other similar features. The conductivity of  $1.0 \times 10^{-4}$  foot/day and the 1-foot thickness were used to model the Giroux Wash fault with this package.

### 5.3.3 Hydraulic Properties

Hydraulic properties were estimated from tests performed on similar strata in other areas because no aquifer test data were available for the Giroux Wash area. Literature values were also used to verify the analogue aquifer test results.

#### 5.3.3.1 Hydraulic Conductivity

Rock types described in the study area were incorporated into the groundwater flow model by assigning representative hydraulic conductivities to each. Stratigraphic variations were incorporated into the numerical model by varying hydraulic conductivity within each layer. This approach was similar to that taken to develop the previous regional groundwater model (PTI 1994).

Hydraulic conductivity values were estimated from previous investigations at the site including Dames & Moore (1982), PTI (1994), and HSI Geotrans (1996). Table 5-1 presents a summary of hydraulic conductivity values used for the individual rock types assigned during discretization of the numerical model and justifications for their use. Quaternary alluvial aquifers, composed of coarser-grained material, typically exhibit conductivities that range from 0.1 to 400 feet/day increasing from the valley edge to center. Conductivity of paleozoic limestone aquifers within the Giroux Wash area typically range from 1 to 20 feet/day. Tertiary volcanic rocks and fine-grained alluvial deposits have hydraulic conductivities that range from 0.0001 to 1 foot/day. Hydraulic conductivity was assigned to specific flow units based on stratigraphic or diagenetic properties (fracturing, mineralization, and dissolution) of that specific rock type. A range of hydraulic conductivity was assigned to rock types identified in the Giroux Wash area. For example, Quaternary alluvial sediments were allowed to vary from 0.01 to 400 feet/day over the model domain. Figure 5-7 displays the range of hydraulic conductivity values assigned to model layer 6. A similar plot, Figure 5-8, shows the variability of hydraulic conductivity over the model space for layer 7.

#### 5.3.3.2 Specific Storage and Specific Yield

Previous aquifer testing performed by Dames & Moore (1982) and HSI Geotrans (1996) determined that storage coefficients ranged from  $4 \times 10^{-3}$  to  $1 \times 10^{-5}$  for confined and semiconfined flow units. Storage coefficients for alluvium at the Nevada Test Site ranging from  $2 \times 10^{-3}$  to  $1 \times 10^{-4}$  are in good agreement with these values.

Specific yield for the unconfined aquifers was estimated at 0.05 to 0.23 from pumping tests in the adjacent areas. Table 5-2 summarizes storage terms used in the modeling study. Published literature data by McWhorter and Sunada (1977), Freeze and Cherry (1979), and Domenico and Schwartz (1990) confirms the storage terms used for the specific rock types encountered within the model domain.

#### 5.3.3.3 Porosity

Table 5-2 also summarizes porosity values assigned to the rock types encountered at Giroux Wash. An effective porosity of 0.25 was used for alluvial strata based on previous investigations completed at the site (PTI 1994). An effective porosity of 0.05 was assigned to the volcanic rocks. Estimated total porosity was converted to effective porosity according to the method of de Marsily (1986).

#### 5.3.4 Aquifer Stresses

There are no active pumping wells located within the groundwater model domain. Also, mine dewatering activities north of the study area will have no impact on the impoundment area because they are on the far side of a groundwater divide formed by the Egan and Butte Ranges. Recharge and evapotranspiration are the only stresses acting on the local groundwater regime.

##### 5.3.4.1 Recharge Calculations

Higher elevations receive more rainfall and allow a greater amount of deep percolation to the aquifers. Only a part of the precipitation will infiltrate through the unsaturated zone and recharge the groundwater system because a large percentage of the precipitation will be lost to evapotranspiration and surface runoff. Maxey and Eakin (1949) developed a water budget for White Pine County, which indicated that the fraction of precipitation recharging the aquifer is dependent on elevation, with an increasing fraction reaching the groundwater at higher elevations.

Therefore, the previous investigation (PTI 1994) calculated recharge by incorporating rainfall amounts predicted according to surface elevation. PTI developed a plot of precipitation vs. elevation based on average annual precipitation measured in gauges in the region. The plot of recharge shows that the highest recharge rates are estimated for the Egan Range area and recharge in the valley floor is lowest (Figure 5-9).

To incorporate the recharge into the groundwater model, the estimated recharge,  $R$  (in inches/year), as a function of elevation,  $E$ , was fit to the following equation with a correlation coefficient of  $r = 0.95$  (coefficient of determination =  $r^2 = 0.90$ ):

$$R = 0.534 \times \exp\left(\frac{0.28E}{1,000}\right) - 3.029 . \quad (5-2)$$

For every model cell, this equation provided an initial estimate for recharge that was based on the elevation of the center of the cell as determined from the topographic map. Recharge was assigned to the highest active model layer.

#### *5.3.4.2 Evaporation and Evapotranspiration Calculations*

In areas where the water table is closer to the land surface—which in the model domain primarily occurs in White River Valley south of the Giroux Wash impoundment—evaporation and transpiration by plants can occur from the water table surface. In fact, evapotranspiration in the lower elevations of Steptoe and White River Valleys generally exceeds precipitation, resulting in a net loss of groundwater from these areas of the basins (Maxey and Eakin 1949).

Therefore, an evapotranspiration curve was developed by assuming a maximum evapotranspiration rate of 48 inches/year for water at the land surface. This value is reasonably consistent with a maximum rate of 41 to 46 inches/year for evapotranspiration from the water table. The extinction depth for evapotranspiration was 20 feet (Frick 1985), and the rate was assumed to decrease linearly with depth.

More recent investigations have determined that there is a complex relationship between pan-evaporation rates and climatic conditions. However, the Giroux Wash area lies in a region of Nevada in which monthly and yearly average evapotranspiration rates fall in the lower end of the range for the state (Shevenell 1996) and thus are not significant contributions to aquifer stresses.

### **5.4 Calibration**

A numerical calibration was performed for the steady-state groundwater flow model to prove that it was reasonably accurate and precise for its intended use of reproducing heads observed in the field. A primary objective of the calibration was to minimize the error of the numerical solution. Calibration of a flow model is a demonstration that the model is capable of reproducing the field-measured heads and fluxes that are the calibration values. The calibration was accomplished by determining the set of parameters, boundary conditions, and aquifer stresses that produced simulated heads that matched observed values, distributed spatially within the aquifer, within an acceptable range of error. This is the method prescribed by many authors including Anderson and Woessner (1992). Hydraulic conductivity was used as the calibration parameter to solve the inverse problem of developing the correct data set to accurately simulate measured heads. A qualitative calibration target set prior to modeling was  $\pm 100$  feet for all observation points evaluated.

#### *5.4.1 Observation Points*

The groundwater flow model was calibrated to seven monitoring wells situated around the periphery of the Giroux Wash impoundment. These wells were installed

by Woodward Clyde Consultants in 1991 and by BHP in 1996. Monitoring wells were completed vertically over a range of several hundred feet. Five of the calibration targets (WCC-G2, WCC-G3, MW-G5, MW-G6, and PZ-G7) were completed in the equivalent of model layer 6, and two of the targets (WCC-G1 and PZ-G8) were completed in the equivalent of model layer 7. WCC-G4 was not included in the calibration because it is located in the region of faulting and volcanic intrusive rocks where it is very difficult to predict the rapid change in heads that occur across it.

#### 5.4.2 Results of Steady-State Calibration

Results of the steady-state calibration statistics are included in Table 5-3. The groundwater sampling event of the first quarter of 1997 was used as the observed comparison for calibration purposes. The results indicate that the groundwater flow model is accurate at reproducing field-observed head values in multiple layers. An industry-standard suite of statistical analyses was performed for these data. The residual mean (RM) is defined as

$$RM = \frac{1}{n} \sum_i^n (h_o - h_s) i \quad , \quad (5-3)$$

where

$n$  is the number of observations or calibration points,

$h_s$  is the simulated head, and

$h_o$  is the observed head.

The residual mean is 2.7 feet for the target points available for calibration.

The absolute residual mean (ARM) is the absolute value of the residual mean, or

$$ARM = \frac{1}{n} \sum_i^n | (h_o - h_s) i | \quad , \quad (5-4)$$

The absolute residual mean is 36.9 feet for the seven calibration points.

The standard deviation (SD) of the simulated heads at the observation points is determined by

$$SD = \left[ \frac{1}{n} \sum_i^n (h_o - h_s)^2 \right]^{0.5} \quad , \quad (5-5)$$

The standard deviation for the model calibration targets was 53.2 feet. Range in heads (HR) for the observation points was 826 feet. A very useful measure of calibration

results is to calculate the SD per HR of the observation points. This ratio gives a sense for the accuracy of the model over the calibrated area. Results of the steady-state calibration gave 0.06 (6%). According to Anderson and Woessner (1992), a calibrated flow model should have an SD/HR value of >15%.

This model appears to be accurate for predicting heads and flows over the area of interest as determined by the generally accepted protocol for quantitative evaluation of groundwater flow models.

Although there were just seven points with which to quantify the model, there were regional data from which to interpret groundwater flow away from the monitoring wells. As described in Section 3.1, groundwater flow originates in the ranges forming flow boundaries on roughly three sides of the model domain, and it flows southward toward the axis of the White River Valley. A qualitative evaluation of model-predicted heads for layer 6 reproduced the overall shape and corresponded closely with the interpreted water table map (Figure 5-11).

### **5.5 Verification and Sensitivity Analysis**

Mass-balance error for the flow model was 0.9%, an acceptable mass-balance error according to Anderson and Woessner (1992).

Model sensitivity analysis, using industry-accepted protocol, was accomplished by adjusting the hydraulic parameters and evaluating the results. Final sensitivity to variation in hydraulic conductivity, vertical conductivity, recharge, and evapotranspiration is displayed on Table 5-4. The model was most sensitive to changes in recharge.

An analysis was performed to determine how sensitive the model is to uncertainty in various model input parameters. The relative sensitivity of the model to changes in input parameters was an indicator of the degree of importance of individual parameters to the simulation results.

The parameter groups varied during the sensitivity analysis were

- horizontal and vertical hydraulic conductivities,
- recharge, and
- evapotranspiration.

The parameter groups were varied by multipliers of 1.5 and 0.5 (i.e.,  $\pm 50\%$ ), for a total of eight simulations. Results of the sensitivity analysis were compared against the calibrated (base case) model. The results (Table 5-4) show that the model is most sensitive to changes in recharge, with horizontal conductivity being the second most sensitive parameter. The model is least sensitive to changes in evapotranspiration and vertical hydraulic conductivity. Even though the increased lateral hydraulic

conductivity case indicates improved statistics compared to the calibrated model, increasing the hydraulic conductivity was not justified, owing to the previous aquifer testing adjacent to the site. In addition, the result of the calibrated model and the increased lateral hydraulic conductivity case were statistically essentially identical.

## **5.6 Predictive Simulations**

A total of 40 simulations, each with a 5,000-day stress period, was performed by using the calibrated groundwater flow model. Output from the HYDRUS\_2D simulation of predicted infiltration velocity was input to the flow model as recharge. Meteoric recharge over the surface of the tailings impoundment was included in the unsaturated zone modeling described in Section 4. Simulations employing the predisposal conditions were assumed after this 200,000-day series of increased recharge by flushing through the vadose zone.

Steady-state simulations were selected for each of these stress periods because of the minor seasonal variations to aquifer stresses within the study area. These variations have been documented by measuring the hydraulic heads in the Giroux Wash monitoring wells over extended periods, as shown in the hydrographs for the WCC monitoring wells adjacent to the impoundment (Figure 5-12). It is apparent from Figure 5-12 that water levels in these wells have been essentially constant since their first sampling event.

An evaluation of the effect of increased recharge was modeled in steady and transient modes to determine what impact the increased infiltration estimated by HYDRUS\_2D through the vadose zone would have on groundwater flow in the area. It was determined from the modeling results, comparing the 5000-day transient case against steady-state, that the system reaches equilibrium or pseudo steady-state within 500 days of the increased recharge stress. Figure 5-13 is a plot of head vs. time for WCC-G1 that displays the onset of steady-state conditions.

## **5.7 Interpretation of Modeling Results**

Only minor changes in head and flux are realized by the aquifers in the region as a result of disposal of flotation tailings in the impoundment. Recharge increases during infiltration of the disposed water over the facility, but 100 years after initial disposal, recharge is predicted to have little impact on the groundwater flow and heads in model layer 6 (Figures 5-14). This observation modeling result is confirmed by comparing the layer-6 predisposal head distribution (Figure 5-11) to the layer-6 head distribution 100 years after disposal began (Figure 5-14).

## **5.8 Model Limitations and Assumptions**

There are no aquifer tests of the saturated zone in the Giroux Wash area on which to base estimates of hydraulic parameters for input to the numerical model. Hydraulic

conductivity—the calibration parameter—was assigned on the basis of analogue rock types in adjacent areas collected during previous investigations. For example, estimated hydraulic conductivity values determined from pumping tests performed on alluvial sediments in Steptoe Valley were applied to the Giroux Wash area. The steady-state flow model is calibrated over the region in which there are observation wells to act as calibration targets. There are a limited number of calibration targets on which to base the model accuracy and precision. Fortunately, all of the observation wells available for calibration were in the area of the impoundment in which the predicted concentrations and groundwater velocities to be resolved were critical for interpretation of future impacts to the POC well. Therefore, the numerical model is accurate for predicting groundwater flow and heads in the area near the impoundment.

**Table 5-1. Transmissivities and Hydraulic Conductivities of Rock Types in Model**

Model Zone Number	Transmissivities (ft <sup>2</sup> /day)		
	X direction	Y direction	Z direction
CONFINED PALEOZOIC CARBONATE ROCK *			
27	32.0	32.0	0.3
28	40.0	40.0	0.4
29	80.0	80.0	0.8
30	160.0	160.0	16.0
31	320.0	320.0	3.2
32	1,600.0	1,600.0	1.6
33	3,200.0	3,200.0	320.0
34	4,000.0	4,000.0	40.0
35	8,000.0	8,000.0	80.0
36	16,000.0	16,000.0	160.0
37	32,000.0	32,000.0	320.0
38	50,000.0	50,000.0	50,000.0
Model Zone Number	Hydraulic Conductivities (ft/day)		
	X direction	Y direction	Z direction
LOWER AND UPPER ARCTURUS FORMATION †			
51	0.05	0.05	$5.0 \times 10^{-5}$
PALEOZOIC CARBONATE ROCKS *			
2	0.001	0.001	0.001
3	0.002	0.002	$2.0 \times 10^{-4}$
6	0.010	0.010	0.010
7	0.020	0.020	0.020
8	0.025	0.025	0.025
9	0.1	0.1	0.0
12	0.4	0.4	0.4
13	0.8	0.8	0.8
14	1.0	1.0	1.0
15	1.2	1.2	1.2
16	1.6	1.6	0.016
17	2.0	2.0	2.0
18	2.3	2.3	2.3
19	3.2	3.2	0.0
21	5.0	5.0	5.0
22	6.4	6.4	6.4
23	8.0	8.0	8.0
24	10.0	10.0	10.0
25	16.0	16.0	0.2
26	20.0	20.0	2.0
52	0.010	0.010	0.001
QUATERNARY ALLUVIUM ‡			
10	0.1	0.1	0.01
39	5.0	5.0	0.5
45	0.010	0.010	0.001
49	400.0	400.0	40
55	1.0	1.0	0.1
59	0.1	0.1	0.0
60	0.001	0.001	$1.0 \times 10^{-6}$



**Table 5-1. Transmissivities and Hydraulic Conductivities of Rock Types in Model, *continued***

Model Zone Number	Hydraulic Conductivity (ft/day)		
	X direction	Y direction	Z direction
TERTIARY SHEEP PASS CONGLOMERATE AND PERMIAN RIB HILL SANDSTONE †			
11	0.2	0.2	0.0
TERTIARY VOLCANIC ROCKS §			
1	$4.8 \times 10^{-4}$	$4.8 \times 10^{-4}$	$4.8 \times 10^{-4}$
4	$4.0 \times 10^{-3}$	$4.0 \times 10^{-3}$	$4.0 \times 10^{-4}$
5	$5.0 \times 10^{-3}$	$5.0 \times 10^{-3}$	$5.0 \times 10^{-4}$
46	$5.0 \times 10^{-2}$	$5.0 \times 10^{-2}$	$5.0 \times 10^{-6}$

\* Dames & Moore (1982, 1988, 1990): Ely Limestone near McGill, 1.1 to 15 ft/day.

† Westec (1991): Giroux Wash, 0.00 to 0.6 ft/day.

‡ Dames & Moore (1982, 1988, 1990): Steptoe Valley, 0.005 to 3 ft/day.

LeedsHill (1981): Steptoe Valley,  $5.7 \times 10^4$  to  $5.7 \times 10^5$  ft/day.

WESTEC (1991): Giroux Wash 0.02 to 0.6 ft/day.

§ WESTEC (1991): Giroux Wash  $1 \times 10^{-3}$  to 0.05 ft/day.

**Table 5-2. Storage Properties Used in Model**

Rock Type	Specific Storage $S_s$	Specific Yield $S_y$	Porosity $\phi$
Quaternary Alluvium	$1 \times 10^{-4} *$	0.5–0.15	0.25
Tertiary Volcanic Rocks	$3 \times 10^{-6} \dagger$ $-7 \times 10^{-5}$	0.02–0.47	0.08
Paleozoic Carbonate Rocks	$2 \times 10^{-5} *$ $-4 \times 10^{-3} \dagger$	—	0.08

\* Dames and Moore (1982, 1988, 1990).

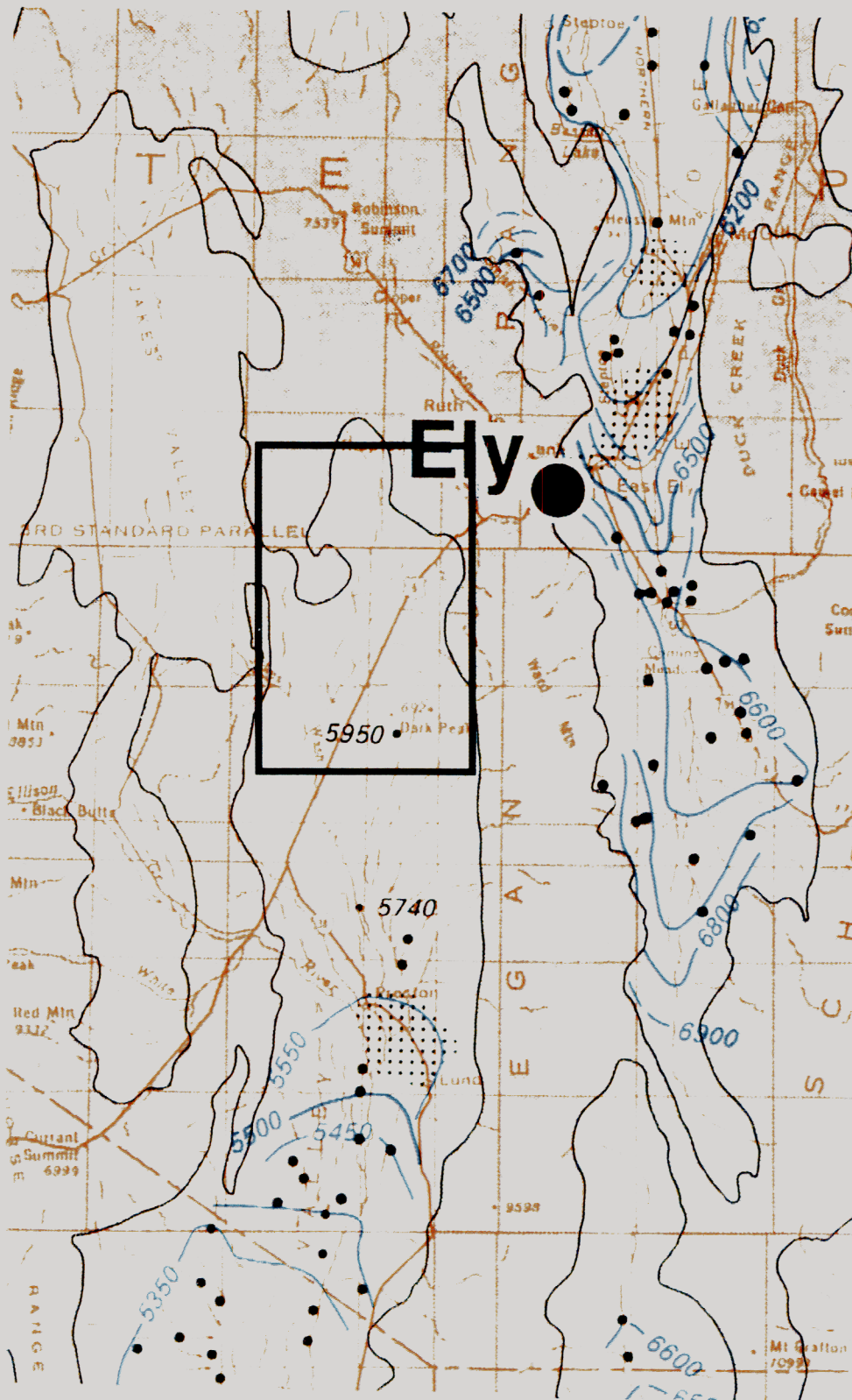
† Morris and Johnson (1967).

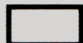
**Table 5-3. Groundwater Flow Model Calibration Statistics**

Well	Observed head (ft)	Simulated head (ft)	Residual (ft)	Absolute Residual (ft)	Residual Squared (ft <sup>2</sup> )
MW-G6	5804.00	5802.13	1.87	1.87	3.50
MW-G5	5805.00	5795.18	9.82	9.82	96.43
WCC-G1	5814.90	5793.87	21.03	21.03	442.26
WCC-G3	6476.80	6386.20	90.60	90.6	8208.36
PZ-G7	6597.50	6614.39	-16.89	16.89	285.27
PZ-G8	6598.00	6700.75	-102.75	102.75	10557.56
WCC-G2	6630.10	6614.72	15.38	15.38	236.54
Observed range in heads:				826.10 ft	
Mean error:				2.72 ft	
Mean absolute error:				36.91 ft	
Standard deviation:				53.22 ft	
Ratio of standard deviation to range in heads:				0.06	

**Table 5-4. Sensitivity Analysis**

Simulation	Residual Mean	Standard Deviation	Ratio of Standard Deviation to Range in Head
Calibrated model	2.70	53.20	0.064
Increase $K_h$ by a factor of 1.5	-0.07	47.26	0.057
Decrease $K_h$ by a factor of 0.5	0.11	64.75	0.078
Increase $K_v$ by a factor of 1.5	2.90	52.46	0.064
Decrease $K_v$ by a factor of 0.5	2.90	52.46	0.064
Increase recharge by a factor of 1.5	-4.97	56.73	0.069
Decrease recharge by a factor of 0.5	10.94	49.08	0.059
Increase evapotranspiration by a factor of 1.5	2.90	52.46	0.064
Decrease evapotranspiration by a factor of 0.5	2.50	52.70	0.064

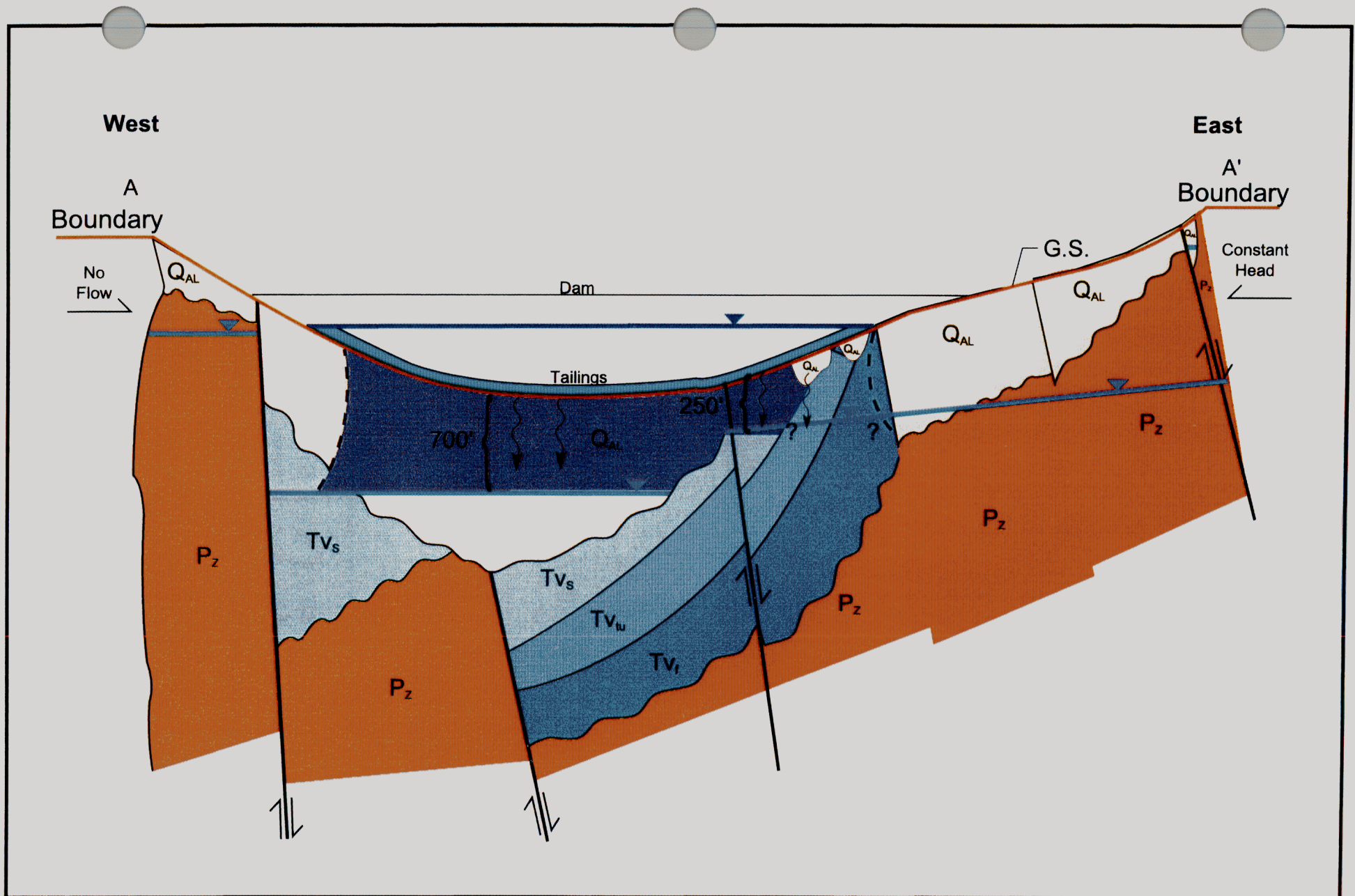


 FDM Model Domain

Generation  
Date:  
8/7/97

Figure 5-1. Regional Water Table  
(after Thomas et al., 1986) and FDM Model Domain.





Generation

Date:

8/4/97

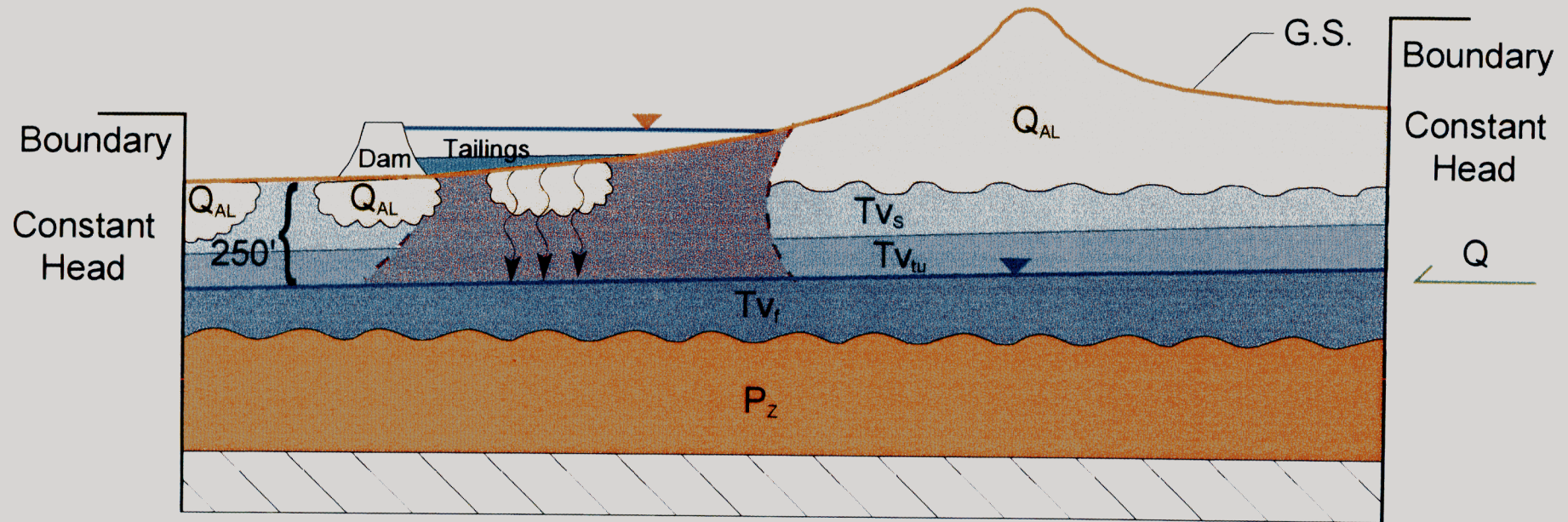
Figure 5-2. East - West Conceptual Flow Schematic.



# Eastern Portion

South

North



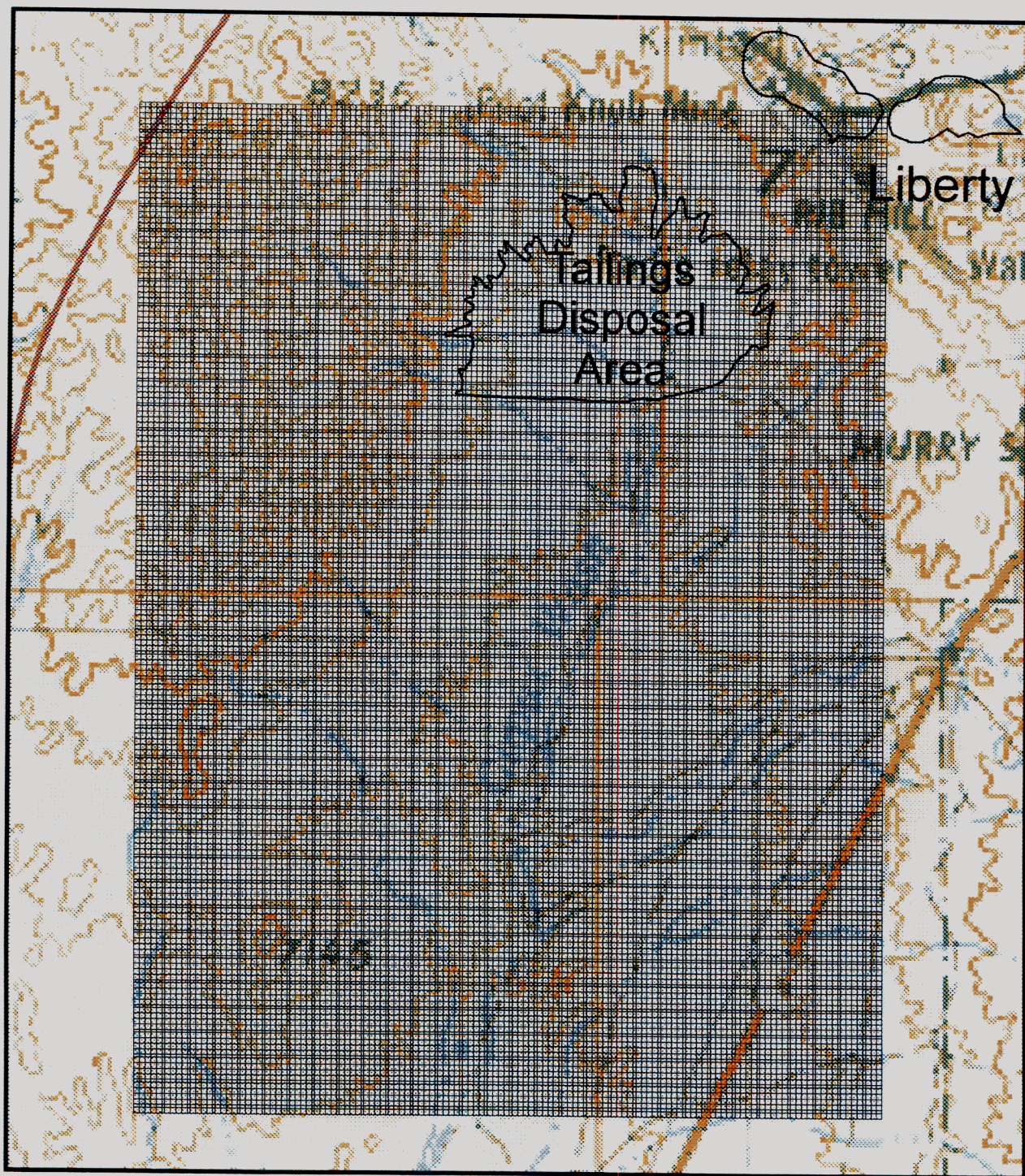
Generation

Date:

8/4/97

Figure 5-3. North - South Conceptual Flow Schematic.



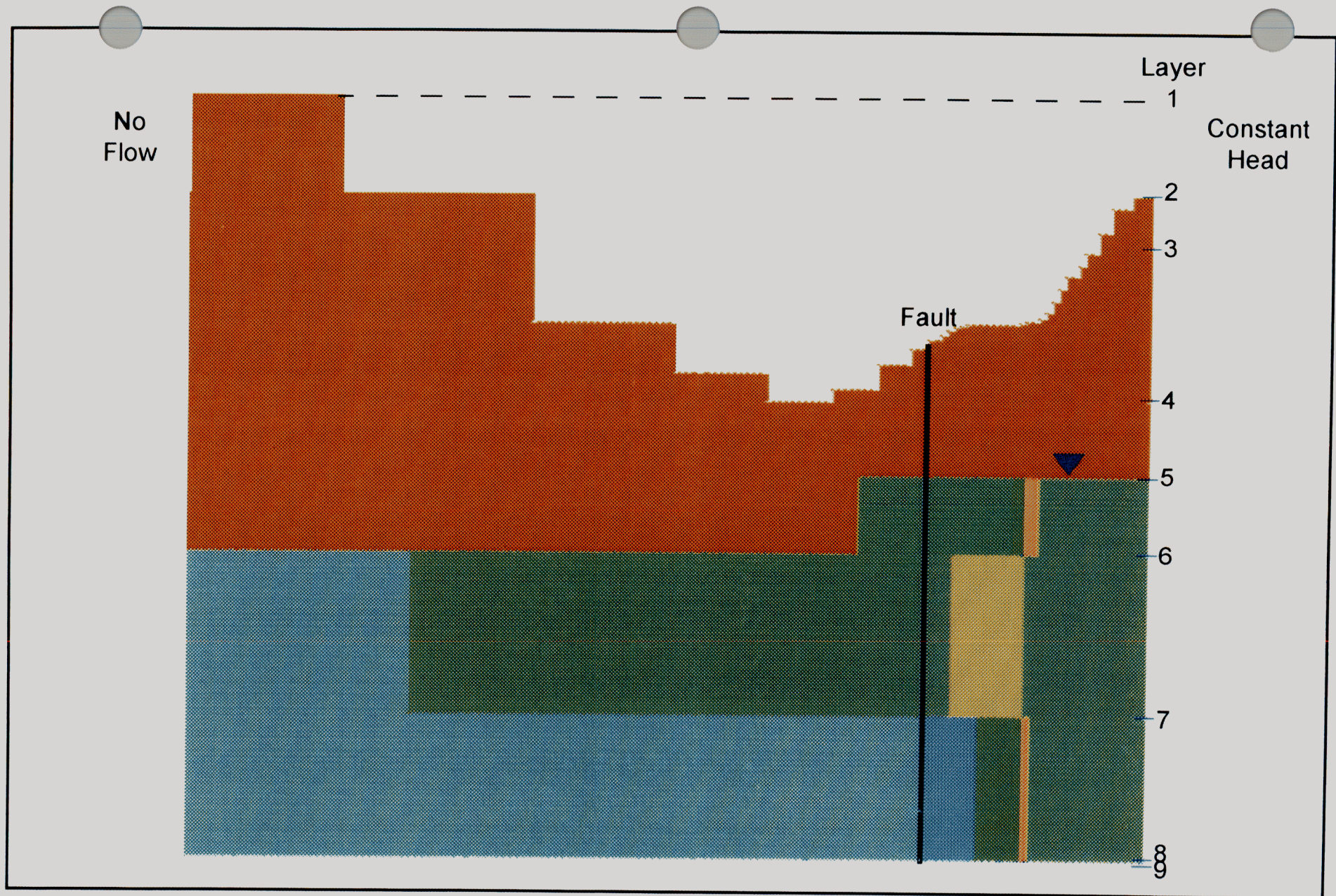


Generation  
Date:  
8/4/97

Figure 5-4. Giroux Wash Impoundment  
Finite Difference Model Grid.

  
Geomega



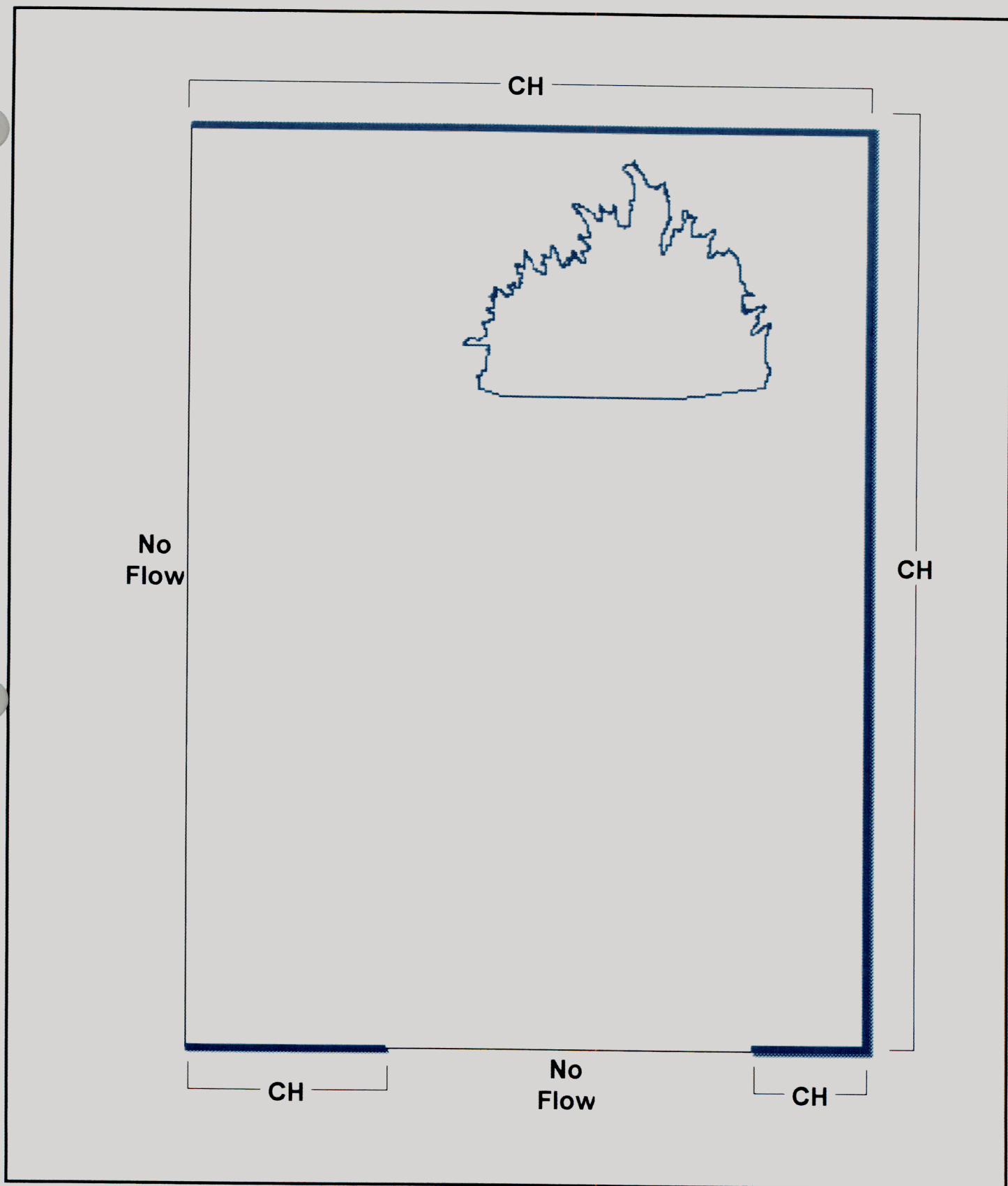


Generation

Date:

8/5/97

Figure5-5. Finite Difference Model Discretization, Section View.

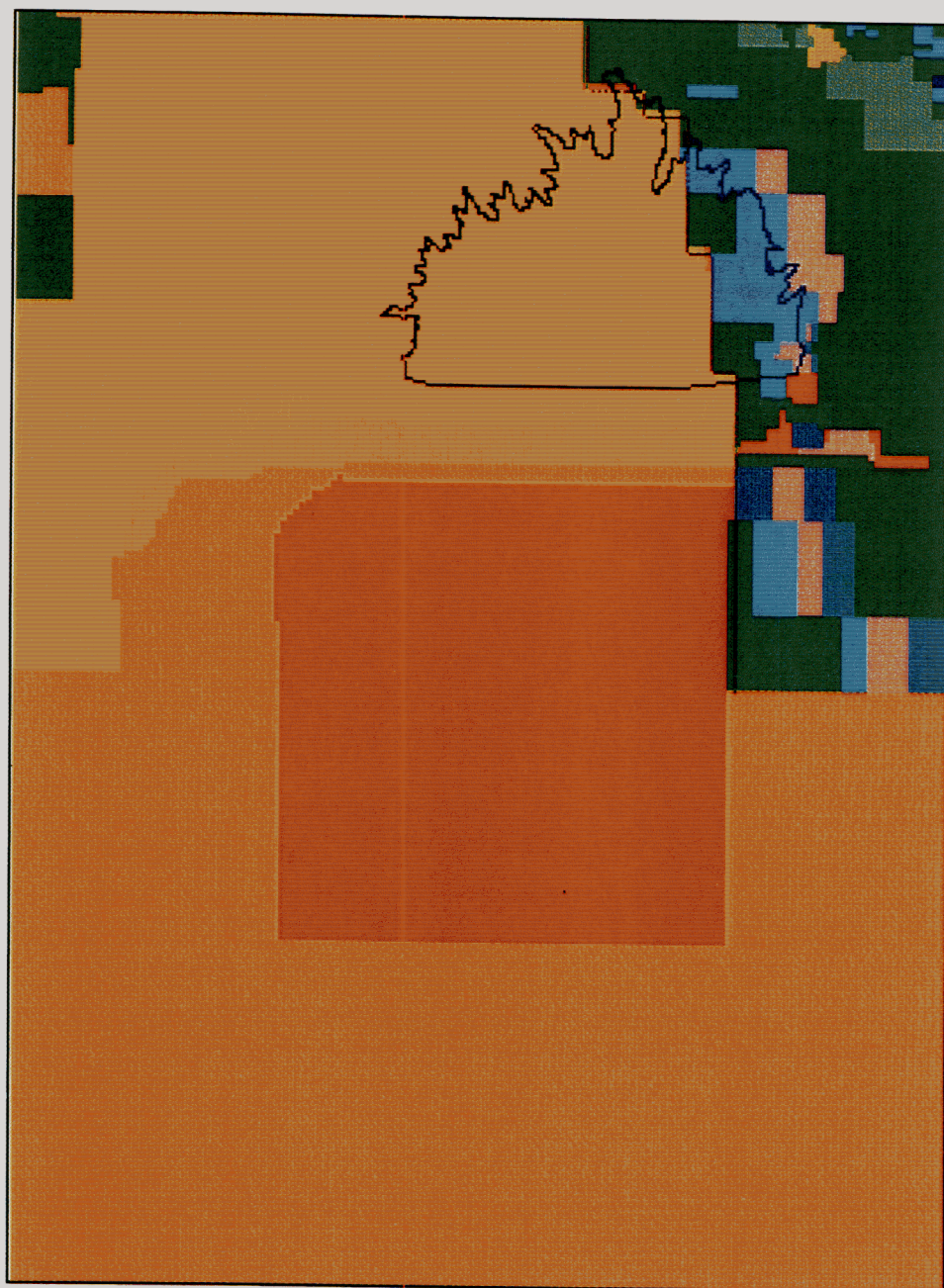
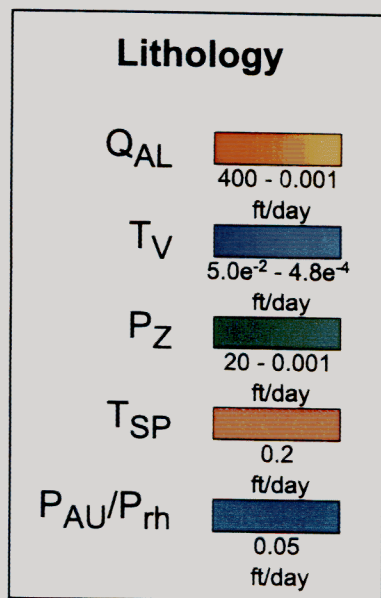


Generation  
Date:  
8/5/97

Figure 5-6. Boundary Conditions  
Assigned, Layer 6.

  
**Geomega**






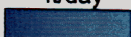
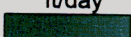
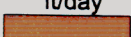
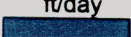
Generation  
Date:  
8/6/97

Figure 5-7. Hydraulic Conductivity Distribution,  
Layer 6.

  
**Geomega**



### Lithology

$Q_{AL}$	
	400 - 0.001 ft/day
$T_V$	
	$5.0e^{-2}$ - $4.8e^{-4}$ ft/day
$P_Z$	
	20 - 0.001 ft/day
$T_{SP}$	
	0.2 ft/day
$P_{AU}/P_{rh}$	
	0.05 ft/day



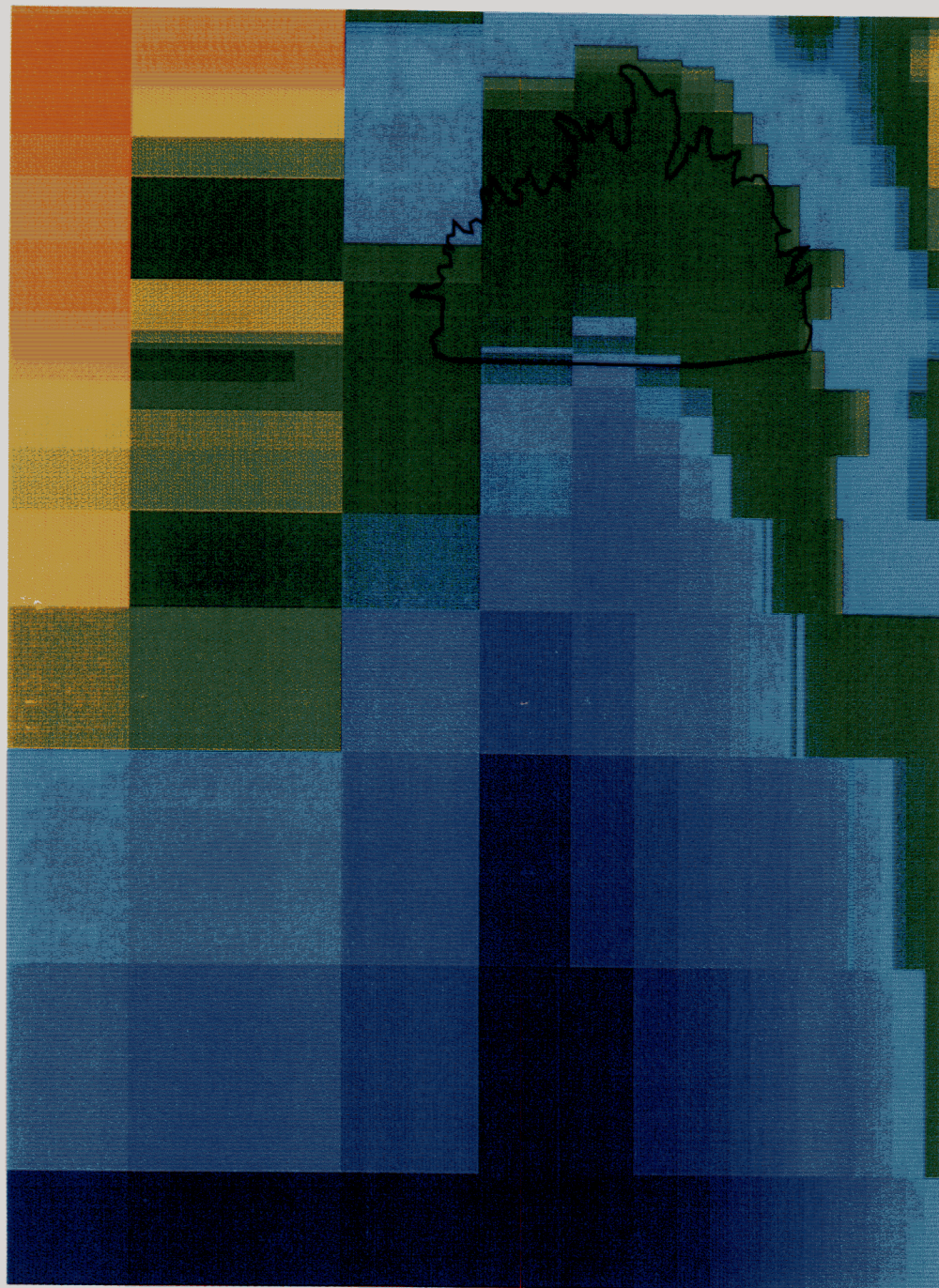
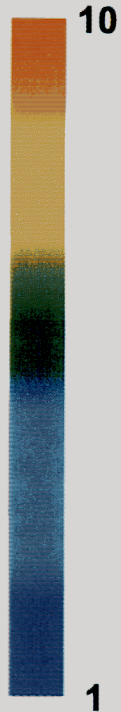
Generation  
Date:  
8/6/97

Figure 5-8. Hydraulic Conductivity Distribution,  
Layer 7.

  
**Geomega**



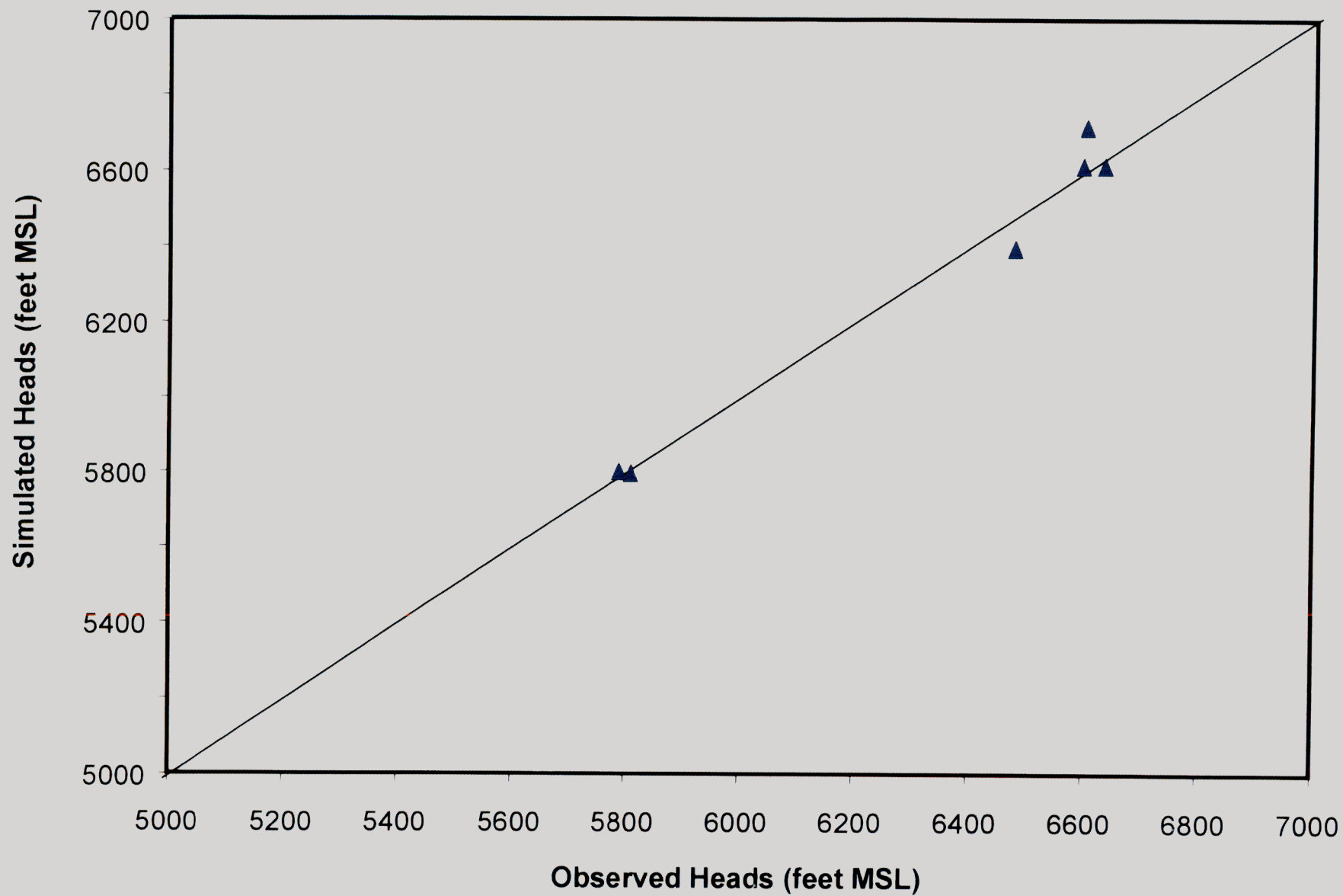
R (in/yr)



Generation  
Date:  
8/5/97

Figure 5-9. Recharge Rates Applied to  
Top Active Model Layer.

  
Geomega

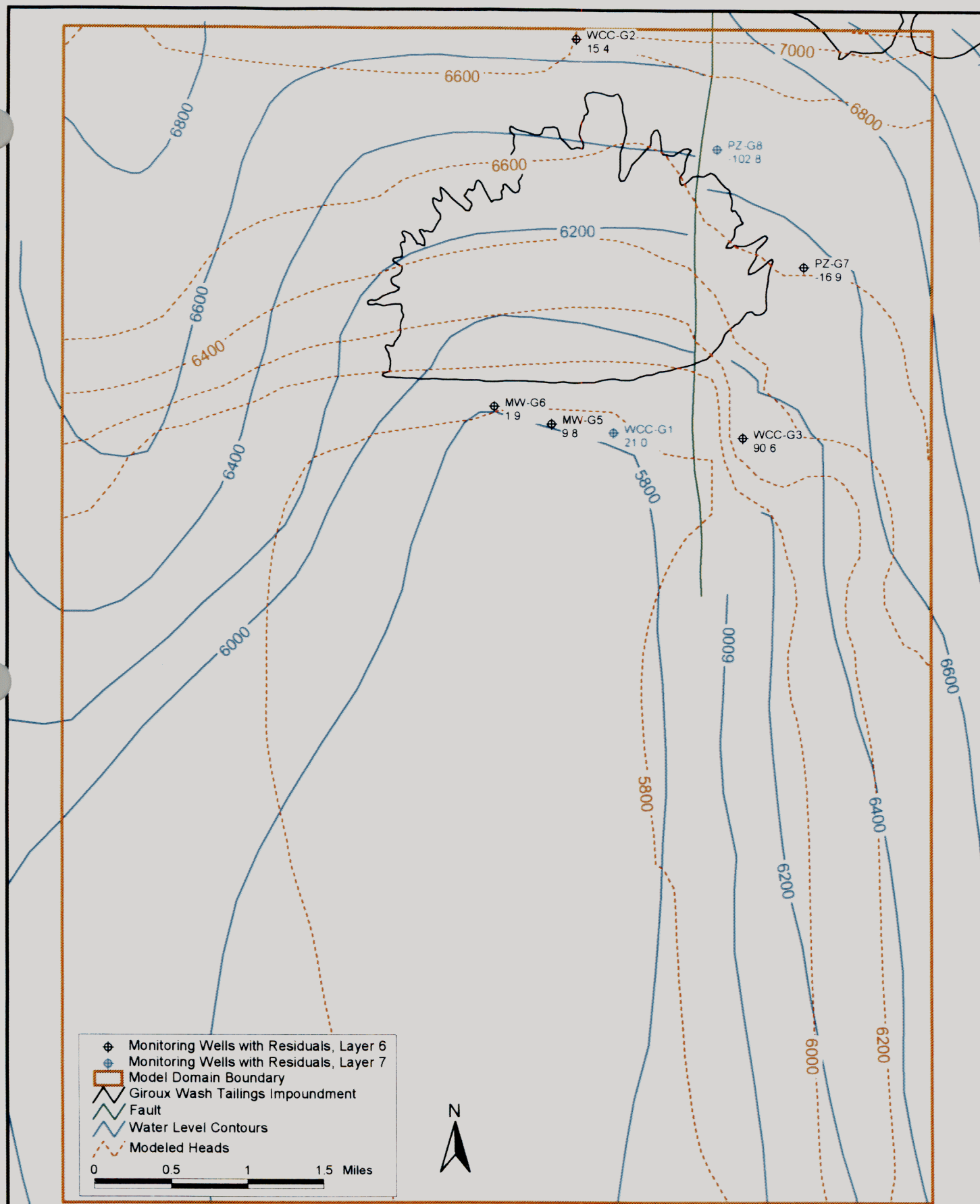


Generation  
Date:  
10/13/97

Figure 5-10. Calibrated Summary of Steady-State Flow Model.



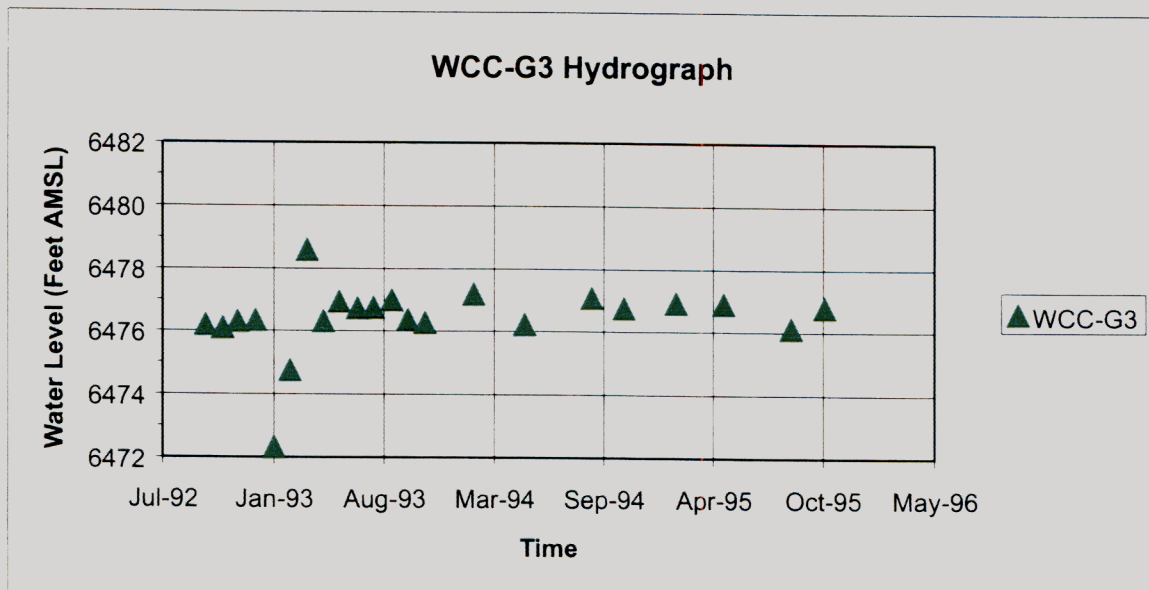
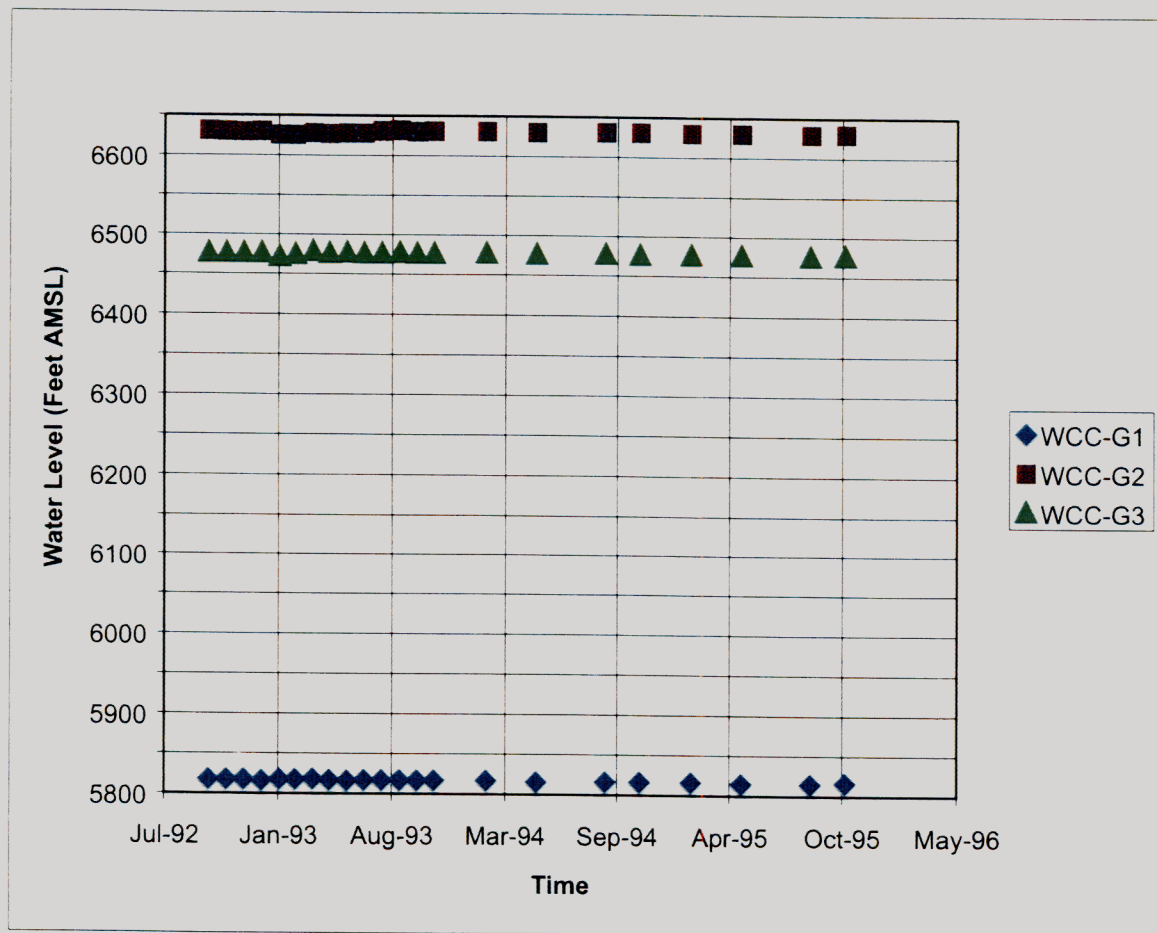




Generation  
Date:  
8/6/97

Figure 5-11.  
Observed vs. Predicted Water Table Map, Layer 6.

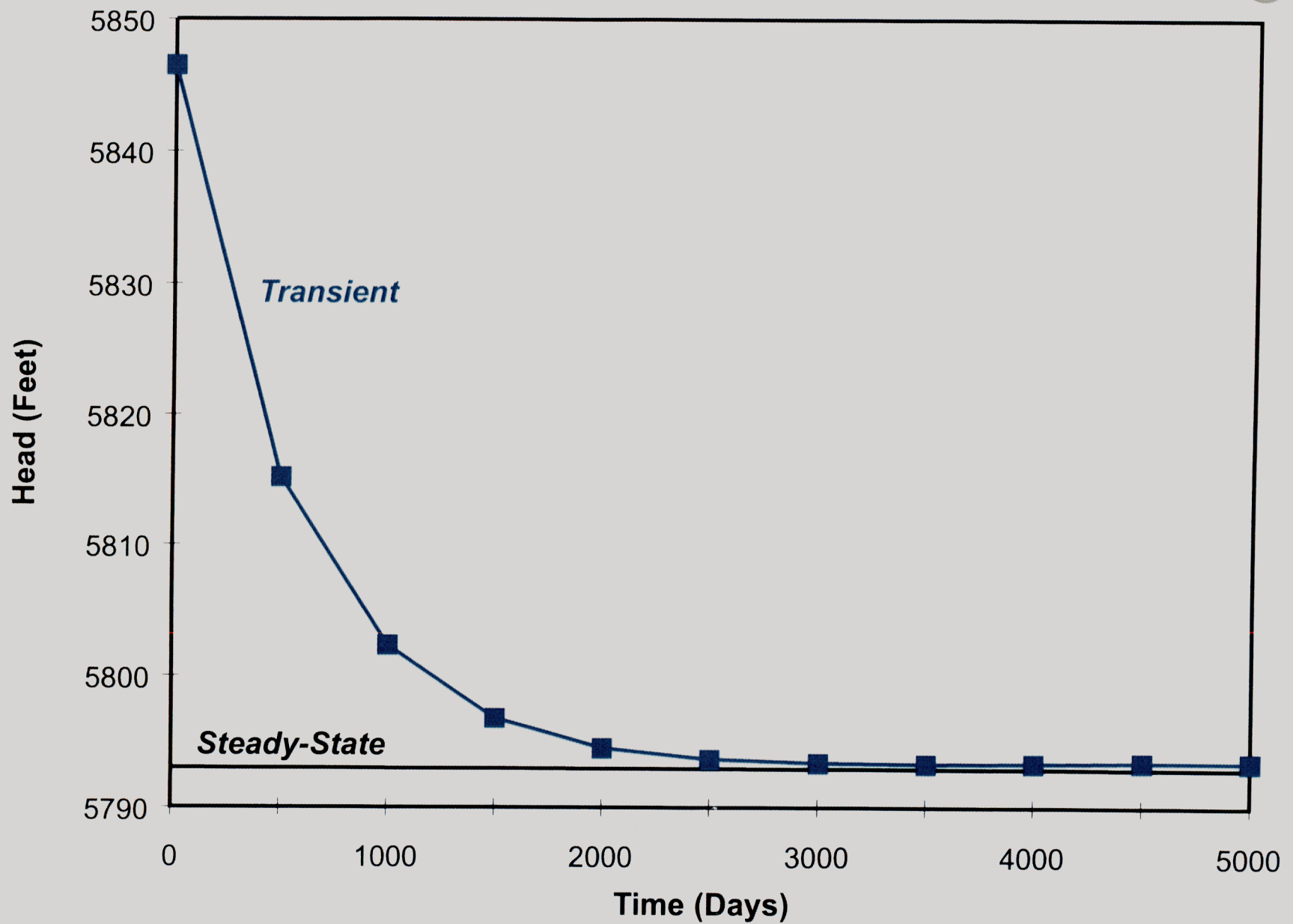




Generation  
Date:  
8/5/97

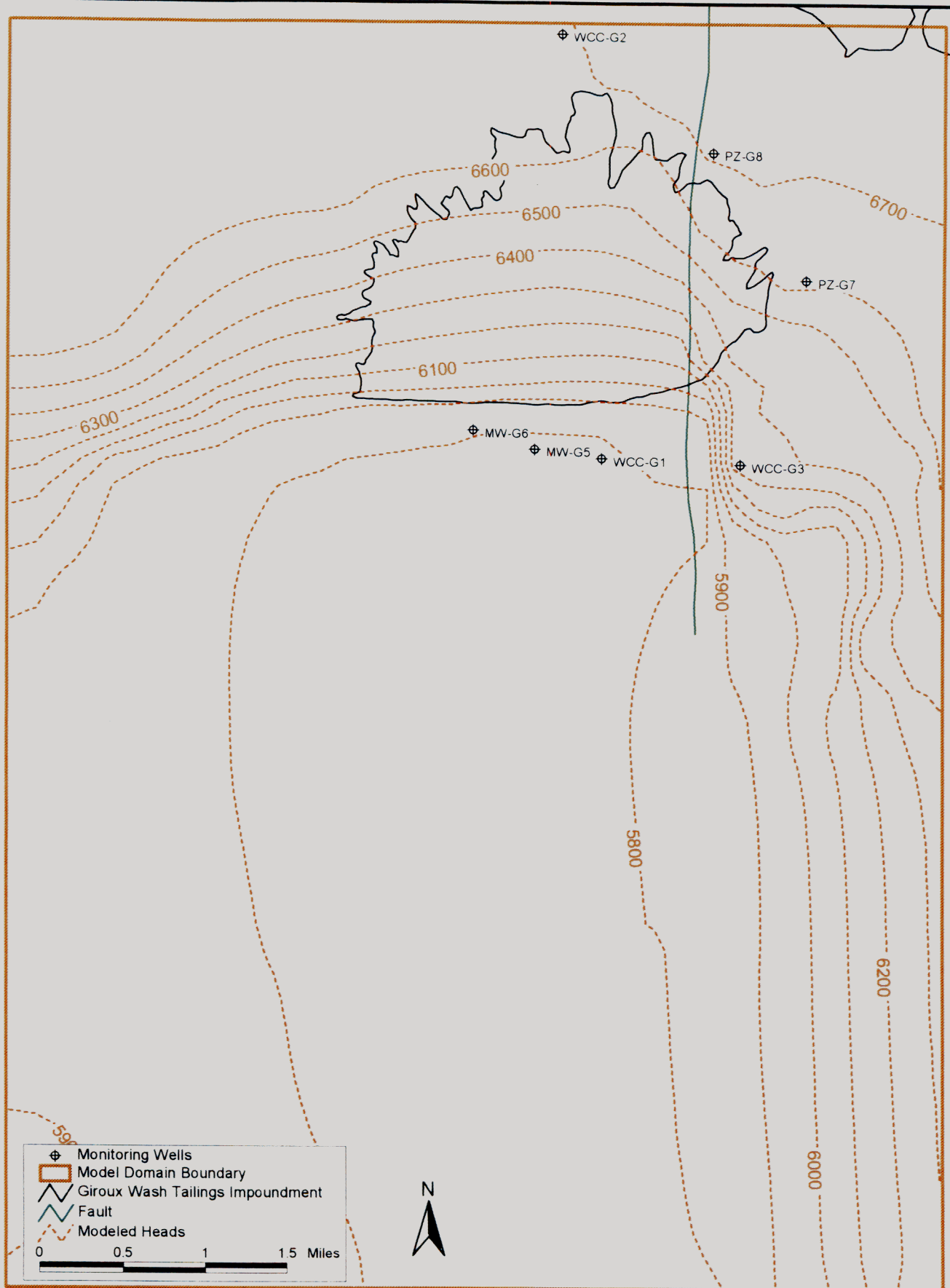
Figure 5-12. Giroux Wash Area Hydrographs.





Generation  
Date:  
8/8/97

Figure 5-13. Comparison of Transient *versus* Steady-State Heads.



Generation  
 Date:  
 8/7/97

Figure 5-14.  
 Predicted Water Table Map, Layer 6, at 100 Years.



## 6. Transport Modeling

The MT3D96 solute transport model was employed to predict aqueous-phase concentrations of sulfate downgradient of the Giroux Wash Tailings Impoundment. This solute transport code was linked to MODFLOW results to incorporate groundwater flows and heads; it was linked to HYDRUS\_2D to incorporate the sulfate concentrations infiltrated downward to the water table. Flow modeling results for the unsaturated and saturated zones that were input to the transport model assumed that climate-controlled parameters such as recharge and evapotranspiration did not change over the life of the simulations. Therefore, these results assume no changes to weather patterns over this region of Nevada for thousands of years.

### 6.1 Conceptual Transport Model

Figure 4-2 depicts the conceptual migration of solute from the floor of the tailings impoundment through the vadose zone and to groundwater aquifers. Surface water disposed of in the impoundment will infiltrate the vadose zone and then migrate vertically to the water table.

### 6.2 Mathematical Model

Transport of COCs at the site was modeled by using the numerical, fully three-dimensional code MT3D. The code solved the advection-dispersion equation (e.g., Zheng 1992):

$$R \frac{\partial C}{\partial t} = \frac{\partial}{\partial x_i} \left( D_{ij} \frac{\partial C}{\partial x_j} \right) - \frac{\partial}{\partial x_i} (v_i C) + \frac{q_s}{\theta} C_{ss} - \lambda \left( C + \frac{\rho_b}{\theta} C_s \right), \quad (6-1)$$

where

$R$  is the retardation factor (dimensionless),

$C$  is chemical concentration in groundwater ( $ML^{-3}$ ),

$t$  is time ( $T$ ),

$x_i$  values are the Cartesian coordinate axes ( $L$ ),

$D_{ij}$  is the hydrodynamic dispersion tensor ( $L^2T^{-1}$ ),

$v_i$  values are the components of average linear groundwater velocity ( $LT^{-1}$ ),

$q_s$  is the volumetric flux of water per unit volume of aquifer representing sources and sinks ( $T^{-1}$ ),

$\theta$  is porosity (dimensionless),

$C_{ss}$  is the concentration of sources or sinks ( $ML^{-3}$ ),

$\lambda$  is the first-order degradation-rate constant ( $T^{-1}$ ),

$\rho_b$  is bulk density ( $ML^{-3}$ ), and

$C_s$  is chemical concentration sorbed to the porous medium ( $MM^{-1}$ ).



The hydrodynamic dispersion tensor was defined by previous authors (e.g., Zheng 1992):

$$D_{xx} = \alpha_L \frac{v_x^2}{|v|} + \alpha_{TH} \frac{v_y^2}{|v|} + \alpha_{TV} \frac{v_z^2}{|v|} + D^* , \quad (6-2)$$

$$D_{xy} = D_{yx} = (\alpha_L - \alpha_{TH}) \frac{v_x v_y}{|v|} , \quad (6-3)$$

where

$\alpha_L$  is the longitudinal dispersivity (L),

$\alpha_{TH}$  is the horizontal transverse dispersivity (L),

$D^*$  is the effective molecular diffusion coefficient ( $L^2 T^{-1}$ ), and

$|v|$  is the magnitude of the velocity vector ( $LT^{-1}$ ).

There is also the third-dimensional component of this tensor that is not included here since it is similar to the horizontal component.

The retardation factor is defined as (Freeze and Cherry 1979):

$$R = 1 + \frac{\rho_b}{\phi} K_d , \quad (6-4)$$

where

$K_d$  is the partition coefficient ( $L^3 M^{-1}$ ),

$\rho_b$  is the bulk density ( $ML^{-3}$ ), and

$\phi$  is porosity (dimensionless).

MT3D solved equation 6-3 by a mixed Eulerian-Lagrangian method. The advection term was solved with the Lagrangian method by using one of three particle-tracking implementations:

- the forward-tracking method of characteristics (MOC),
- the backward-tracking modified method of characteristics (MMOC), or
- a hybrid of these two methods (HMOC).

The dispersion and chemical reaction terms were solved through a conventional explicit Eulerian block-centered finite-difference implementation.

Implementation of a numerical contaminant transport model requires the use of assumptions and approximations that simplify the physical system. The principal simplifying assumptions used in this transport model include the following:

- sorption follows a reversible linear isotherm and
- degradation follows a first-order rate-reaction law.

### **6.3 Model Design Parameters**

The average linear groundwater velocities were obtained from the MODFLOW groundwater-flow model, and they were used as input to the MT3D96 transport model.

#### **6.3.1 Solute Fluxes**

Background concentrations for sulfate and TDS were incorporated as 29 mg/L and 378 mg/L, respectively. A contaminant source was input into MT3D96 as temporal and spatially variable sulfate concentrations. The TDS concentration is assumed to be proportional to the sulfate concentration (Section 1.3). These concentrations were predicted by HYDRUS\_2D as contaminant flux through the vadose zone to the water table. Sulfate concentration flux to the groundwater system was predicted over the lateral extent of the Giroux Wash impoundment. Concentrations are predicted for beneath the impoundment during the life of the anticipated transport through the unsaturated zone (forty 5000-day stress periods). Following the 200,000 day period of sulfate transport through the unsaturated zone, all water recharging the model was assumed to be at the background groundwater concentration of 29 mg/L of sulfate.

#### **6.3.2 Dispersivity**

The estimated longitudinal dispersivity ( $\alpha_L$ ) length of 450 feet was based on the scale of the problem evaluated. An average distance from the lower center part of the impoundment, where the centroid of the plume is anticipated, to the WCC-G1 POC well is 4,500 feet. Dispersivity equal to 10% of the distance the plume will travel is a reasonable estimate (Domenico and Schwartz 1990), and the value of 450 feet was derived from this. The ratios of transverse dispersivity ( $\alpha_T$ ) to  $\alpha_L$  of 0.33 and of vertical dispersivity ( $\alpha_V$ ) to  $\alpha_L$  of 0.0533 were used from previous studies (PTI 1994).

#### **6.3.3 Molecular Diffusion**

Molecular diffusion was estimated at  $1 \times 10^{-5}$  cm<sup>2</sup>/s for the entire model domain. This value was chosen during previous site investigations (PTI 1994).

#### **6.3.4 Chemical Reactions**

No chemical reactions, including sorption or biodegradation, were assigned or simulated in the groundwater transport model. Conservative transport was assumed. Only hydrodynamic dispersion and dilution via groundwater flux through the system were responsible for attenuating sulfate concentrations.

#### **6.4 Predictive Transient Simulations**

A series of forty 5000-day stress periods (548 years, as required for the complete flushing of the vadose zone predicted by HYDRUS\_2D [Section 4.8]) was run using MT3D96 to simulate sulfate transport from the tailings impoundment area during disposal and postdisposal of processed water. During this period, all solutes from the tailings impoundment percolated to groundwater finishing with background solute concentrations throughout the vadose zone. Beyond these 40 stress periods, the transport model was then run for an additional 1,096 years at predisposal conditions, assuming steady flow, to estimate maximum sulfate concentration at the POC well WCC-G1. Groundwater flow and heads from MODFLOW were input into the transport model, and sulfate flux to the groundwater as predicted by HYDRUS\_2D was also incorporated into the model.

The suite of transport solvers was evaluated via a simple test case, and it was determined that the hybrid method of characteristics (HMOC) particle-tracking solver was appropriate for solving this field problem. HMOC gave the best combination of accuracy and processing speed. The HMOC solver uses the method of characteristics (MOC) particle-tracking algorithm in areas with sharp concentration fronts and the modified method of characteristics (MMOC) in areas without sharp concentration fronts. This solver minimizes numerical dispersion while optimizing the processing speed of the problem. Processing speed was important because the modeling was simulating multiple-layer three-dimensional transport for more than 1600 years. Numerical oscillations appeared in the upstream finite-difference model solver, and because of these instabilities, it was not deployed. The pure MMOC solver was not employed because of the potential problems with nonuniform flow fields and the possibility for advection-dominated transport. MOC required the most time to complete the test case simulation and was therefore not used.

#### **6.5 Interpretation of Modeling Results**

##### **6.5.1 Case 1—3,000 mg/L TDS and 2,100 mg/L Sulfate Source**

Simulated sulfate concentrations reach a maximum of approximately 41 mg/L, 750 years in the future at the POC well, WCC-G1 (Figure 6-1). This value is an increase of only 12 mg/L above the naturally occurring groundwater sulfate concentrations. Sulfate concentrations are predicted to plateau for several hundred years and then gradually decrease at the POC well after 1,200 years. The modeled sulfate

concentrations remained above the background concentrations for the remainder of the simulation, but steadily decreased.

A breakthrough curve for TDS at the POC well, assuming a 3,000 mg/L source concentration, is shown in Figure 6-2. Predicted TDS concentrations can be scaled to the modeled sulfate concentrations because there is a linear relationship between sulfate and TDS concentrations in the infiltrating water. By adjusting the predicted increases in sulfate concentrations by the ratio of TDS to sulfate concentration for a 3,000 mg/L concentration source in the impoundment, the resulting increases in TDS concentrations at the POC well can be calculated. At 750 years in the future, the TDS concentrations at the POC well reach a maximum of 395 mg/L.

It can be interpreted from these breakthrough curves (Figures 6-1 and 6-2) that sulfate and TDS will not exceed 41 and 395 mg/L, respectively. These values are below the State of Nevada Drinking Water Standards. The highest concentrations of these two constituents at the POC well will not be realized until approximately 750 years after disposal was initiated.

Isoconcentration maps constructed at 96 years in the future show that sulfate reaches highest concentrations in layer 5, with a maximum simulated value of 204 mg/L (Figure 6-3). Lower concentrations are predicted in layer 6 and 7, in which the maximum levels simulated at 96 years are 64 mg/L and 41 mg/L respectively (Figures 6-4 and 6-5). Maximum solute flux to the water table is predicted approximately 96 years from the present. The modeled concentrations 548 years in the future are displayed for layers 6 and 7 in Figures 6-6 and 6-7, respectively. Maximum sulfate concentrations after 548 years are predicted as 90 mg/L in layer 6 and 62 mg/L in layer 7 beneath the impoundment structure. The total mass of disposed water will be flushed through the vadose zone by 548 years after disposal operations cease.

Sulfate concentrations for layers 6 and 7 after 1,644 years of transport are shown in Figures 6-8 and 6-9, respectively. The maximum concentrations are 49 mg/L and 55 mg/L for layers 6 and 7, respectively. This transport time is after the predicted sulfate concentrations at the POC have begun to gradually decrease.

#### **6.5.2 Case 2—4,000 mg/L TDS and 2,400 mg/L Sulfate Source**

A breakthrough curve for TDS and sulfate constituents, assuming a 4,000 mg/L source, at the POC well is included (Figure 6-10). Predicted TDS concentrations can be scaled to the modeled sulfate concentrations because there is a linear relationship between sulfate and TDS concentrations in the infiltrating recharge water. By adjusting the predicted increases in sulfate concentrations by the ratio of TDS to sulfate concentration for a 4,000 mg/L concentration source in the impoundment, the resulting TDS concentrations at the POC well peak at slightly less than 400 mg/L.

Maximum sulfate concentrations will occur at the same time as in Case 1, but are estimated to be approximately 44 mg/L. This estimate was obtained by taking the ratio of sulfate concentration at the source for Case 2 to that for Case 1 (2,760 mg/L : 2,100 mg/L) and multiplying modeled increases in sulfate concentrations by that value.

#### **6.5.3 Case 3—5,000 mg/L TDS and 3,000 mg/L Sulfate Source**

A breakthrough curve for TDS and sulfate constituents, assuming a 5,000 mg/L source, at the POC well is included (Figure 6-11). The same relationships as described above were incorporated to predict TDS concentrations for a 5,000 mg/L source. By adjusting these predicted values for a 5,000 mg/L concentration source in the impoundment, the resulting TDS concentrations in the POC well in layer 7 reach maximum concentration of 405 mg/L.

Maximum sulfate concentration will occur at the same time as in Case 1, but is estimated to be approximately 48 mg/L. This estimate was obtained by taking the ratio of sulfate concentration at the source for Case 3 to that for Case 1 (3,450 mg/L : 2,100 mg/L) and multiplying modeled sulfate concentrations by that value.

#### **6.5.4 Simulations of the Barge-Operating Channel**

A series of barge-operating scenarios was simulated to evaluate a range of possible events from the most likely to the worst-case. The times of solute breakthrough to the water table and of complete solute removal from the vadose zone are dependent on the flow rates through the vadose zone. However, a faster breakthrough in the western part of the impoundment does not necessarily correspond to a change in predicted groundwater concentrations because breakthrough in this area will not occur until well after impoundment closure. By the time infiltrating solutes reach the water table, the infiltration rate through the vadose zone is controlled by the ambient recharge rate. Hence, when compared to the original modeling scenario, breakthrough from the barge-operating channel happens sooner, but by the time solutes flux to the water table, the percolation rate and solute fluxes are comparable between the two scenarios.

##### **6.5.4.1 10-Foot-Deep Barge-Operating Channel in Addition to a 5-Foot Ponding Depth**

The barge-operating channel area will make up a small portion (<1%) of the ultimate impoundment footprint, lying solely above the western part of Giroux Wash where the water table is deepest (>750 feet). The small areal extent of the barge-operating channel and its lack of influence on the eastern part of the impoundment reduced the significance of infiltration from the supernatant pond to the water table.

The barge-operating channel area of the impoundment was modeled by assuming a 10-foot ponding depth with a 5-foot head applied to the rest of the impoundment. This



scenario resulted in little change to the magnitude of the solute concentration reaching the water table and the rate at which the solutes entered the groundwater. The primary change caused by the imposition of a 10-foot head in the barge-operating channel area was that solute breakthrough in the western part of the impoundment occurred approximately 35 years sooner (Figure 6-12). The barge-operating channel resides solely in the western part of the impoundment and does not influence model results for the eastern part of the impoundment, where the 5-foot head would actually not occur with the operation of the channel.

If the barge-operating channel is maintained at a 10- to 15-foot head on the western part of the impoundment, there will be little variability in the solute concentration and flow rate at the water table owing to the depth of the vadose zone there. In the western part, infiltration will not reach the water table for more than 100 years after impoundment closure. Even under the increased recharge rate resulting from operating the barge-operating channel, the solute front will percolate less than half the distance to the water table during the 16-year impoundment operation. After closure, the transport mechanism will be dominated by the rate of ambient recharge. Hence, concentrations and flow rates at the water table are similar to the three modeled cases (Sections 6.5.1 through 6.5.3). However, the solute front in the barge-operating channel area has a "head start" over the solute front in other areas and, hence, will reach the water table sooner.

#### *6.5.4.2 10-Foot-Deep Barge-Operating Channel Without 5-Foot Ponding Depth*

The effects of infiltration due to a 10-foot barge-operating channel without the 5-foot head across the impoundment had little influence on the solute concentrations reaching the water table on the western side of the impoundment. The solute front under the barge-operating channel area will reach groundwater as described above. The solute front under the remainder of the western part of the impoundment would reach the groundwater approximately 84 years later than in the 5-foot head case (Figure 6-13).

The effects on the solute concentration reaching the water table on the eastern side of the impoundment were more significant. Although the solute concentrations in the pore water of the vadose zone did not change, the flow rate during impoundment operation was reduced by a factor of 6. Hence, the solutes would reach the water table in the eastern part approximately 11 years later than in the 5-foot head case (Figure 6-14). In addition, the rate at which this infiltration would enter the groundwater was 6 times slower. Therefore, the rate of solute transport to the groundwater is reduced by a factor of 6, and the predicted solute concentration observed in the groundwater was reduced.

#### **6.5.4.3 Constant 5-Foot Ponding Depth vs. Barge-Operating Channel Modeling**

From results reported in Sections 6.5.1 and 6.5.4.2, it is apparent that applying a constant 5-foot head across the impoundment maximizes solute concentrations and minimizes travel times compared to the application of the barge-operating channel. This result is due to the relatively shallow depth to groundwater in the eastern part of the impoundment and the fact that the barge-operating channel will be located solely in the western part of the impoundment. The 750-foot depth to groundwater in the western part of the impoundment mitigates any significant difference between the 5-foot head and 10-foot head applied to the barge-operating channel area. However, removing the 5 feet of head from the eastern part of the impoundment results in a reduction of the solute concentrations predicted in the groundwater. Predicted groundwater sulfate concentrations at the location of the Case 1 maximum (Section 6.5.1) decrease from 204 mg/L to 110 mg/L. In contrast, predicted groundwater sulfate concentrations in the barge-operating channel increase a minimal amount from 62 mg/L to 79 mg/L.

#### **6.5.5 Maximum Solute Concentrations at the Vadose Zone/Water Table Interface**

The predicted sulfate and TDS concentrations using the 5-foot head assumption are greatest at a location in the northeast part of the tailings impoundment. The concentrations in the infiltrating water and the resulting increase in the groundwater are shown in Figures 6-15 and 6-16 for the Case 1 sulfate and TDS source concentrations, respectively.

### **6.6 Model Limitations and Assumptions**

These simulations assume that there are no major climatological changes in this area of Nevada over the entire simulation length. The simulations were conducted for almost 2,000 years, given the rate of groundwater flow compared to the size of the model domain, making the lack of climatological change an important assumption. However, a discussion on model sensitivity provided in Section 4.9 identifies that climatological variation will not significantly increase predicted concentrations.

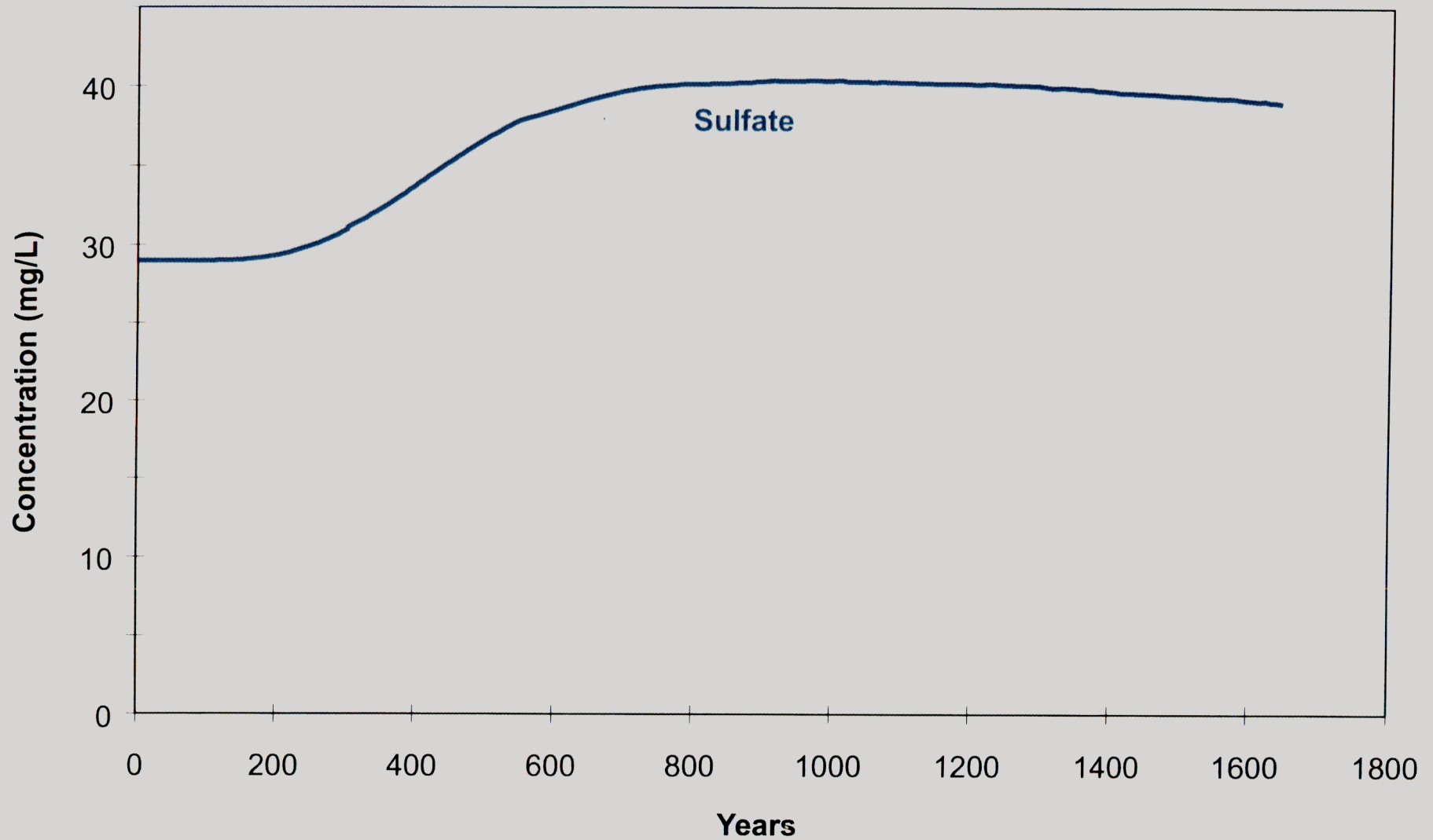
The limited area for the transport model simulation owing to the interest focused on the POC well (WCC-G1) constrained the predictive results to the immediate vicinity of Giroux Wash. Predictions of the fate of the sulfate and TDS far downgradient of the WCC-G1 monitoring well were not completed during this investigation. Although having initial conditions would have enabled checking the assumed dispersivity and other solute transport parameters, there were no initial conditions to calibrate the solute transport model to.

The resolution of the modeled sulfate concentrations reflect the model domain discretization. The vertical discretization results in an averaging of the solute concentrations through out the individual model cell thickness (200 feet  $\times$  200 feet).

The conservative assumptions of no attenuation of the TDS and sulfate built into the three groundwater solute transport cases represent a worst case scenario for the sulfate transport in the ground water.

**Table 6-1. Solute Transport Properties Used in Model**

Parameter	Value	Reference
Longitudinal dispersivity ( $\alpha_L$ )	450 feet	10% of the distance from POC to the lower center of impoundment
Transverse dispersivity ( $\alpha_T$ )	150 feet	Ratio of $\alpha_T$ to $\alpha_L$ used by PTI (1994)
Vertical dispersivity ( $\alpha_v$ )	24 feet	Ratio of $\alpha_v$ to $\alpha_L$ used by PTI (1994)
Porosity ( $\phi$ )	0.25 or 0.08	See Table 5-2
Molecular diffusion	$1 \times 10^{-5} \text{ cm}^2/\text{day}$	PTI (1994)
Partition coefficient ( $K_d$ )	0	Conservative transport assumption
Decay constant $K$	0	Conservative transport assumption

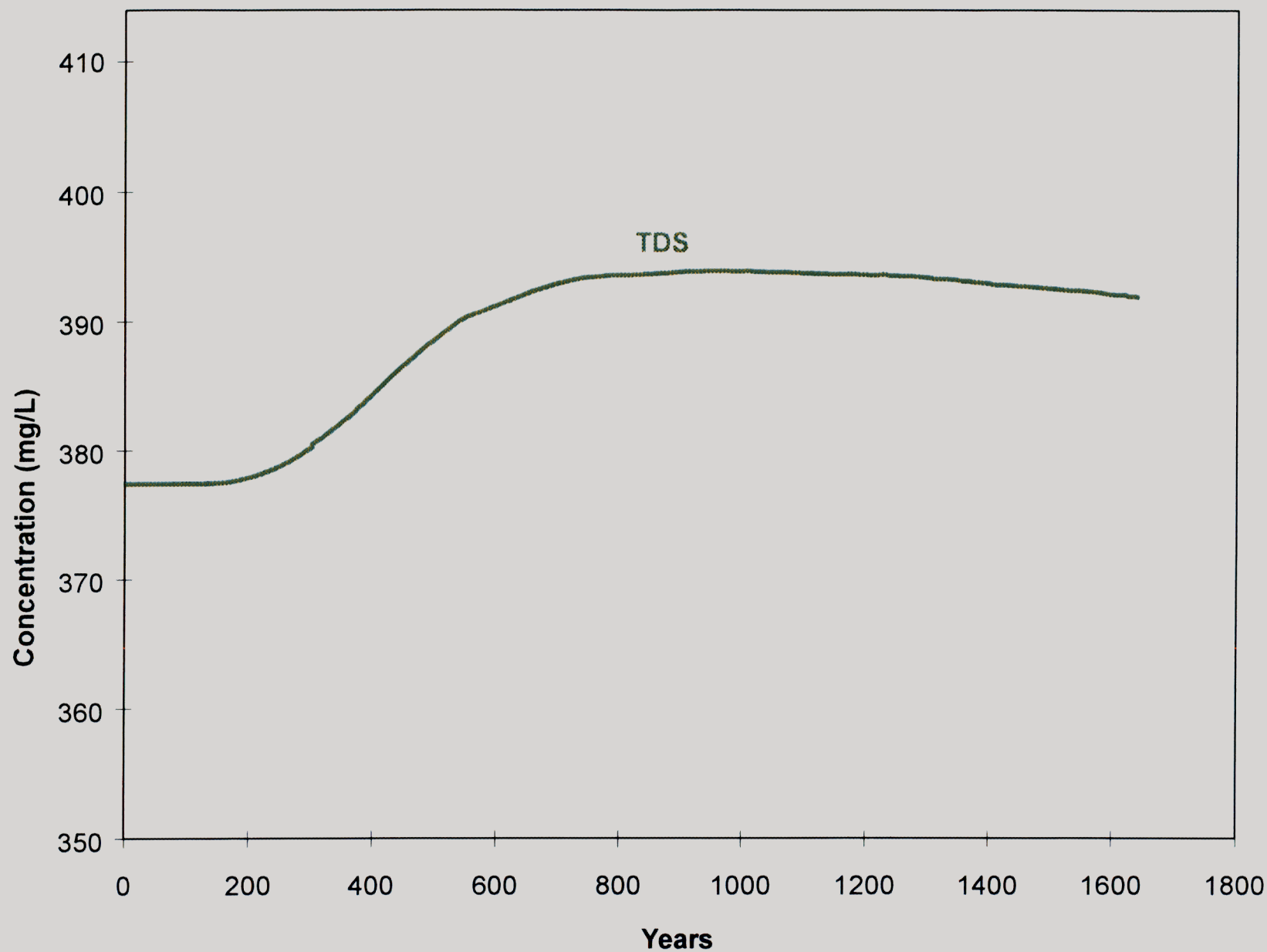


Generation  
Date:  
8/7/97

Figure 6-1. Modeled Sulfate Concentrations *versus* Time  
at WCC-G1 Assuming 3,040 mg/L TDS Source.



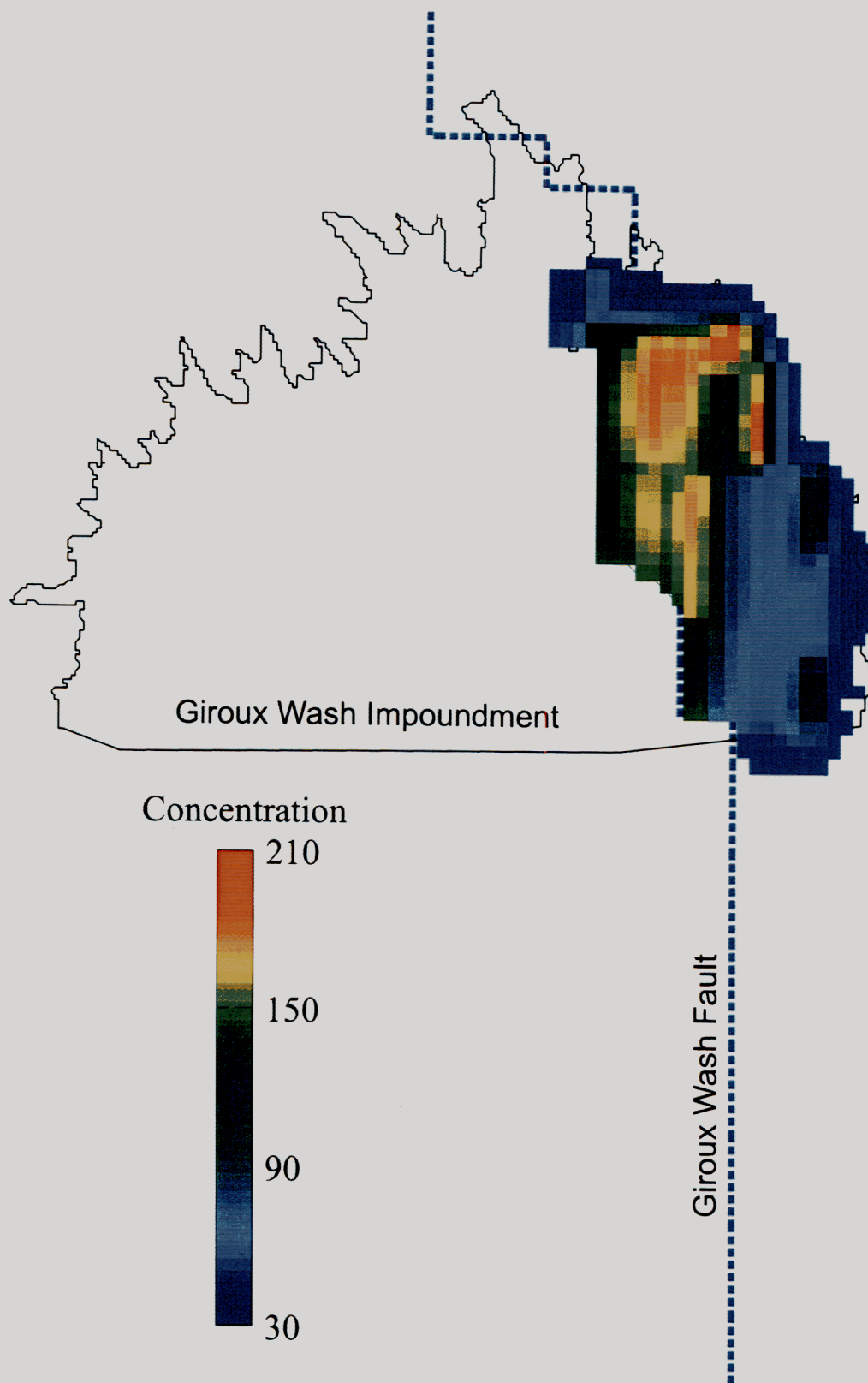




Generation  
Date:  
8/7/97

Figure 6-2. Modeled TDS Concentrations *versus* Time  
at WCC-G1 Assuming 3,040 mg/L TDS Source.

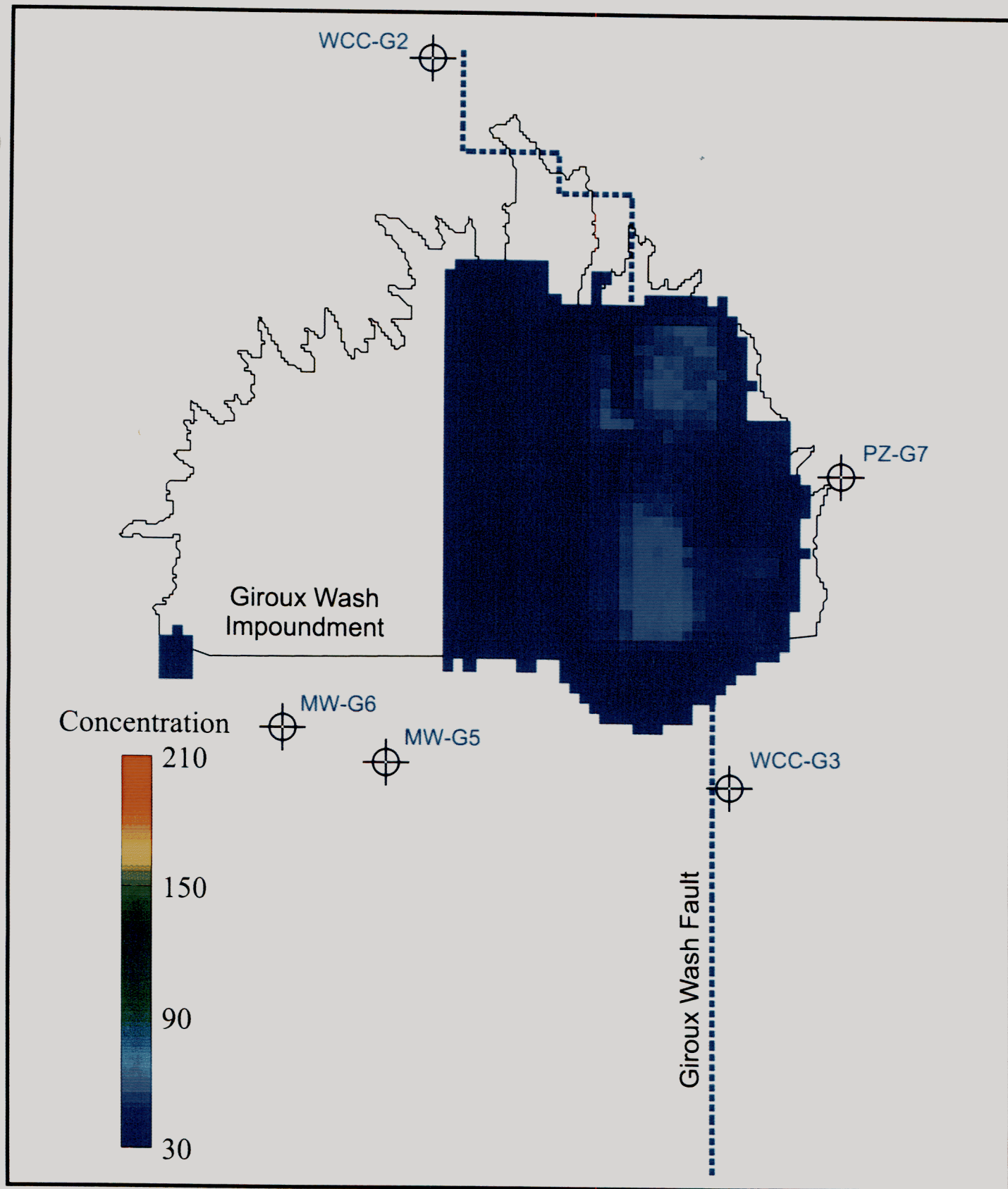




Generation  
Date:  
8/6/97

Figure 6-3. Predicted Sulfate Isoconcentrations  
in Layer 5 at 96 Years.

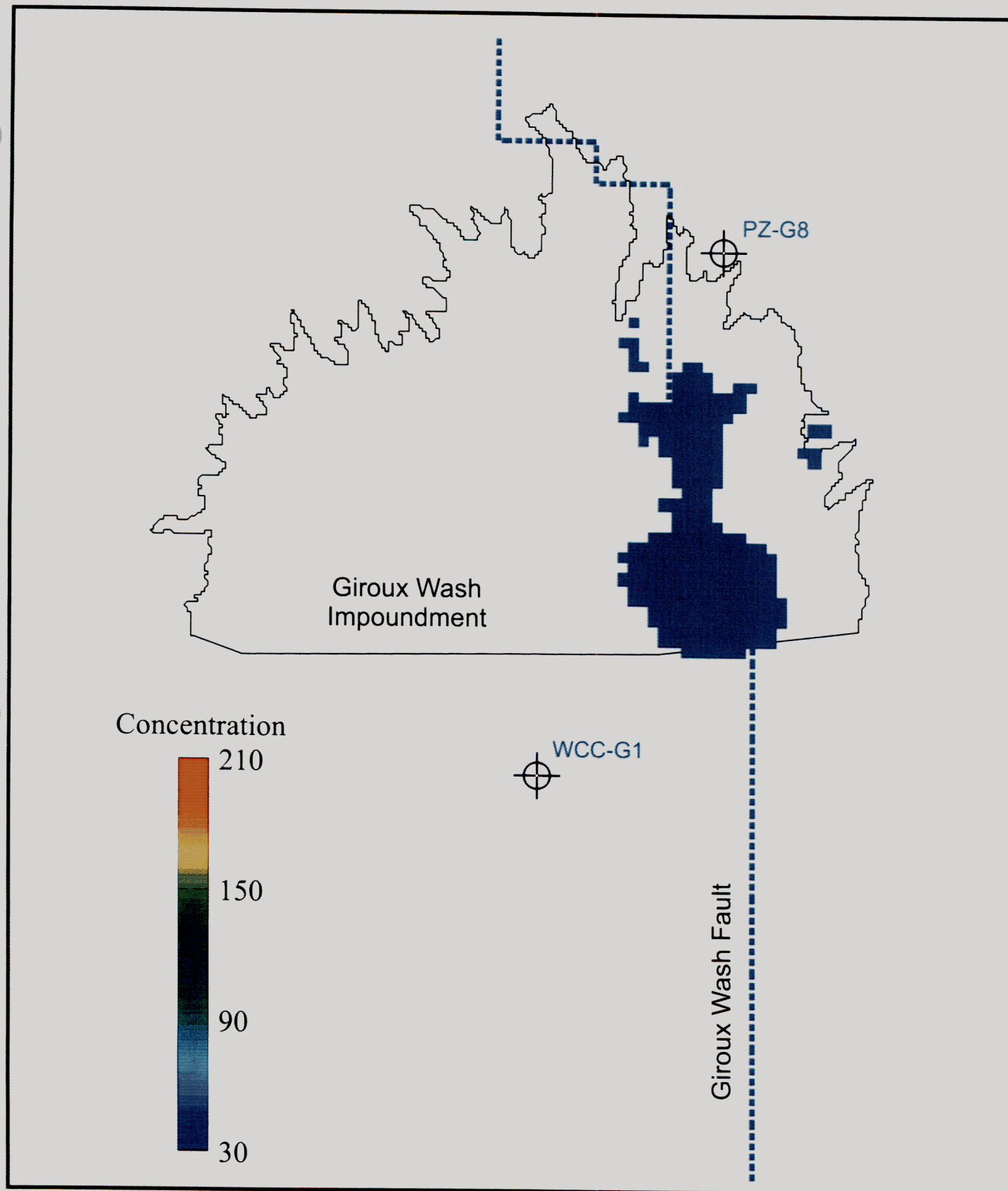
  
**Geomega**



Generation  
Date:  
8/6/97

Figure 6-4. Predicted Sulfate Isoconcentrations  
in Layer 6 at 96 Years.



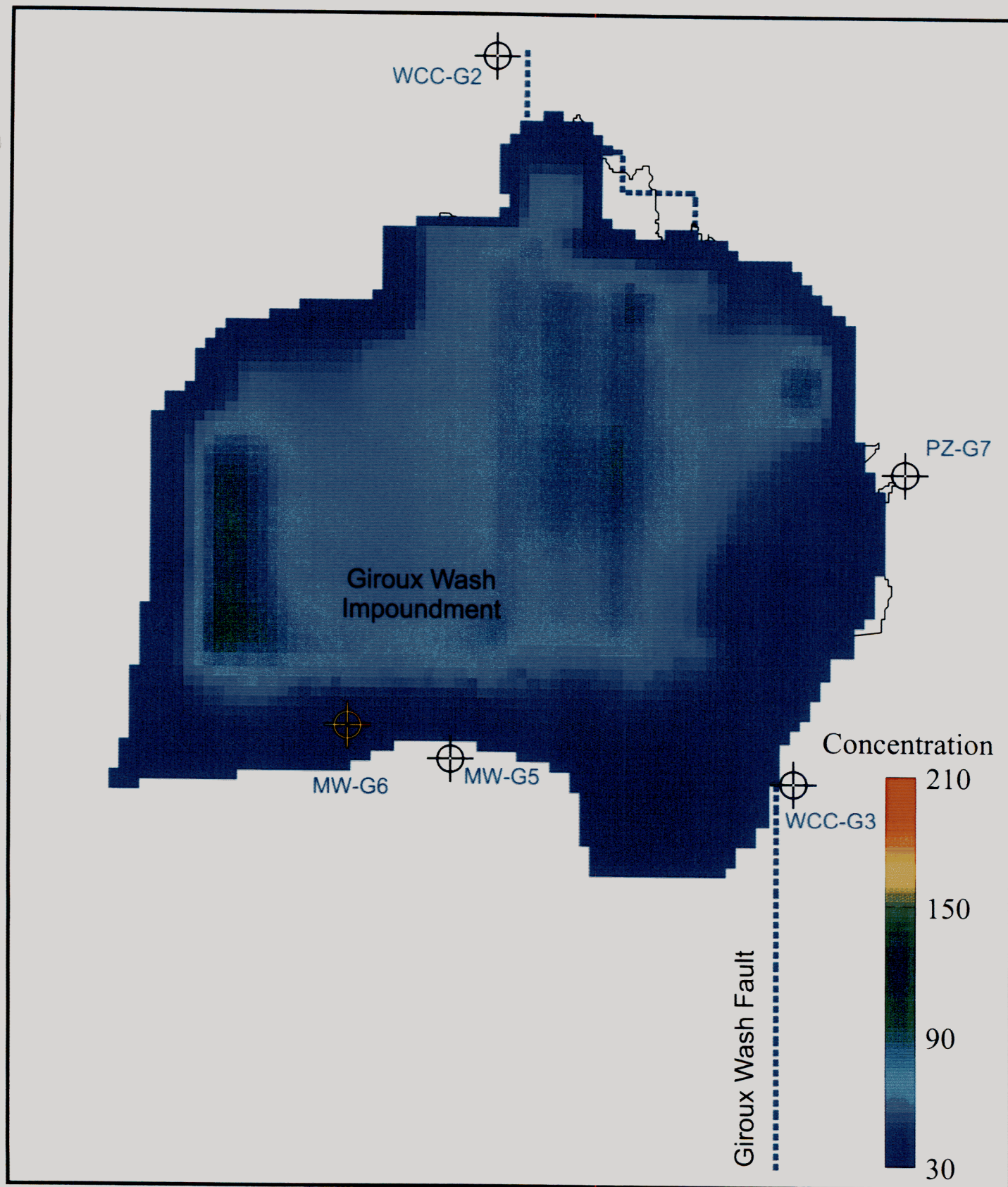


Generation  
Date:  
8/6/97

Figure 6-5. Predicted Sulfate Isoconcentrations  
in Layer 7 at 96 Years.





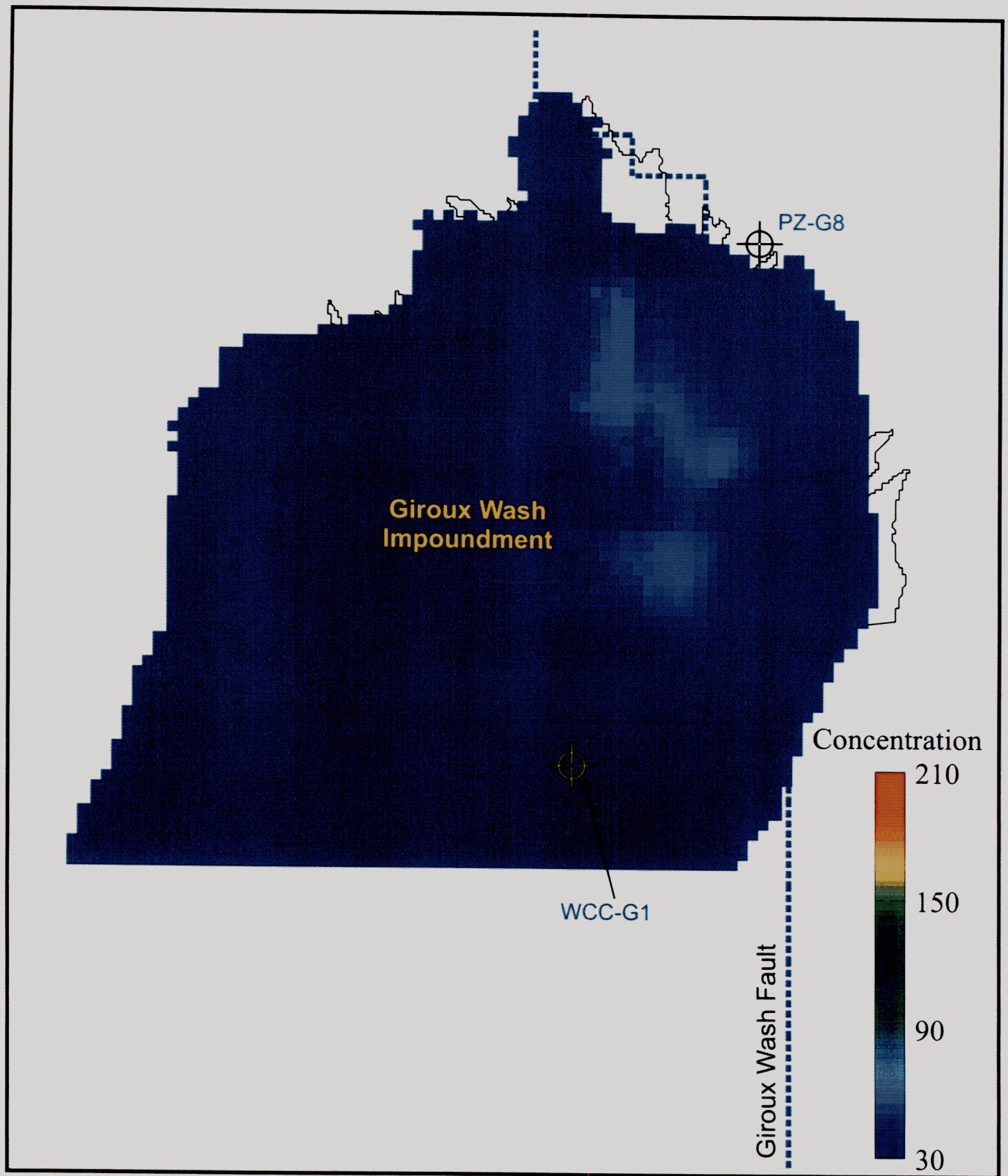


Generation  
Date:  
8/7/97

Figure 6-6. Predicted Sulfate Isoconcentrations  
in Layer 6 at 548 Years.

  
**Geomega**



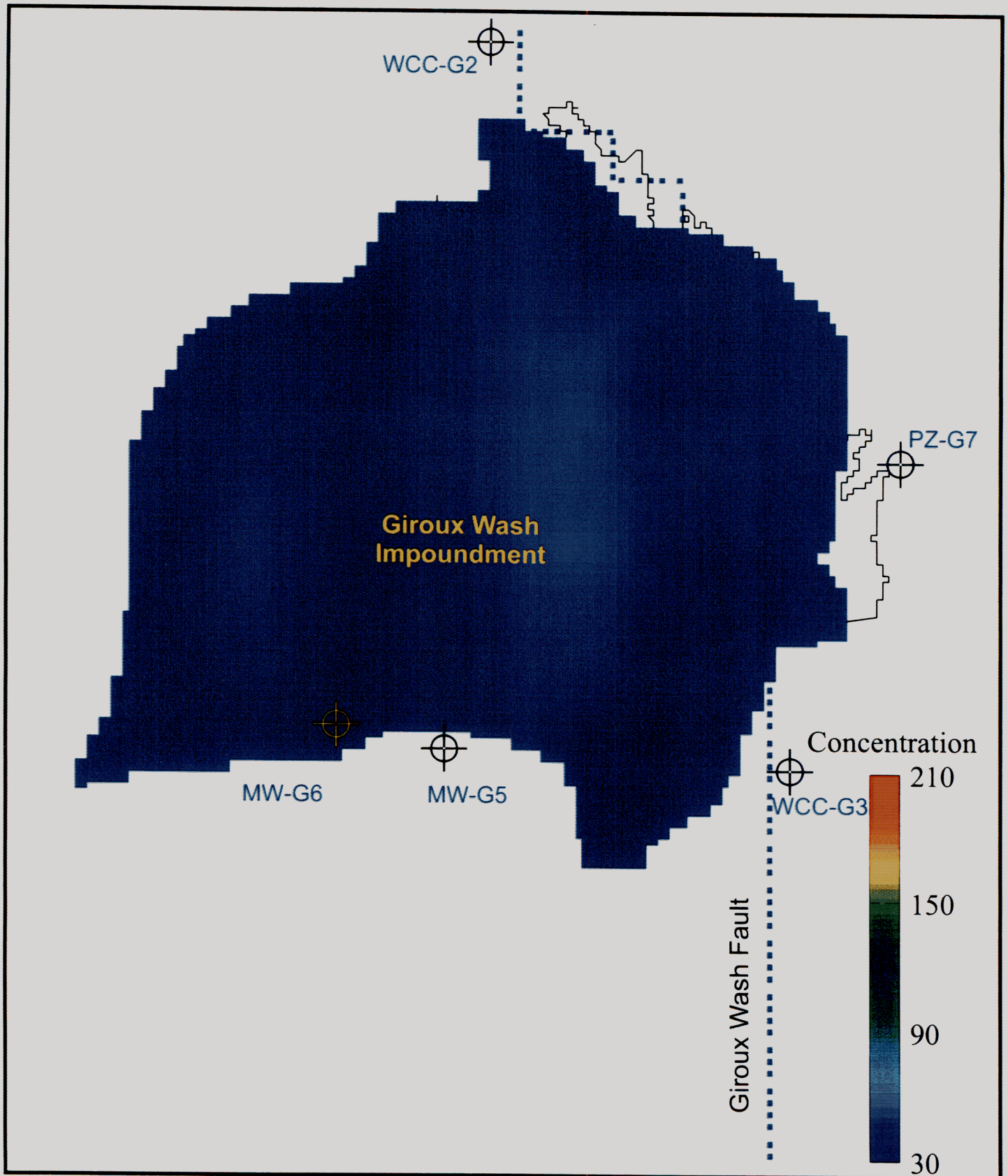


Generation  
Date:  
8/7/97

Figure 6-7. Predicted Sulfate Isoconcentrations  
in Layer 7 at 548 Years.





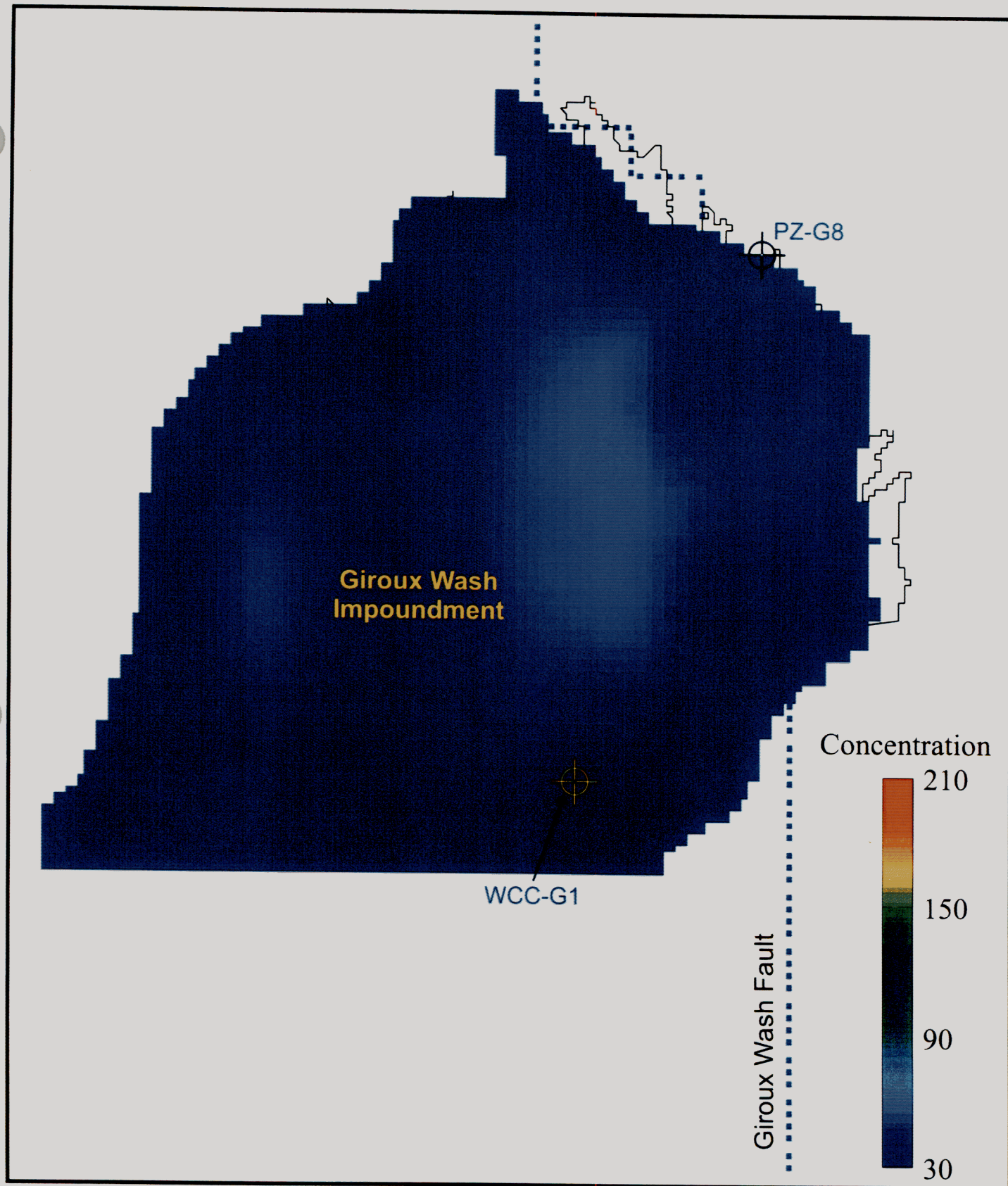


Generation  
Date:  
8/7/97

Figure 6-8. Predicted Sulfate Isoconcentrations  
in Layer 6 at 1644 Years.

  
**Geomega**

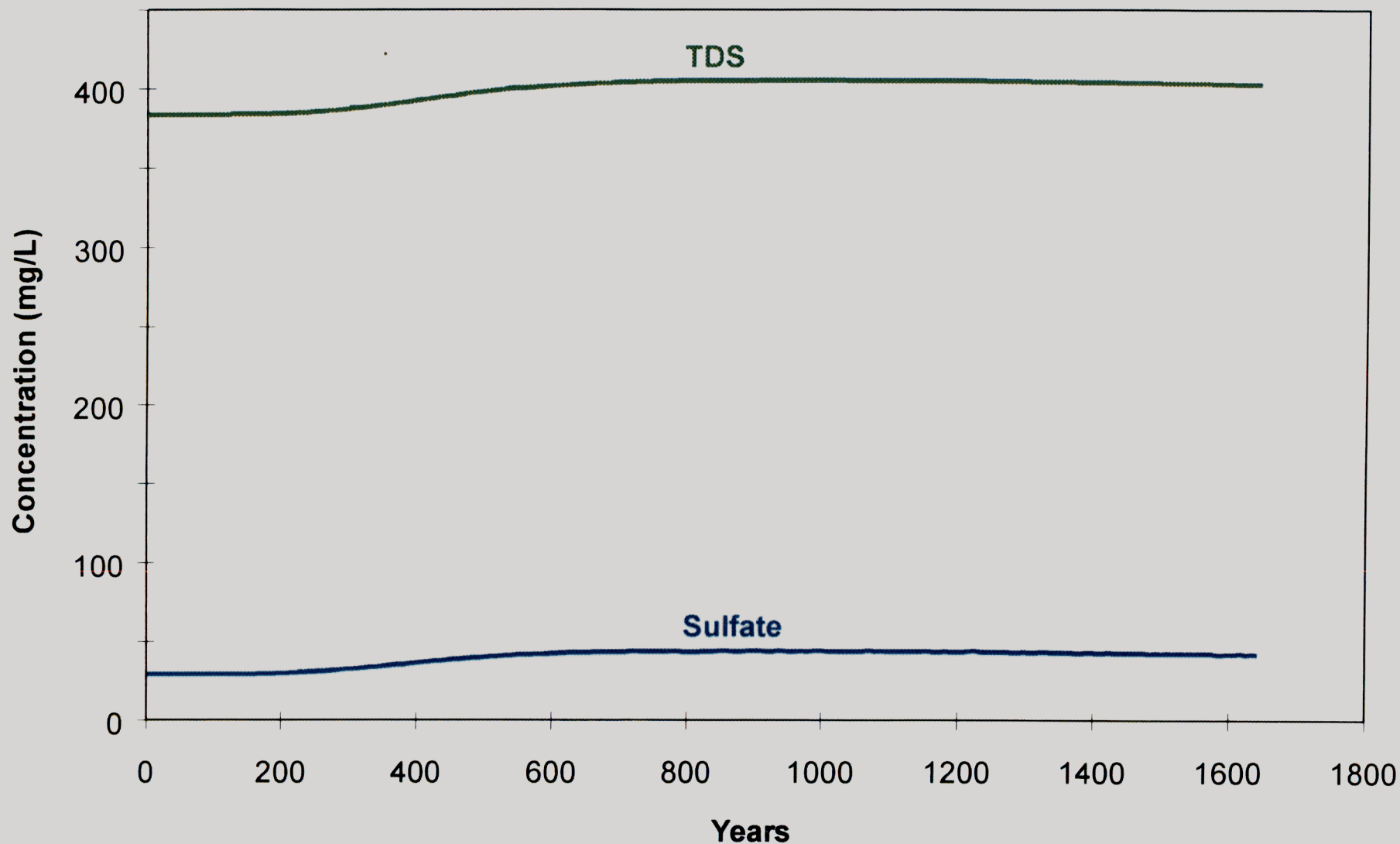




Generation  
Date:  
8/7/97

Figure 6-9. Predicted Sulfate Isoconcentrations  
in Layer 7 at 1644 Years.

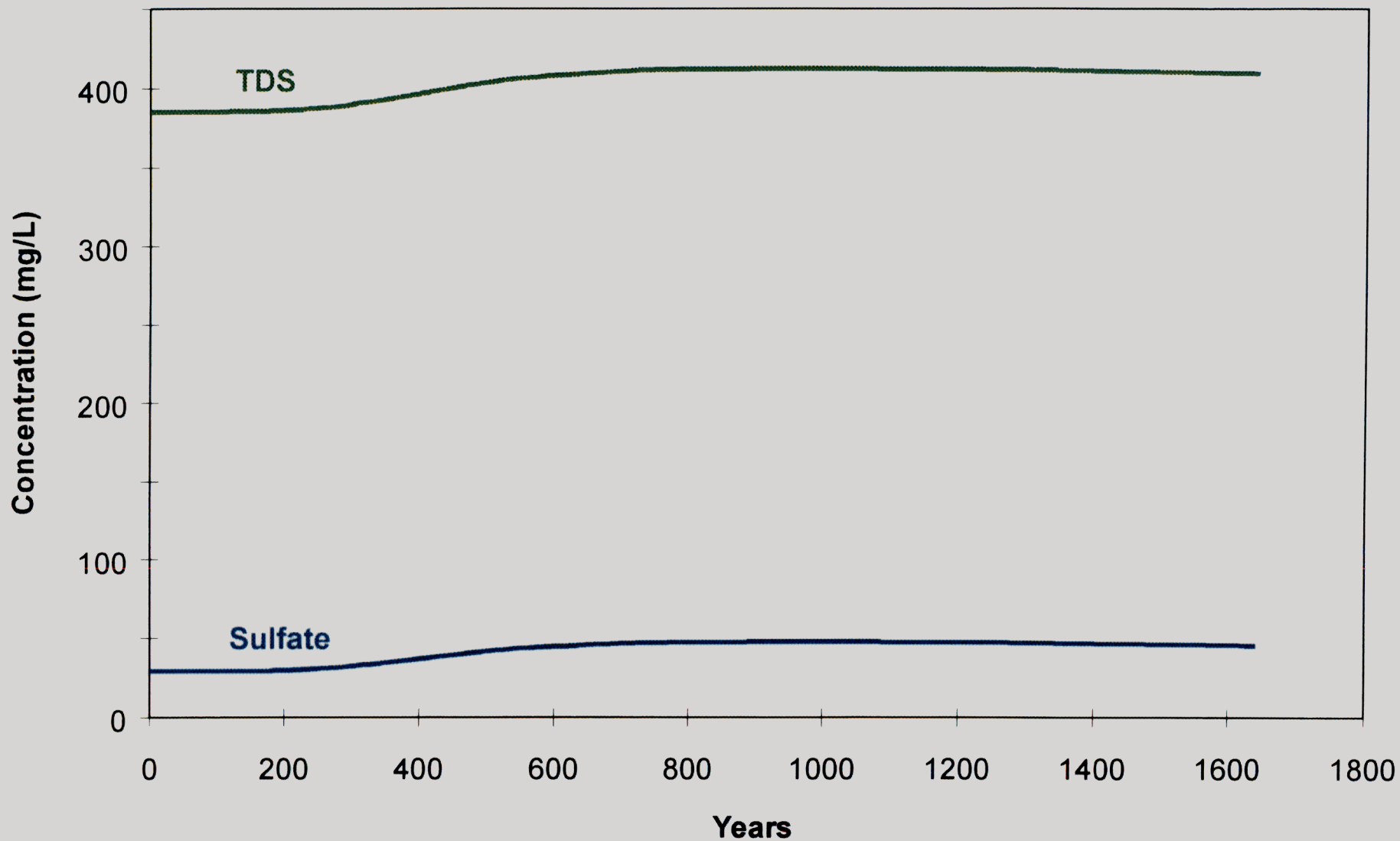




Generation  
Date:  
8/7/97

Figure 6-10. Modeled Sulfate and TDS Concentrations *versus* Time  
at WCC-G1 Assuming 4,000 mg/L TDS Source.

  
**Geomega**

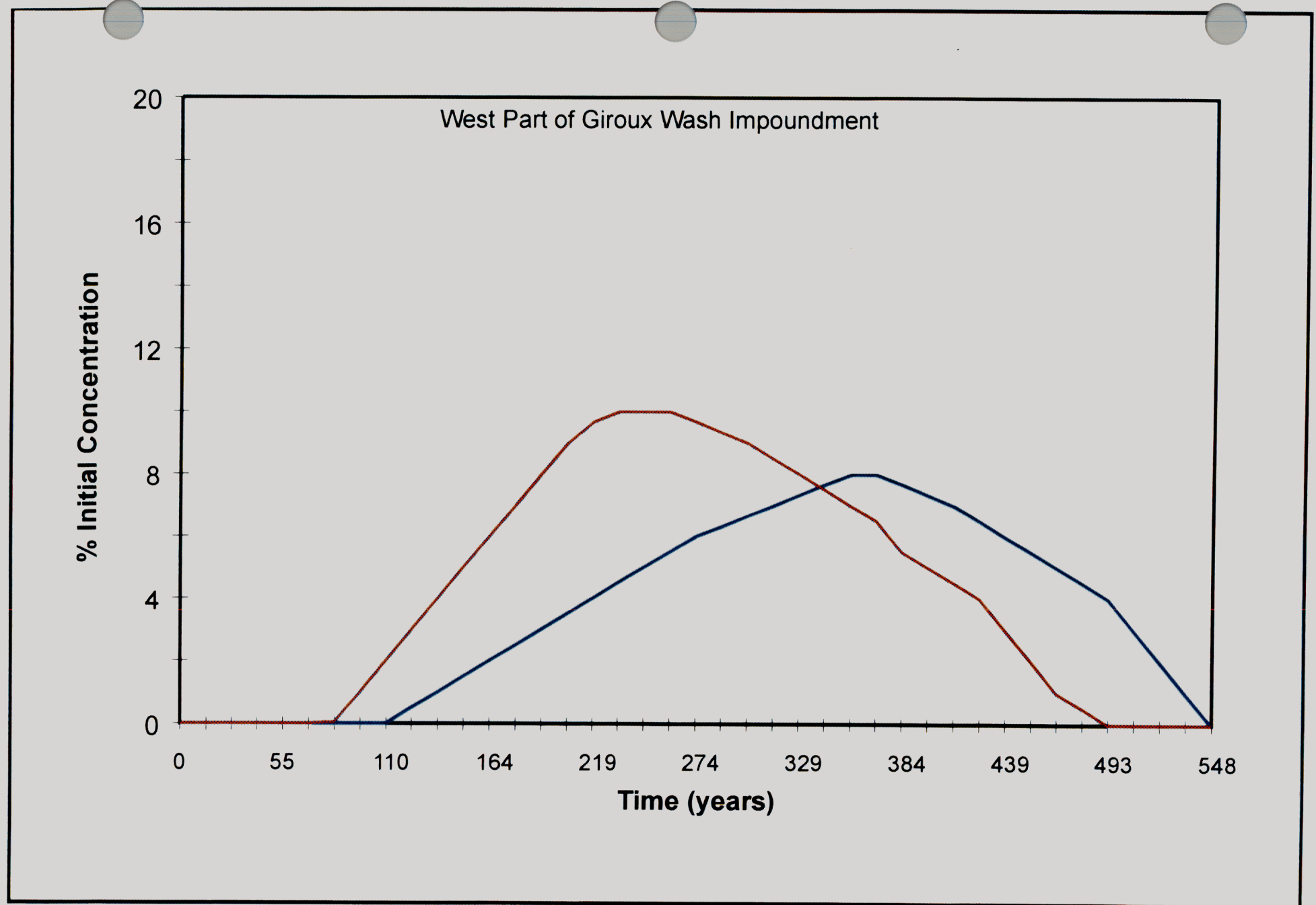


Generation  
Date:  
8/7/97

Figure 6-11. Modeled Sulfate and TDS Concentrations *versus* Time  
at WCC-G1 Assuming 5,000 mg/L TDS Source.

  
**Geomega**

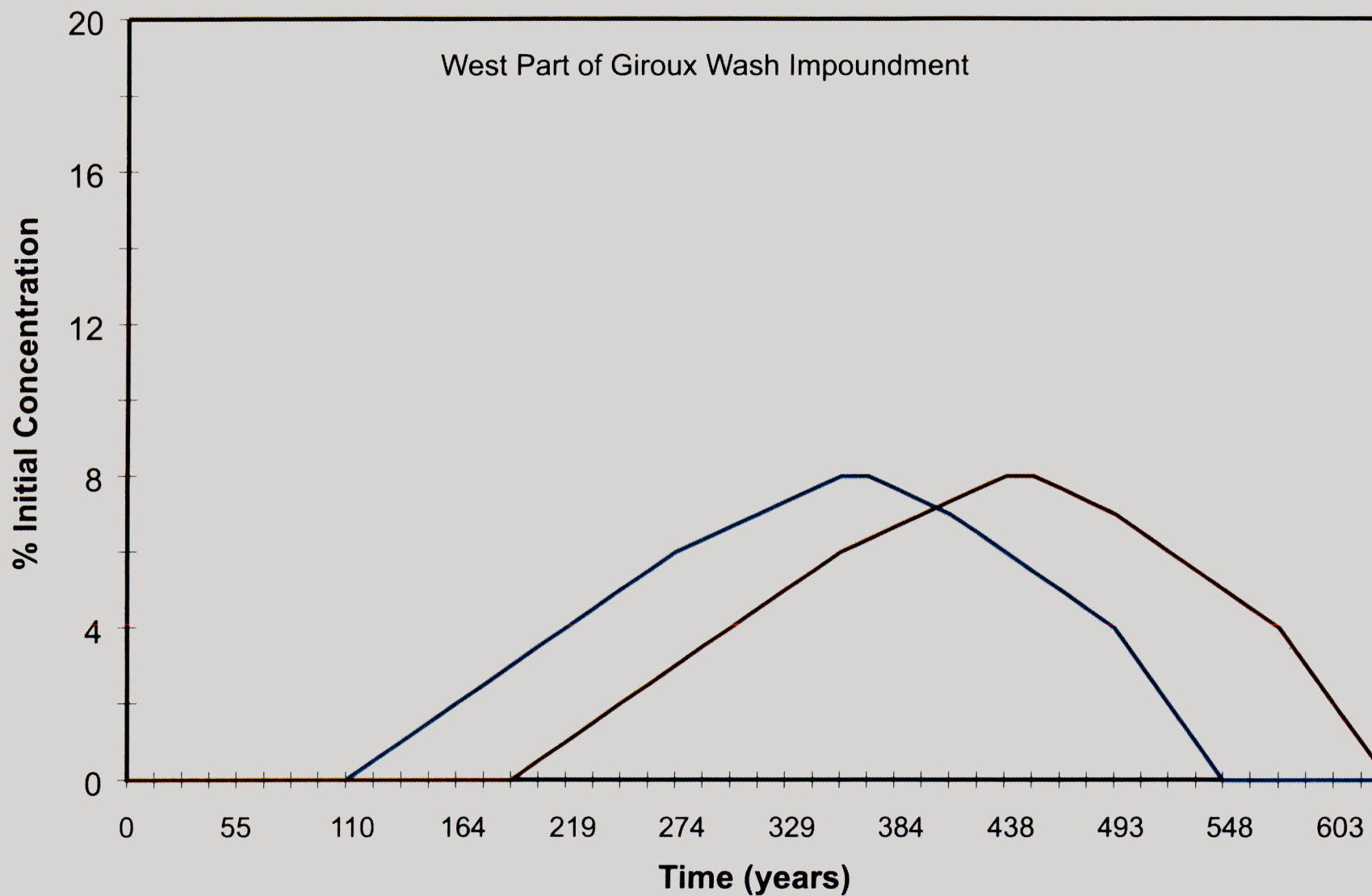




Generation  
Date:  
10/10/97

Figure 6-12. Predicted Solute Concentrations in the Vadose Zone for the Barge Canal (magenta) and 5-Foot Head (blue) Simulations.

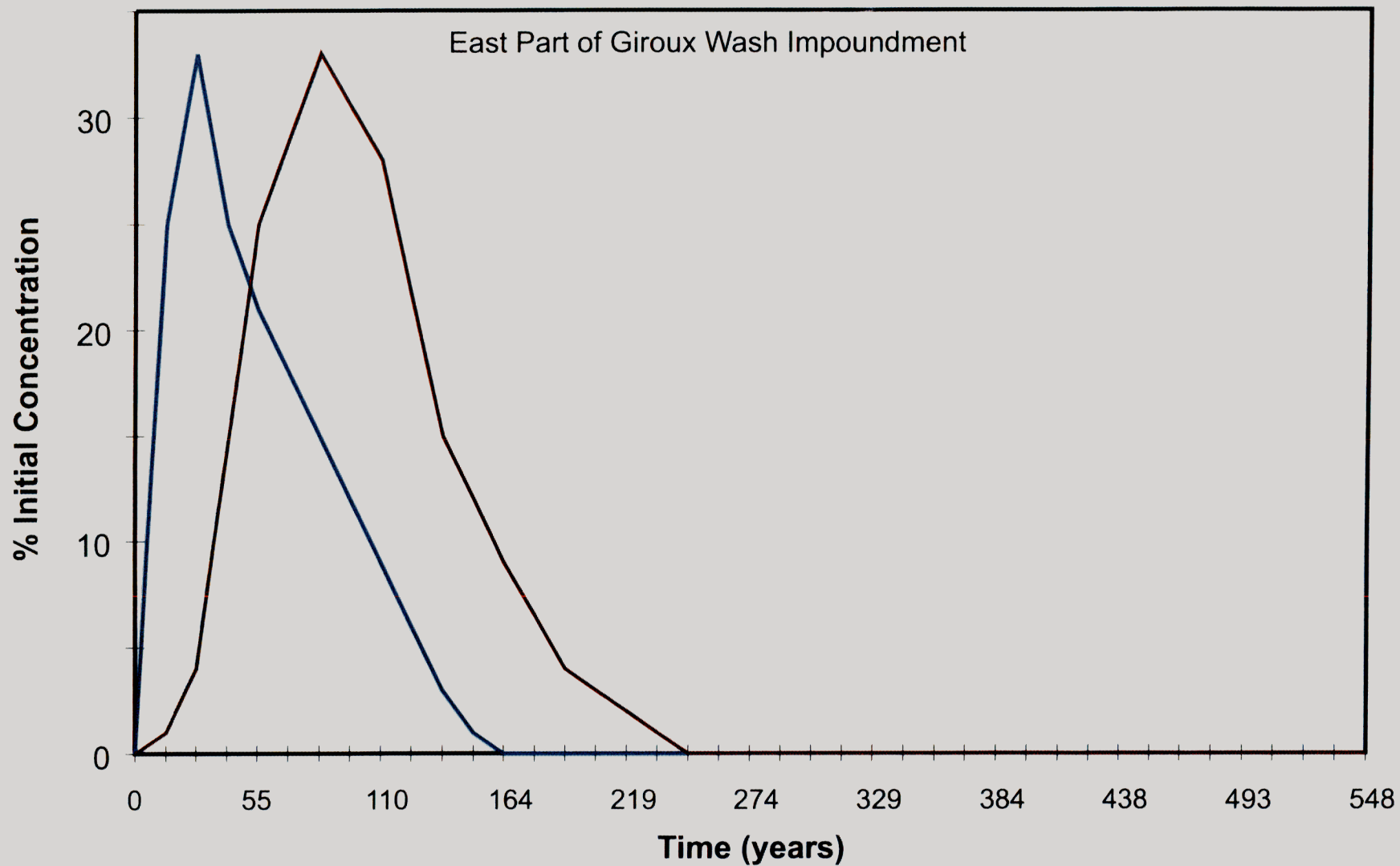




Generation  
Date:  
10/10/97

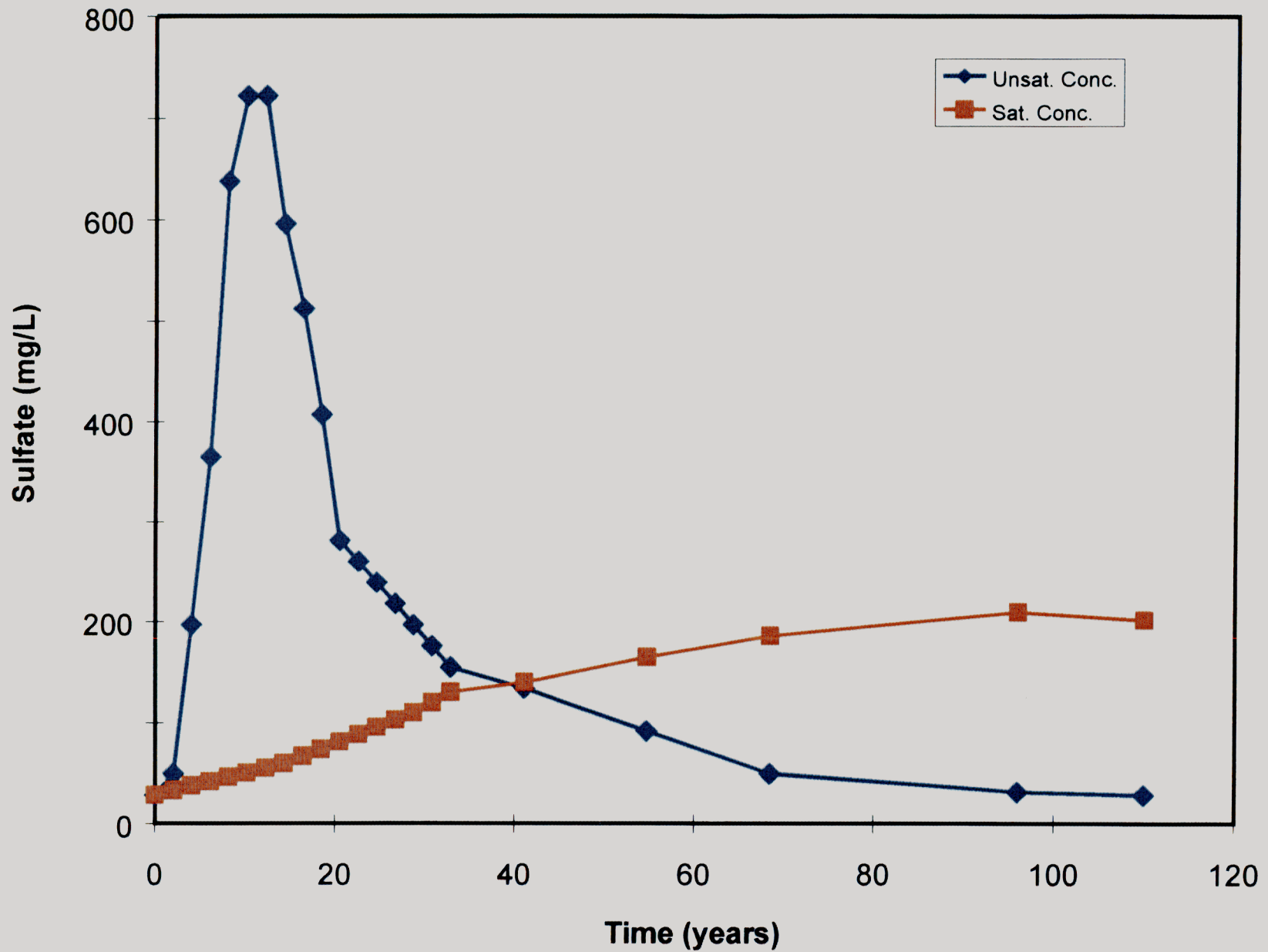
Figure 6-13. Predicted Solute Concentrations in the Vadose Zone not covered by the Barge Canal (magenta) and 5-Foot Head (blue) Simulations.

  
**Geomega**



Generation  
Date:  
10/10/97

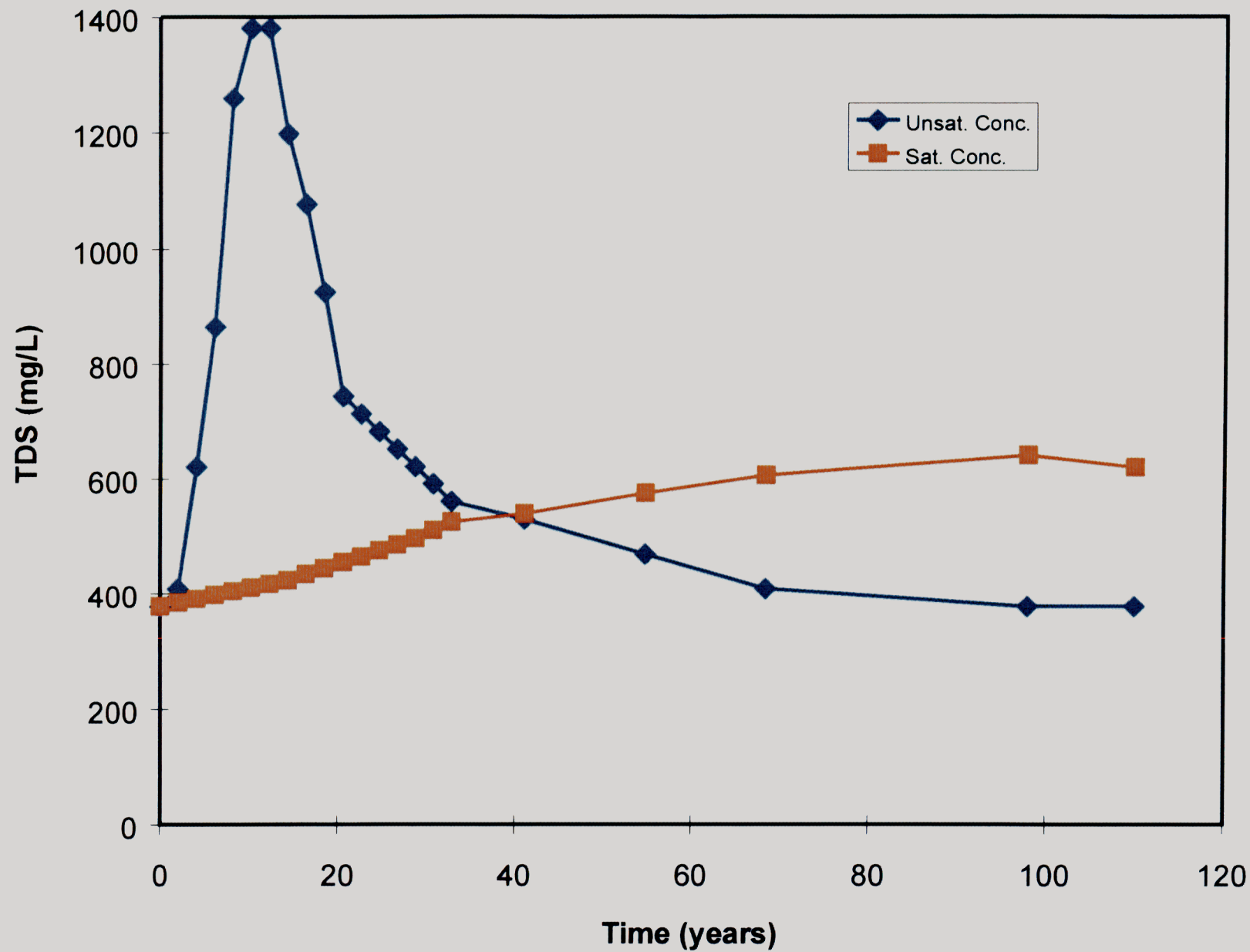
Figure 6-14. Predicted Solute Concentrations in the Vadose Zone for the Barge Canal (magenta) and 5-Foot Head (blue) Simulations.



Generation  
Date:  
10/10/97

Figure 6-15. Predicted Vadose Zone and Groundwater  
Sulfate Concentrations.

  
**Geomega**



Generation  
Date:  
10/10/97

Figure 6-16. Predicted Vadose Zone and Groundwater  
TDS Concentrations.

  
**Geomega**



## 7. Conclusions

Groundwater flow and solute transport modeling was completed for the Giroux Wash Tailings Impoundment pursuant to Section 2.9.2 of the February 27, 1997, *Work Plan—Robinson Operations*. Well-benchmarked U.S. Geological Survey and U.S. Environmental Protection Agency models were combined to quantify tailings solution percolation and solute transport through the vadose zone to groundwater, followed by saturated zone flow and solute transport to the downgradient compliance point (well WCC-G1).

The subregional Giroux Wash model assumed continued tailings solution deposition into the impoundment for the remaining mine life of 16 years. Postclosure conditions implemented in the model assumed that no cap or cover will be installed over the impoundment. The model evaluated three cases of tailings solution concentrations—3,000 mg/L, 4,000 mg/L, and 5,000 mg/L—to account for TDS variations in mill process water. The model accounted for future impoundment development through sequentially increased impoundment surface area and volume. The model implemented the following conservative flow and transport assumptions:

- Seepage will occur over the entire footprint of the impoundment for the operational life of the facility.
- The supernatant pond was assumed to provide an equivalent head across the lateral extent of the impoundment.
- No sorption or retarded transport of solutes will occur.
- The solutes will not be subject to any chemical reactions.
- Worst-case scenarios for source concentrations were modeled.
- Low-permeability soils (i.e., "B" horizon) were not incorporated in the vadose zone model.

These assumptions provided for maximum predicted flow velocities and advective solute transport. The model assumed that future climatic conditions in east-central Nevada would remain similar to current conditions over the modeled period of 1,644 years.

The purpose for conducting this modeling effort was twofold:

- to evaluate tailings solution percolation through the unsaturated zone below the impoundment and
- to assess the potential for degradation of state waters.

The model was successful in addressing these two objectives, as discussed in Sections 7.1 to 7.3.

## **7.1 Tailings Solution Percolation Through the Unsaturated Zone**

Unsaturated zone modeling predicted tailings solution percolation and solute transport through alluvium and volcanic rock composing the Giroux Wash subsurface. The travel time required for the initial wetting front to reach groundwater differs considerably across the Giroux Wash fault because of the differences in depth to groundwater.

West of the fault, a thick alluvial sequence underlies Giroux Wash, with groundwater residing approximately 750 feet below ground surface. Model results indicate that the initial wetting front will require 100 years to reach groundwater west of the fault, with percolation continuing 548 years thereafter until free water residing within the impoundment completely percolates through the vadose zone to groundwater.

East of the fault, relatively thin alluvium and volcanic rock compose the Giroux Wash subsurface, hosting groundwater at approximately 250 feet below ground surface. The initial wetting front will require 16 years to reach groundwater east of the fault, with tailings solution continuing to percolate for 100 years thereafter.

Conservative model assumptions (maximized relative solute concentrations and minimized travel time) within the bounds of the Giroux Wash characterization were implemented to quantify peak solute concentration discharging to groundwater via vertical tailings solution percolation. West of the Giroux Wash fault, peak conservative solute concentration reaching the water table is approximately 8% of the impounded tailings solution concentration, after approximately 356 years. East of the fault, peak solute concentration reaches approximately 33% of the impounded tailing water after approximately 36 years.

## **7.2 Potential for Groundwater Degradation**

Saturated zone solute transport modeling predicted that peak conservative solute concentration will increase by 10 to 20 mg/L (owing to tailings solution migration) over the next 500 to 1,000 years at WCC-G1 and then gradually decrease back to baseline concentrations at 1,370 years in the future.

The model results predict a maximum TDS of 387 mg/L at well WCC-G1. The peak TDS concentration is predicted to occur within 500 years at the earliest, given an impounded tailings solution TDS concentration of 5,000 mg/L. Model results therefore indicate that vertical percolation of tailings solution from the impoundment to groundwater underlying Giroux Wash will not lead to an exceedance of NDEP water-quality standards for TDS of 1,000 mg/L.

Model results predict a maximum sulfate concentration of 48 mg/L at well WCC-G1 as early as 600 years in the future, given an impounded tailings solution sulfate concentration of 5,000 mg/L. These results support TDS modeling results discussed

above and indicate that sulfate concentrations will not exceed the NDEP water-quality standard of 500 mg/L at well WCC-G1.

### **7.3 Barge-Operating Channel**

The results of the barge-operating channel modeling evaluation (Sections 6.5.4.1 through 6.5.4.3) support the use of the channel as a means to minimize infiltration of tailings solution to the relatively shallow groundwater in the volcanic bedrock under the eastern part of the impoundment. Operation of the channel over the 750-foot-deep alluvium under the western part of the impoundment slows infiltration in the eastern part and reduces the predicted groundwater solute concentrations there.

Planned barge operation will minimize the volume of infiltrating water in the channel by reclaiming water back to the mill circuit. Under these conditions, the ponded water that acts as the driving force for infiltration will be localized and limited to an approximately 10- to 15-foot depth. This infiltration will increase the infiltration rate of solutes from the barge-operating channel. However, the depth of the vadose zone underlying the channel will mitigate solute transport, resulting in a slight increase in predicted groundwater solute concentrations beneath the barge-operating channel (see Figure 6-12) compared to the decrease in predicted groundwater solute concentrations in the eastern part of the impoundment.

### **7.4 Summary**

In summary, conservative transport parameters assigned for transport modeling results indicate that subsurface discharge of percolating tailings solution will not lead to degradation of state waters, as solute concentrations do not exceed NDEP water-quality standards at the downgradient compliance point (monitoring well WCC-G1).

## 8. Recommendations

Groundwater flow and solute transport modeling for the Giroux Wash Tailings Impoundment predicts slow, vertical percolation of tailings solution through the Giroux Wash vadose zone to groundwater. Model results predict no substantial increase in conservative solute concentration in groundwater at the compliance monitoring point (WCC-G1). Consequently, model results indicate no degradation of state waters. The model results support continued operation of the tailings impoundment throughout the remaining mine life of approximately 16 years.

Results of the modeling effort, which incorporated conservative flow and transport assumptions, are germane to evaluating any potential benefits of lining the barge-operating channel. Although tailings deposition will displace free water as the impoundment is filled, the model incorporated an initial 5-foot free hydraulic head (SRK, 1997) across the entire impoundment footprint, as a conservative starting condition. This starting hydraulic head is equivalent to the average head in the supernatant pond and barge-operating channel, and thus the model assumes that the supernatant pond covers the entire impoundment. Model results indicate no degradation of state waters at the POC from tailings solution infiltration. Therefore, under current and future operating conditions, vertical tailings solution infiltration from the unlined barge-operating channel (ultimately covering only a small fraction—i.e., <1%—of the total impoundment footprint) will not lead to degradation of state waters.

## 9. References

- Anderson, M.P., and W.W. Woessner. 1992. *Applied Groundwater Modeling*. Academic Press, Inc. San Diego, California.
- Bedinger, M.S., J.R. Harril, and J.M. Thomas. 1984. Maps showing ground-water units and withdrawal, Basin and Range Province, Nevada. 1:500,000. U.S. Geological Survey Water-Resources Investigations Report WRI 83-4119-A.
- Brokaw, A.L., and P.J. Barosh. 1968. Geologic map of the Riepetown quadrangle, White Pine County, Nevada: U.S. Geological Survey Geologic Quadrangle Map GQ-758.
- Burbey, T.J., and D.E. Prudic. 1991. Conceptual evaluation of regional ground-water flow in the carbonate-rock province of the Great Basin, Nevada, Utah, and adjacent states. U.S. Geological Survey Professional Paper 1409-D.
- Dames & Moore. 1982. Geotechnical evaluation, tailings remining project, McGill, Nevada. Prepared for Kennecott Minerals Co. by Dames & Moore, Salt Lake City, Utah.
- Dames & Moore. 1987. Phase I Report, Hydrogeology Studies, Nevada Mines Operation, McGill, Nevada for Kennecott. Job no. 1375-074-18. Dames & Moore, Salt Lake City, Utah.
- Dames & Moore. 1988. Phase IIA Report, Hydrogeology Studies, Lane City Area. Dames & Moore, Salt Lake City, Utah.
- Dames & Moore. 1990. Phase IIB Report, Hydrogeology Studies. Dames & Moore, Salt Lake City, Utah.
- de Marsily, G. 1986. *Quantitative Hydrogeology*. Academic Press, San Diego, California.
- Domenico, P.A. and F.W. Schwartz. 1990. *Physical and Chemical Hydrogeology*. John Wiley & Sons, New York, NY.
- Eakin, T.E., J.L. Hughes, and D.O. Moore. 1967. Water-resources appraisal of Steptoe Valley, White Pine and Elko Counties, Nevada. State of Nevada, Department of Conservation and Natural Resources, Water Resources Reconnaissance Series, Report 42.



Einaudi, M.T. 1982. Description of skarns associated with porphyry copper plutons, in Titley, S.R., ed., *Advances in geology of the porphyry copper deposits, southwestern North America*: Tucson, University of Arizona Press, p. 139–183.

Fournier, R.O. 1967a. The porphyry copper deposit exposed in the Liberty open-pit mine near Ely, Nevada. Part I. Syngenetic formation: *Economic Geology*, 62:57–81.

Frick, E.A. 1985. Quantitative analysis of groundwater flow in valley-fill deposits in Steptoe Valley, Nevada. Thesis. University of Nevada, Reno, Nevada. 192 pp.

Freeze, R.A. and J.A. Cherry. 1979. *Groundwater*. Prentice-Hall, Englewood Cliffs, New Jersey.

Gans, P.B., and E.L. Miller. 1983. Style of mid-Tertiary extension in east-central Nevada. In W.P. Nash and K.D. Gurgel (Eds.). *Geological excursions in the overthrust belt and metamorphic core complexes of the Intermountain region*. Utah Geol. Mineral Surv. Special Study 59.

Geomega. 1997a. Giroux Wash Tailings Impoundment TDS Mobility Testing. Prepared for BHP Copper–Nevada Mining Company, Robinson Operations.

Geomega. 1997b. Giroux Wash Tailings Impoundment Soil Column Attenuation Testing. Prepared for BHP Copper–Nevada Mining Company, Robinson Operations.

Hose, R.K. and M.C. Blake, Jr. 1976. Geology and mineral resources of White Pine County, Nevada. Part I. Geology. Nevada Bureau of Mines and Geology, Bulletin 85.

Houghton, J.G., C.M. Sakamoto, and R.O. Gifford. 1975. Nevada's weather and climate. Nevada Bureau of Mines and Geology, Special Publication 2, University of Nevada, Reno, Nevada.

James, L.P. 1976. Zoned alteration in limestone at porphyry copper deposits, Ely, Nevada. *Econ. Geol.* 71:488–512.

Jury, W.A., W.R. Gardner, and W.H. Gardner. 1991. *Soil Physics*. John Wiley and Sons, Inc., New York.

LeedsHill. 1981a. Groundwater investigation, phase 1, Technical report for the White Pine Power Project. Prepared for Los Angeles Department of Water and Power by Leeds, Hill and Jewett, Inc., San Francisco, California.

Maxey, G.B. and T.E. Eakin. 1949. Groundwater in White River Valley, White Pine, Nye, and Lincoln Counties, Nevada. State of Nevada, Office of the State Engineer, Water Resources Bulletin No. 8.

McDonald, J.M., and A.W. Harbaugh. 1988. *A modular three-dimensional finite difference ground-water flow model*. Techniques of Water Resources Investigations of the U.S. Geological Survey, Book 6.

McWhorter, D.B. and D.K. Sunada 1977. *Ground-Water Hydrology and Hydraulics*. Water Resources Publications, Highlands Ranch, Colorado.

Maurer, D.K., R.W. Plume, J.M. Thomas, and A.K. Johnson. 1996. *Water Resources and Effects of Changes in Groundwater Use Along the Carlin Trend, North-Central Nevada*: U.S. Geological Survey Water-Resources Investigations Report 96-4134.

Morris, D.A., and A.I. Johnson. 1967. *Summary of Hydrological and Physical Properties of Rock and Soil Materials*. U.S. Geological Survey Water Supply Paper 1839-D.

PTI. 1994. *The Hydrogeochemistry of the Robinson District, White Pine County, Nevada*. Prepared for Magma Nevada Mining Company.

Rumbaugh, J.O., III. 1997. Environmental Simulations, Inc. *Groundwater Vistas Version 1.88*.

Seedorff, E. (Ed.). 1993. *Summer Field Trip (RMD), Geology and Mineralization*. Geological Society of Nevada, Elko. Special Publication 17.

Shevenell, L. 1996. *Statewide Potential Evapotranspiration Maps for Nevada*, Nevada Bureau of Mines and Geology Report 48, University of Nevada, Reno, Nevada.

Simunek, J., M. Sejna, and M.Th. van Genuchten. 1996. *HYDRUS\_2D: Simulating Water Flow and Solute Transport in Two-Dimensional Variably Saturated Media*, U.S. Department of Agriculture, Riverside, California.

Smith, R.M. 1976. *Geology and mineral resources of White Pine County, Nevada. Part II. Mineral Resources*. Nevada Bureau of Mines and Geology, Bulletin 85.

SRK. 1997. *Water Balance for Giroux Wash Tailings Impoundment, White Pine County, Nevada*. Prepared for BHP Copper-Nevada Mining Company, Robinson Operations.

Thomas, J.M., J.L. Mason, and J.D. Crabtree. 1986. *Ground-water levels in the Great Basin region of Nevada, Utah, and adjacent states. 1:1,000,000*. U.S. Geological Survey Hydrologic Investigations Atlas (Atlas HA-694-B).

Welsh Engineering, Inc. 1991. *Design Report, Magma Nevada Mining Company, Robinson Project Tailings Impoundment*.

WESTEC. 1991. Design Report, Magma Nevada Mining Company, Robinson Project, Tailings Impoundment. Prepared for Magma Nevada Mining Company.

Westra, G. 1982. Alteration and mineralization in the Ruth porphyry copper deposit near Ely, Nevada. *Econ. Geol.* 77:950-970.

Woodward-Clyde Consultants. 1991. Preliminary hydrogeological investigation of the flow regime between the Liberty and Ruth pits and the Murry and Ward Mountain Springs for the Robinson mine site, White Pine County, Nevada. Prepared for Magma Copper Company, San Manuel, Arizona, by Woodward-Clyde Consultants, Denver, Colorado.

Woodward-Clyde Consultants. 1992. Hydrogeologic investigation and groundwater modeling, open pit and Giroux Wash areas, Robinson Mine project, Ely, Nevada. Prepared for Magma Copper Company, San Manuel, Arizona by Woodward-Clyde Consultants, Denver, Colorado.

Zheng, C. 1996. *MT3D96, A Modular Three-Dimensional Transport Model for Simulation of Advection, Dispersion and Chemical Reactions of Contaminants in Groundwater Systems*. S.S. Papadopoulos & Associates, Inc., Rockville, Maryland. June 1996.

Zheng, C. 1992. *MT3D: A Modular Three-Dimensional Transport Model for Simulation of Advection, Dispersion and Chemical Reactions of Contaminants in Groundwater Systems*. S.S. Papadopoulos & Associates, Inc.

Zones, C. 1961. Groundwater Potentialities in the Crescent Valley, Eureka and Lander Counties, Nevada. U.S. Geological Survey Water-Supply Paper 1581.

**Model provided to NDEP on CD-ROM**

**Please contact Geomega to receive model on CD-ROM**